ERDA Report
COO-3127-11

VAPOR PRESSURE ISOTOPE EFFECT IN $^{13}CCIF_3$ / $^{12}CCIF_3$ BY CRYOGENIC DISTILLATION KINETICS

by

Henry J. Wieck and Takanobu Ishida

Brooklyn College of
The City University of New York
Brooklyn, New York 11210

August, 1975

DISCLAIMER

ABSTRACT

The vapor pressure of $^{13}CClF_3$ relative to the vapor pressure of $^{12}CClF_3$ has been measured as a function of temperature between 169° and 206°K by using a modified Bigeleisen distillation column. The transient build-up of the isotopic concentration gradient along the length of the packed column during the start-up period was monitored by taking samples from the condenser section as a function of time. The gaseous samples were completely oxidized to carbon dioxide in the presence of a platinum catalyst and a large excess of oxygen at temperatures between 1050 and 1100°C. The combustion products were purified by means of gas-chromatography, and the purified carbon dioxide samples were analyzed in a Nier-type isotope-ratio mass-spectrometer. The data of each distillation run were reduced in the light of Cohen's theory of the kinetics of square cascade of close-separation stages.

The vapor pressure isotope effect for the carbon substitution in $CClF_3$ at temperatures between 169° and 206°K has been found to be an inverse effect and to be rather insensitive to changes in temperature. The relative vapor pressure may be expressed as

$$\ln \frac{P'}{P} = \frac{(1.5 \pm 14.1)}{T^2} - \frac{(0.159 \pm 0.076)}{T} ,$$

or

$$\ln \frac{P'}{P} = \frac{(0.173 \pm 0.098)}{T} - (0.11 \pm 0.53) \times 10^{-3} ,$$

where P' and P are the vapor pressures of $^{12}CClF_3$ and $^{13}CClF_3$, respectively. To the first-order, the presence of chlorine isotopes would not affect the fractionation of carbon isotopes by the distillation of $CClF_3$.

Thesis Approved by:

Takanobu Ishida
Professor of Chemistry
Thesis Adviser

Harmon L. Finston
Professor of Chemistry

P. Gary Mennitt
Professor of Chemistry

David E. Goldberg
Chairman
Department of Chemistry
Brooklyn College of the
City University of New York

VAPOR PRESSURE ISOTOPE EFFECT IN $^{13}CClF_3/^{12}CClF_3$ BY CRYOGENIC DISTILLATION KINETICS

A Thesis

Presented to the Graduate Faculty

of the Department of Chemistry

Brooklyn College

City University of New York

In Partial Fulfillment

of the Requirements of the Degree of

Master of Arts

by

Henry J. Wieck

August 1975

DEDICATION

Dedicated with love to: My Mother, my happiness was hers,

My Father, my accomplishments are his,

My wife, Nancy, my life is hers.

TABLE OF CONTENTS

TABLE OF CONTENTS (continued)

LIST OF TABLES

LIST OF FIGURES

LIST OF FIGURES (continued)

I. INTRODUCTION

The purpose of this study is to experimentally determine the separation factor for ^{13}C from its natural abundance by means of a low temperature distillation of chlorotrifluoromethane.

Carbon-13 is a stable isotope that occurs at a natural abundance of 1.11%. The very fact that it is not radioactive has recently attracted the interests of biomedical scientists to its potential use as a tracer for carbon in medical and biological studies. Recent advances for detection and/or determination of carbon-13, by NMR, have made its use particularly attractive. In such tracer studies the technique will not only trace the path of the carbon-13, but also determine its molecular environment.

Currently carbon-13 is being enriched up to 95.5%[1] by means of cryogenic distillation of carbon monoxide and also by a combination of the carbon dioxide-carbamate process[2] and the thermal diffusion of methane[3]. Other methods that have been investigated, but have not proceeded to production scale include the following. Urey fractionated carbon-13 from natural enrichment by means of a carbon-isotope exchange between an aqueous solution of sodium cyanide and gaseous hydrogen cyanide[4];

$$H^{13}CN + {}^{12}CN^- = H^{12}CN + {}^{13}CN^-.$$

The equilibrium constant was found to be 1.026 at room temperature, but in addition to the obvious toxicity of the substance, polymerization of HCN sets in gradually, which leads to equivalent loss of isotopes in a cascade operation. A system that consists of cuprous chloride-ammonium chloride solution and carbon monoxide (COCO system) developed at Oak-Ridge National Laboratory, employs thermal reflux at both ends. The

stage separation factor for this system is 1.015 at room temperature and the isotope exchange is rapid enough to obtain a stage height of less than 1.5 times the column diameter[5]. Another exchange system developed at Oak Ridge consists of a ketone cyanohydrin and aqueous cyanide solution. It has a very high separation factor of about 1.04 but requires a chemical reflux[5].

The carbon dioxide-carbamate exchange was developed by T.I. Taylor and his students at Columbia University and has since been scaled up by Mound Laboratory for enriching ^{13}C from its natural abundance to about 93%. The effective stage separation factor depends on the choice of carbamate, the temperature, the solvent, the pressure and the flow rate. The Mound process utilizes carbamate of n-dibutylamine dissolved in triethylamine and yields an effective single stage separation factor of 1.01[6]. Because of the limited solubility of carbamate and the rather high vapor pressure of the amine, the carbamate process is generally limited to operation at temperatures in the range of 25-40°C.

Unlike processes such as distillation or isotope exchange reactions, thermal diffusion is a non-equilibrium process. Although the process is thermodynamically unfavorable, the thermal diffusion process originally devised by Clasius-Dickel[7] has been widely used for the purpose of isotope separation. This is primarily due to the simplicity of the apparatus and the rather large separation factor the process yields. This process is used at Mound Laboratory for the further enrichment of the product of the carbamate process.

Before proceeding further it seems appropriate to discuss certain basic terminology and the relative advantages and disadvantages of the various processes. A separating stage is a unit of the separation process,

all fed with material of the same composition and producing partially separated product streams of the same composition. When the degree of separation effected by a single stage falls short of the desired separation between product and feed material, it is necessary to connect stages in series. A group of stages connected in series is referred to as a cascade. The degree of separation effected by a unit stage is expressed in terms of the separation factor. Referring to figure 1, the stage separation factor, α, is defined as:

$$\alpha = \frac{\text{Abundance Ratio in Heads}}{\text{Abundance Ratio in Tails}} = \frac{R'}{R''} = \frac{N}{N''}\,\frac{1-N''}{N'} \qquad (1)$$

Since α for an isotope exchange is generally close to unity (except for hydrogen isotopes) it is sometimes convenient to use ϵ, defined as

$$\epsilon = \alpha - 1 \qquad (2)$$

For a distillation process α is equal to the ratio of the vapor pressures of two isotopic molecules at a given temperature. As a rule of thumb ϵ for a distillation process for enrichment of isotopes of second period elements (Li - F) does not exceed 10^{-2}. In Mound Laboratory CCl_3F (Freon-11) was distilled at 24°C and the separation factor was found to be $1.0019 \pm .0003$.[3] For an exchange process the separation factor is proportional to the equilibrium constant. They are not necessarily identical since an isotopic substitution at equivalent atomic positions in a given molecule does not lead to isotopic fractionation[8]. Generally ϵ often exceeds $2 \sim 3 \times 10^{-2}$ which is attributable to a large change in bond-order around the substituted atom as it is exchanged between two chemical species. The disadvantage of the exchange process is that it

Fiqure 1. Separation Stage

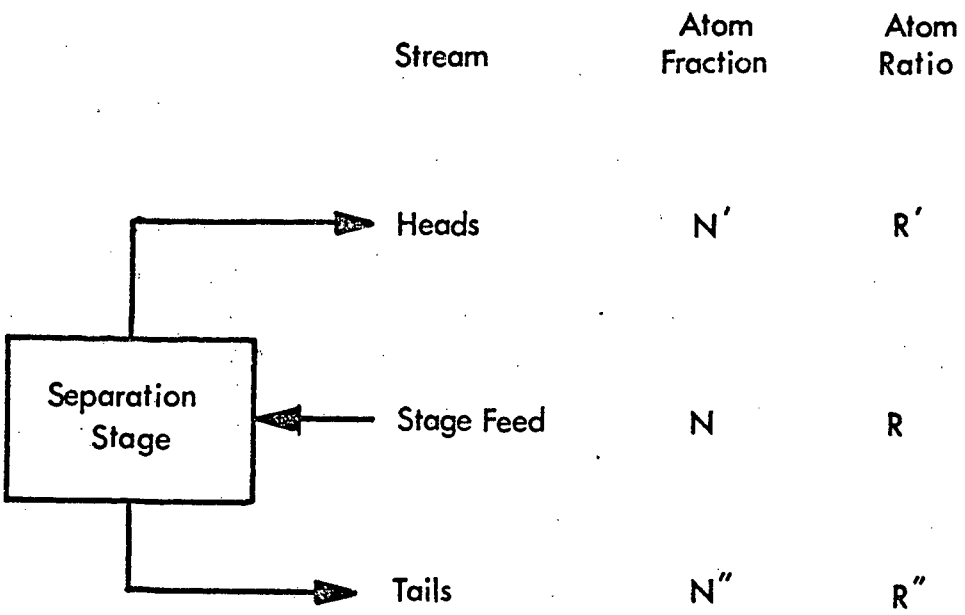

usually requires a chemical reflux at both ends of the cascade. Such a chemical reflux is necessary to achieve complete conversion of one chemical species into the other at the end of the cascade, without any loss of isotopes from the system. This usually leads to costly chemical waste. The carbamate process achieves the reflux by thermal means; the carbamate is thermally decomposed at one end, while carbon dioxide and amine are thermally combined to form carbamate at the other end of the cascade. Such an exchange process is called an exchange distillation, and has the advantages of both the exchange and distillation processes. The more important merits of a distillation lie in the absence of chemical reflux and in a large material throughput, which is a very important consideration in an industrial size plant. Thus a distillation plant which handles a substance with a molecular weight of 100 and a density of 2 g/cc would be 20 times smaller in volume than an exchange plant handling 1 molar solutions.

The recently discovered method of laser-activated isotope separation has a special advantage of being capable of yielding a large separation factor, i.e., of the order of tens and hundreds for α.[9] At its present cradle stage of development, the material throughput is exceedingly limited due to the fact that the laser activation has to be achieved in the gaseous state of very low pressure, typically of the order of a torr. This is a necessary requirement for the achievement of the extreme high selectivity. The future of laser isotope separation seems to depend on ultra powerful laser technology and a compromise between selectivity and throughput.

In Subsection I-1 that follows the general theory of vapor pressure isotope effect will be presented first. It will then be followed in Sub-

section I-2 by a discussion of preliminary investigations that lead to the choice of fluoronated-hydrocarbons as a distillation material. Finally, in Subsection I-3 the outline of the investigation will be given.

I-1. Theory of Vapor Pressure Isotope Effect

The vapor pressure of a chemically and isotopically pure liquid is determined by the dynamic equilibrium between two species, namely, the molecules in the gas phase and the molecules in the liquid phase. The vapor pressure of such a substance can be expressed in terms of the partition function of these two species. It follows that the difference in the vapor pressure of a pair of isotopic liquids of the same substance is expressible in terms of 4 partition functions, two partition functions for each isotopic species.

Bigeleisen[10] developed a fundamental theory of vapor pressure isotope effect based on the assumptions of the simple cell model of liquids, and the Born-Oppenheimer approximation. According to this theory, the ratio of the vapor pressures of the light isotopic species, P', to that of the heavier isotopic species, P, is given by

$$\ln \frac{P'}{P} = \ln \frac{s}{s'} f_c - \ln \frac{s}{s'} f_g \qquad (3)$$

where s' and s are the symetry numbers of the light and heavy isotopic species, respectively, and f_c and f_g are the isotopic ratio of the

reduced partition functions in the condensed phase and the gas phase, respectively. They are "reduced" in the sense that they are the ratio of the partition functions to its classical limit, in other words:

$$\frac{s}{s'} f = \frac{\left(Q/Q'\right)_{qm}}{\left(Q/Q'\right)_{cl}} = \frac{\left(Q_{qm}/Q_{cl}\right)}{\left(Q'_{qm}/Q'_{cl}\right)} \tag{4}$$

where Q' and Q are partition functions of the light and heavy species, respectively, and the subscripts qm and cl represent the quantum mechanical and classical respectively.

Within the framework of the Born-Oppenheimer approximation and under the assumptions that the potential is harmonic, and that the translational and rotational partition functions are classical, $\frac{s}{s'} f$ can be expressed as[7]:

$$\frac{s}{s'} f = \prod_{i=1} \frac{u}{u'_i} \frac{e^{-u_i/2}\left(1-e^{-u_i'}\right)}{e^{-u_i'/2}\left(1-e^{-u_i}\right)} \tag{5}$$

where the product is taken over all degrees of internal vibrational freedom, and u is defined as:

$$u = \frac{hc\omega}{kT} \tag{6}$$

in which h is Plancks constant, c the velocity of light, ω the normal frequency in units of wave numbers (cm^{-1}), k the Boltzman constant and T the absolute temperature.

When T is very large or when ω's are small Equation 5 reduces to

$$\ln \frac{s}{s'} = \frac{1}{24} \sum_i \left(u_i'^2 - u_i^2 \right) \tag{7}$$

$$= \frac{1}{T^2} \frac{1}{24} \left(\frac{hc}{k} \right)^2 \sum_i \left(\omega_i'^2 - \omega_i^2 \right) \tag{8}$$

When the temperature is low or when ω's are large Equation 5 approaches:

$$\ln \frac{s}{s'} = \sum_i \frac{u_i' - u_i}{2} \tag{9}$$

$$= \frac{1}{T} \frac{hc}{2k} \left(\omega_i' - \omega_i \right) \tag{10}$$

In the simple cell model, $\ln \frac{s}{s'} f_c$ in Equation 3 is evaluated by associating three translational degrees of freedom, three rotational degrees of freedom, and 3N-6 internal degrees of freedom, with each molecule. Furthermore the translational and rotational motions are assumed to be oscillatory in nature. Due to the relatively weak external force (as compared to the forces within the molecule) the frequency of these ω , of external oscillation, are small, i.e. $< 150\ cm^{-1}$. Thus $\ln \frac{s}{s'} f_c$ in Equation 3 can be thought of as consisting of two types of terms, one attributable to the weak external oscillations, which is proportional to $\frac{1}{T^2}$ in accordance with equation 8, and the other to the internal vibrations in the condensed phase which is proportional to $\frac{1}{T}$

in agreement with Equation 10. The other term in Equation 3, $\ln \frac{s}{s'} f_g$, of course contributes additional terms which are proportional to $\frac{1}{T}$. Consequently, as a first approximation to equation 3, Bigeleisen[10] derived the following relationship:

$$\ln\left(\frac{P'}{P}\right) = \frac{A}{T^2} - \frac{B}{T} \tag{11}$$

where
$$A = \frac{1}{24}\left(\frac{hc}{k}\right)^2 \sum^{6} \left(\omega'^{2}_{ext} - \omega^{2}_{ext} \right) \tag{12}$$

and
$$B = \left(\frac{hc}{2k}\right)\left\{\left[\sum \omega'_g - \sum \omega'_c\right] - \left[\sum \omega_g - \sum \omega_c\right]\right\} \tag{13}$$

It is seen that A depends entirely on the external vibrations while B represents the isotopic difference in the zero-point energy shift on condensation. It has been shown that A and B are always positive. According to Equation 11, the vapor pressure of the lighter isotope is greater than the vapor pressure of the heavier isotope at sufficiently low temperature, while the effect could be reversed as temperature increases above a certain point. If such a crossover temperature happens to be within the range of liquid temperature, i.e., at a temperature above the triple point and below the boiling point, then the inverse vapor pressure effect is expected to be advantageous in isotope production. The reason for this will be explained briefly in the following paragraph.

Due to the fact that isotope separation is a close separation

(small ϵ), an isotope production plant requires a large number of separation stages. At initial start up of a plant, all stages are charged with material of natural enrichment and, the refluxers on both ends of the column are started. During the initial transient period an isotopic concentration gradient is gradually established along the length of the cascade. When the enrichment in the product end of the cascade reaches a steady level, slow product withdrawal is initiated, accompanied by a corresponding material input at the feed point along the cascade. During the transient period the cascade is operated at total reflux at both ends, i.e., no material is withdrawn from the system. This transient period increases with holdup (the amount of desired material held up in the system). According to the theory developed by Cohen[11] the transient period is shorter when ϵ is negative. For a distillation frationation of carbon-13 the negative ϵ corresponds to the inverse vapor pressure isotope effect. A preliminary investigation, to be outlined in the next subsection, showed the probability of finding such an inverse effect in the liquid temperature range would be substantial for fluorochloro-methanes.

I-2. Investigations leading to the choice of Fluorochloromethanes.

Methane-^{13}C has a lower vapor pressure than $^{12}CH_4$, at liquid methane temperature[12], while ^{13}C substitution in carbon tetrachloride leads to a slightly inverse isotope effect at 35 degrees centigrade[13]. This is a

consequence of the fact that external (translational and rotational) modes vanish to negligible levels, as a result of the symmetric substitution of the peripheral positions by heavy chlorine atoms, thus leading to a small A factor in equation 11. The smallness of the inverse effect in CCl_4 is attributable to the high temperature, the prohibited interaction between the rotation and internal motion of a tetrahedral molecule, and possibly due to a counteracting effect of $^{35}Cl/^{37}Cl$ fractionation that could take place simultaneously. A high molecular weight and a large moment of inertia reduce the magnitude of the $\frac{1}{T^2}$ term, thus favoring the inverse effect at low temperatures. The zero-point energy shift term is enhanced by strong interactions of liquid phase external modes with strongly infrared active internal mode actions, in which the center atom actively participates[14]. Presence of fluorine atoms in a molecule brings the melting and boiling points down to levels that are much lower than those of the corresponding chloro-derivatives, thus raising the possibility of the occurence of the crossover temperature within the liquid range rather than in the solid. Presence of other halogens in a molecule increases the electronic polarizability, which enhances the dipole-induced dipole interaction. However, introduction of too many halogens, except fluorine, increases the melting point and liquid molar volume to too high a level, so that any inverse effect of the liquid vapor pressure would become negligibly small. One of these "Freons", chlorotrifluoromethane ("Freon-13") has C_3v symmetry which is sufficiently non-symmetric to allow its carbon atom to participate in the normal vibrations that can interact with the external modes in the liquid. It has a melting point of -180°C and a normal boiling point of -82°C, which can be conveniently handled by the cryogenic distillation column

TABLE I

SUMMARY OF PHASE TRANSITION DATA OF SOME FLUOROHALOMETHANES

Molecule		M.W.	n-M.P.	n-B.P.	Critical Point		
			(°C)	(°C)	T_c(°C)	P_c(atom)	V_c(ml/mole)
	CH_4	16	-182	-161	- 83	45	99
	CH_3F	34	-142	- 78			
	CH_2F_2	52		- 52	78	58	121
Freon-23	CHF_3	70	-163	- 82	33	47	136
Freon-14	CF_4	88	-184	-129	- 45	37	140
	CCl_4	154	- 23	76	283	45	276
Freon-11	CCl_3F	137.5	-110	24	198	44	248
Freon-12	CCl_2F_2	121	-158	- 25	112	41	217
Freon-13	$CClF_3$	104.5	-180	- 82	29	39	180
	$CHCl_3$	119.5	- 64	61	263	54	239
Freon-21	$CHCl_2F$	103	-135	9	179	51	197
Freon-22	$CHClF_2$	86.5	-160	- 41	96	49	165
	CBr_2F_2	210	-110	24			
Kulene-131	$CBrF_3$	149	-176	- 57	67	39	200

that was made available by Prof. Jacob Bigeleisen of the University of Rochester. Preliminary calculations[15], on the zero-point energy shift on condensation, based on Wolfsberg theory[14] of London dispersion forces in liquids, showed that Freon-13, Freon-12, and Freon-14 have a good possibility of yielding the inverse isotope effect. Freon-13 was chosen for this study.

I-3. Outline of Investigation.

The separation factor for ^{13}C fractionation in the cryogenic distillation of $CClF_3$ has been determined in the following manner. A portion of $CClF_3$ manufactured by Matheson Gas Products which is 99.0% pure, was purified by gas-chromatography and distilled under total reflux in a cryogenic distillation column, which was designed and built by J. Bigeleisen[16] and modified during this investigation. The build up of the carbon-13 enrichment gradient along the column was monitored as a function of time. This transient behavior under total reflux was analysed according to the theory of K. Cohen[11] leading to determination of the stage separation factor and the number of theoretical stages. The separation factor was thus obtained as a function of temperature. The data was fit to Bigeleisen's formula, Equation 11, and the result was compared with a theoretical calculation based on the theory of the simple cell model. In Chapter II (Experimental), the experimental procedures will be discussed

in detail. The method of data reduction by Cohen's theory will be presented in Chapter III (Data Reduction). The derivation of the formula used in the data reduction will also be given in that chapter. An extension of Cohen's theory to accommodate the need of the present investigation which primarily deals with the inverse isotope effect has been developed, and a paper is currently in print. A preprint of the paper will be found in Appendix I.

II. EXPERIMENTAL

The low temperature distillation of Freon-13 ($CClF_3$) dictated the construction of various apparatus. The three major pieces of apparatus constructed, a preparative gas-chromatograph, a low-temperature distillation column, and a combustion train, are described in the following Section (II-1). It was found to be necessary that reliable vapor pressure data be obtained for Freon-13. The acquisition of this data is described in Section II-2. Actual experimental procedures are presented in detail in Section II-3.

II-1. Design and Construction.

Preliminary purity analyses of Freon-13 were performed on a Perkin-Elmer model 990 chromatograph. The results indicated the presence of considerable amounts of impurities. After removal of the major impurity, air, by bulb to bulb distillation, other impurities were shown to be freons. Low boiling impurities would lead to erroneous interpretation of isotopic analysis of the distillate with respect to the distillation column characteristics. In order to bring the level of these impurities down to a more acceptable level, 1 ppm, a preparative gas-chromatograph purification system was designed and constructed. (Fig. 2)

The distillation column of the Bigeleisen type was generously donated by its creator Professor Jacob Bigeleisen of the University of Rochester. Since its movement from Rochester, New York the column has been cleaned, reassembled and modified in several significant ways.

In order to perform isotopic-ratio analysis of the Freon-13 samples taken from the column, it was found to be necessary to convert the Freon-13 samples to carbon dioxide. The conversion is accomplished by

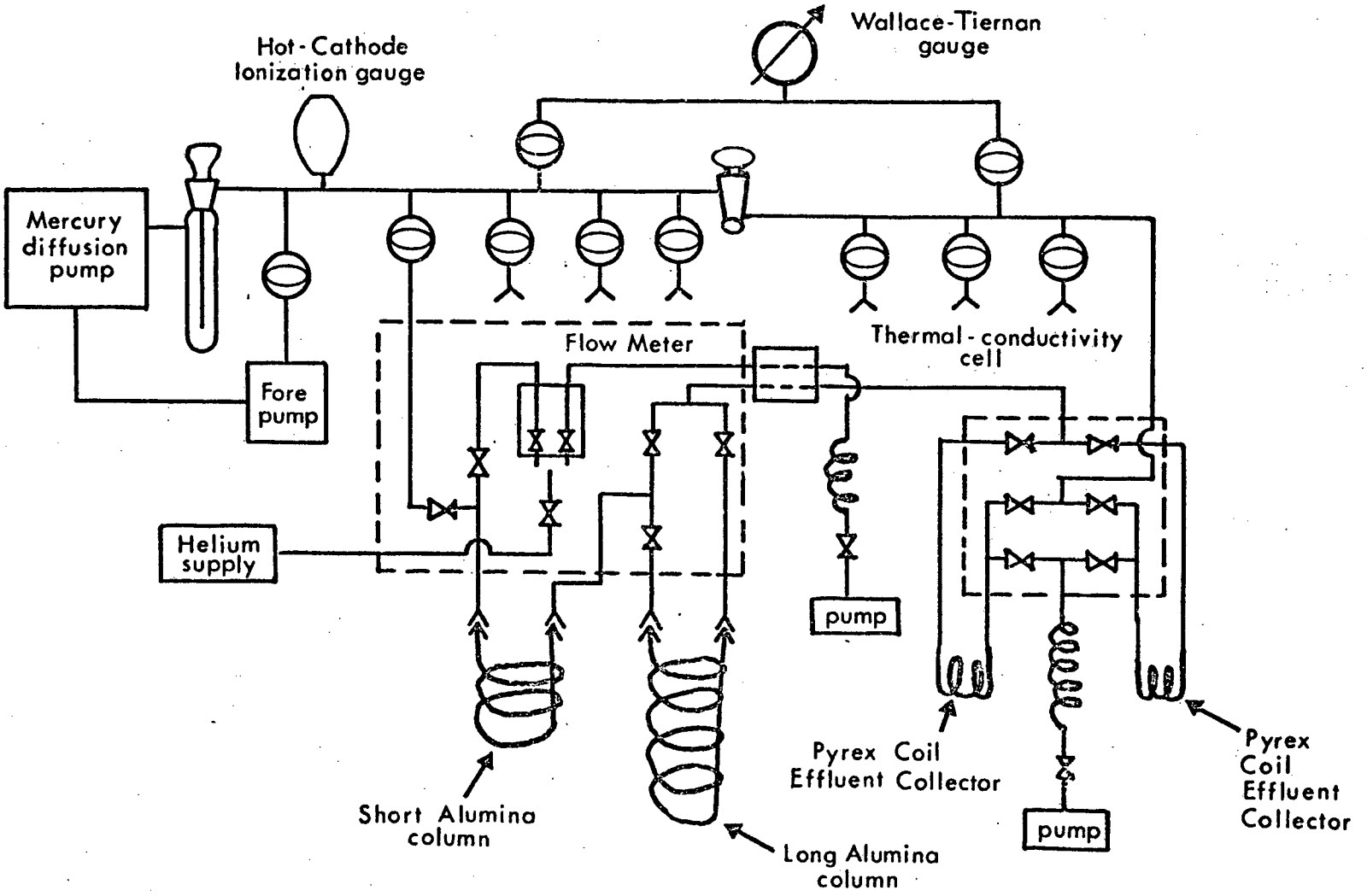

Figure 2. Preparative G/C for Freon-13 Purification.

use of a specially designed and constructed combustion train (Fig. 3). Freons, especially highly fluorinated ones, are chemically very stable. A combustion train, similar to that of McKenna, Priest and Staple[17], with some modifications suggested by Professor T.S. Ma of Brooklyn College, was fabricated in quartz.

A) Preparative gas-chromatograph

Approximately 30 ml of liquid $CClF_3$ were required for the distillation experiments. In order to facilitate the purification of this quantity of material a high-vacuum system which incorporates a gas-chromatograph was constructed. A schematic of the apparatus is shown in Fig. 3. It was found that this system was capable of processing about 1/30 of a mole of $CClF_3$ during any one chromatographic run.

The system may be thought of as consisting of four major parts. These are:

1) Support or service vacuum system

2) Chromatographic columns

3) Thermal conductivity sensor and

4) effluent collection system.

The service vacuum system is constructed of Pyrex glass. It is depicted as several horizontal lines at the top of Fig. 2. High vacuum of the order of 10^{-6} torr is maintained by an Eck and Krebs two stage mercury-diffusion pump. Vacuum readings are made using a Veeco Instrument's Hot-Cathode Ionization gauge and Ionization Gauge Controller. The manifold itself contains several ports each consisting of a high-vacuum stopcock and 10/30 standard taper joint. A Wallace-Tiernan

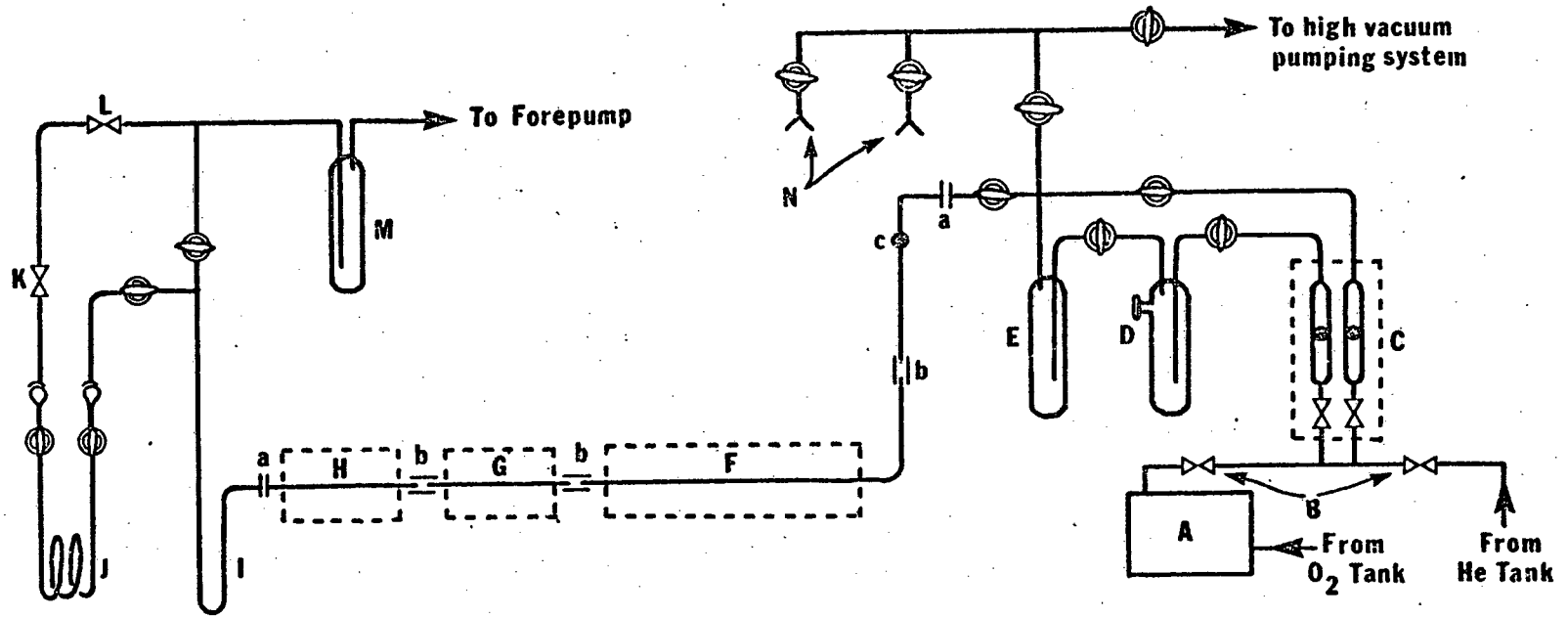

A; Oxygen-purification train
B; Shut-off valves
C; Twin rotometer with needle valves
D; Injection port with silicone rubber
E; Combustion-sample trap
F; Quartz tube with platinum gauze and crushed quartz
G; Pyrex tube with silver wool packing
H; Pyrex tube with NaF packing
I; U-Tube with silica gel packing
J; Removable coiled CO_2 trap
K; Metering value
L; Shut-off valve
M; LN_2-trap
N, Combustion sample inlet ports

a; silicone-rubber
O ring couplings
b; silicone-rubber
tubing connections
c; constriction

Figure 3. Combustion Train.

differential pressure gauge is mounted on the manifold to give pressure readings in the 0-800 torr range.

The chromatographic column assembly is constructed primarily of stainless-steel. It connects to the service manifold via a metal to glass seal. Incorporated in its construction is a dual flow meter-needle valve assembly, which allows setting of both column and reference helium flow rates. All valves on the chromatographic column assembly are Hoke Co.'s bellows sealed, Kel-F tipped valves. All connections (except those to flow-meter) are silver-soldered. Four stainless-steel 18/5 ball and socket joints allow easy attachment or replacement of chromatographic columns. According to design either both columns may be used in tandem, or the second column may be bypassed. The idea of tandem column operation is according to Bigeleisen[18].

Columns for the separation of Freons were prepared of Alumina. The first column is 2 meters long while the second is 6 meters long. Both are made of 3/8" O.D. soft copper tubing. They are equipped with 18/5 ball and socket joints for attachment to the main chromatographic assembly. The joint is sealed with Apeizon black wax sealant.

The thermal conductivity cell and controller were supplied by Gow-Mac. Output is recorded on a Leeds and Northrup Speedomax H recorder. The reference side of the cell is connected to a fore pump via a thin stainless-steel capillary.

The effluent collector system was designed in such a way as to avoid interruption of gas flow through the system while collecting fractions. It is constructed of stainless-steel tubing and Hoke Co.'s bellows sealed, Kel-F tipped valves. All joints are silver soldered. Connection to the two pyrex effluent collector coils is via Kovar seals. The

effluent collector assembly is connected to the service manifold via a Kover seal.

B) Distillation Column and Its Support System.

The low-temperature distillation column was originally designed by Bigeleisen and Ribnikar[19] at Brookhaven National Laboratory. It was applied for studies of vapor pressure isotope effect in N_2O at 184°K. Subsequently it was used in distillation studies of C_2H_3D and $^{12}CH_2=^{13}CH_2$ by Bigeleisen, Cragg and Jeevanandam[12] for their study of isotopic methanes. This well travelled column was transported from the University of Rochester along with its brass housing and service vacuum line. The column received at the outset of this work differed from the original in several alterations[12,17,20], which are described in these publications. It was found necessary to include further modifications and refinements for our work.

As a preliminary step the column was re-assembled in our laboratory in much the same configuration as most recently used[12]. The column was thoroughly cleaned before reassembly and the column packing, Podbelniak's Nichrome "Helipak" packing No. 2916 was cleaned using benzene in a Soxhlet extractor. The column was repacked with 76 grams of packing. All connections linking the column with its service vacuum line were reconstructed employing silver solder. The entire column and service line were leak tested using a highly sensitive (min. detectable leak - 5×10^{-11} atm cc/sec) helium leak detector (DuPont Instruments model 25-120B) and any necessary repairs were made. It was found that the service line and column were able to attain a vacuum of 10^{-5} torr, a rather good vacuum considering the capillaries involved and the large surface area of the packing.

Isotopic analysis of samples taken during the preliminary runs indicated that we were indeed observing the inverse isotope effect in the temperature region studied ($185^{o}K$ to $200^{o}K$). Analysis of the preliminary runs using the theory of K. Cohen proved impossible since we had not observed the transient behavior of the column. It was determined that

1) Sampling would have to begin as soon after charging of the column as possible.

2) Sampling rate would have to be increased to approximately 1 sample every 15 minutes during the first hours of a distillation and

3) That temperature stabilization of the column be improved.

The modification of the column involved dismantling of the original column assembly. The vacuum jacket of the column was cut open and the column stripped of all wiring and mirroring. A pyrex well was sealed on the upper shoulder of the boiler. A 100 ohm platinum resistance element, whose calibration is traceable to the National Bureau of Standards, was glued into the well to insure good thermal contact. The column wall and vacuum jacket were remirrored. The boiler was then rewired with a heating element of 180 ohms (at room temperature) resistance. Because of the increase in the number of electrical leads to be fed through the vacuum jacket a new uranium-glass electrical feed-through was glass blown onto the column assembly. Connection of the inner part of the feedthrough and the heater and platinum resistance element were made using teflon-coated copper wires. The vacuum jacket was then resealed. The column was repacked with 76 grams of Podbelniak Nichrome Heli-pak #2916 which had been cleaned in a Soxhlet extraction

with benzene for three days.

A differential capacitance gauge, Setra Systems Model 236, was installed on the boiler sampling line. This capacitance gauge has a full range of ± 1,000 torr differential pressure and a sensitivity of 0.1 torr. The electronics are self contained in the sensor head, and are capable of providing a 5 VDC output of sufficient power to drive a recorder with an input impedance of 5 kilo ohms. An auxiliary control box to provide a regulated input of 24 VDC and circuits for remote sensitivity, zeroing and calibration adjustments was constructed.

A thermocouple well, approximately 16 inches long, was fabricated from 1/16" O.D. stainless steel. The well was silver soldered onto the top of the column and extended into the condenser (see Fig. 4). An Iron-Constantan thermocouple was inserted into the open end of the well. This new modification allows monitoring of the condenser temperature, a capability not previously available.

The preliminary runs indicated that the cooling rate was more than had been observed by previous workers.

In an effort to locate the exact source of the problem a series of short experiments were performed and it was found that the cork insulation on the bell-shaped cover that surrounds the condenser was inadequate. To rectify this difficulty the column was modified by installing an annular vacuum jacket around the bell shaped cover that surrounds the condenser, so as to reduce the radial heat loss. The modification is shown in Fig. 4.

The column was then reassembled and is depicted in Figure 5.

The column service vacuum system (depicted in Figure 6) received

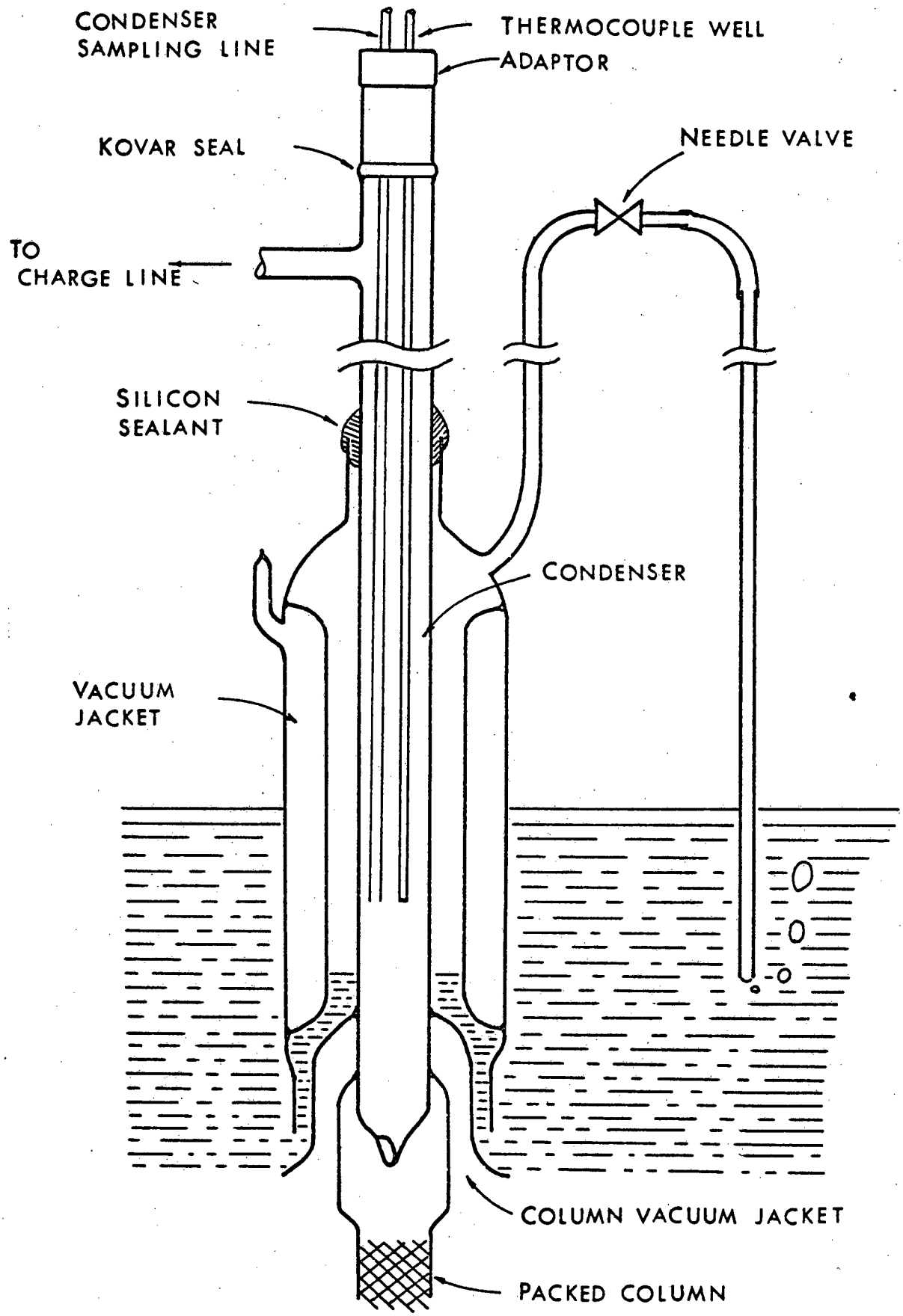

Figure 4. Modified Condenser

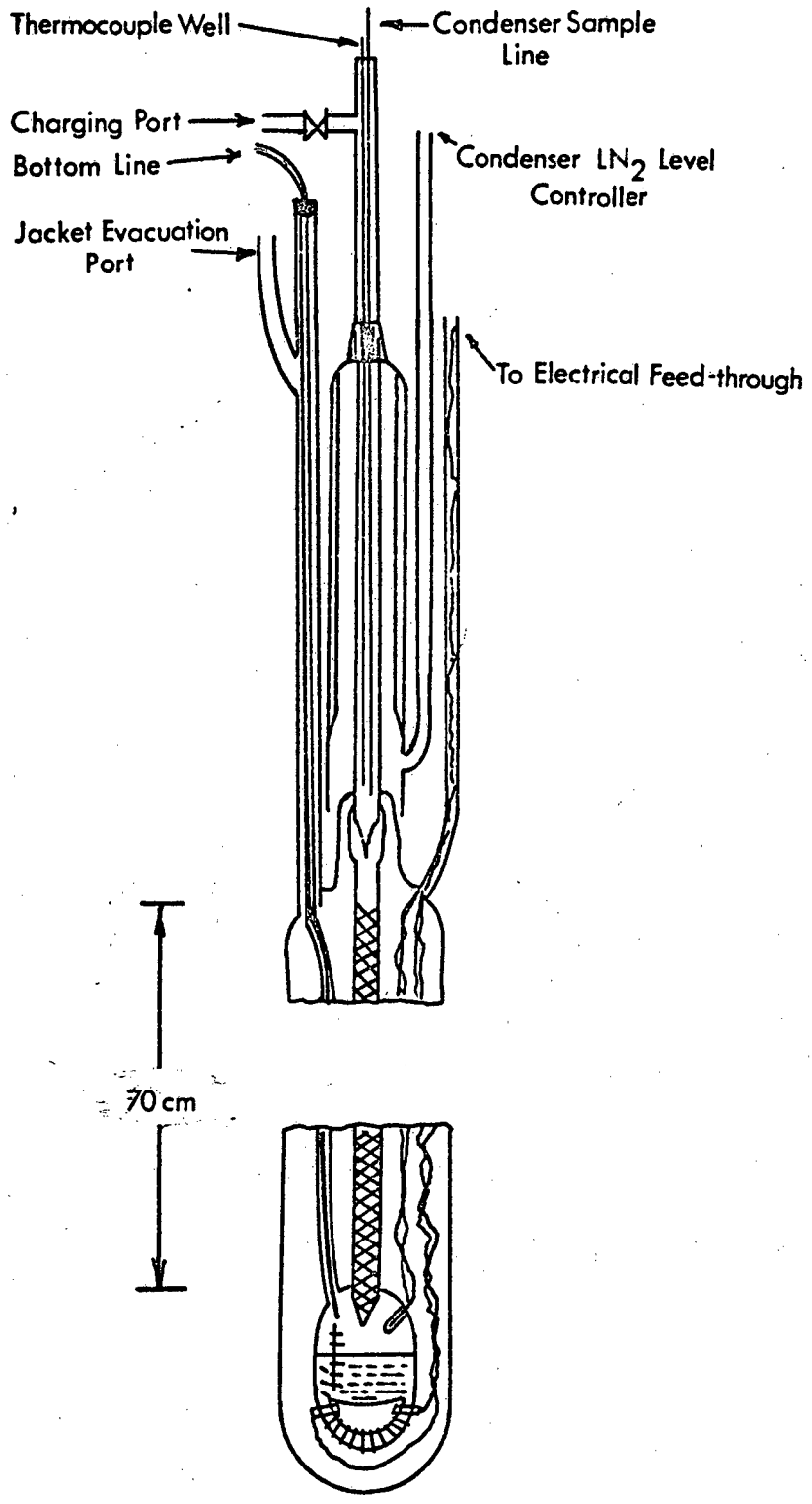

Figure 5. The Modified Cryogenic Distillation Column.

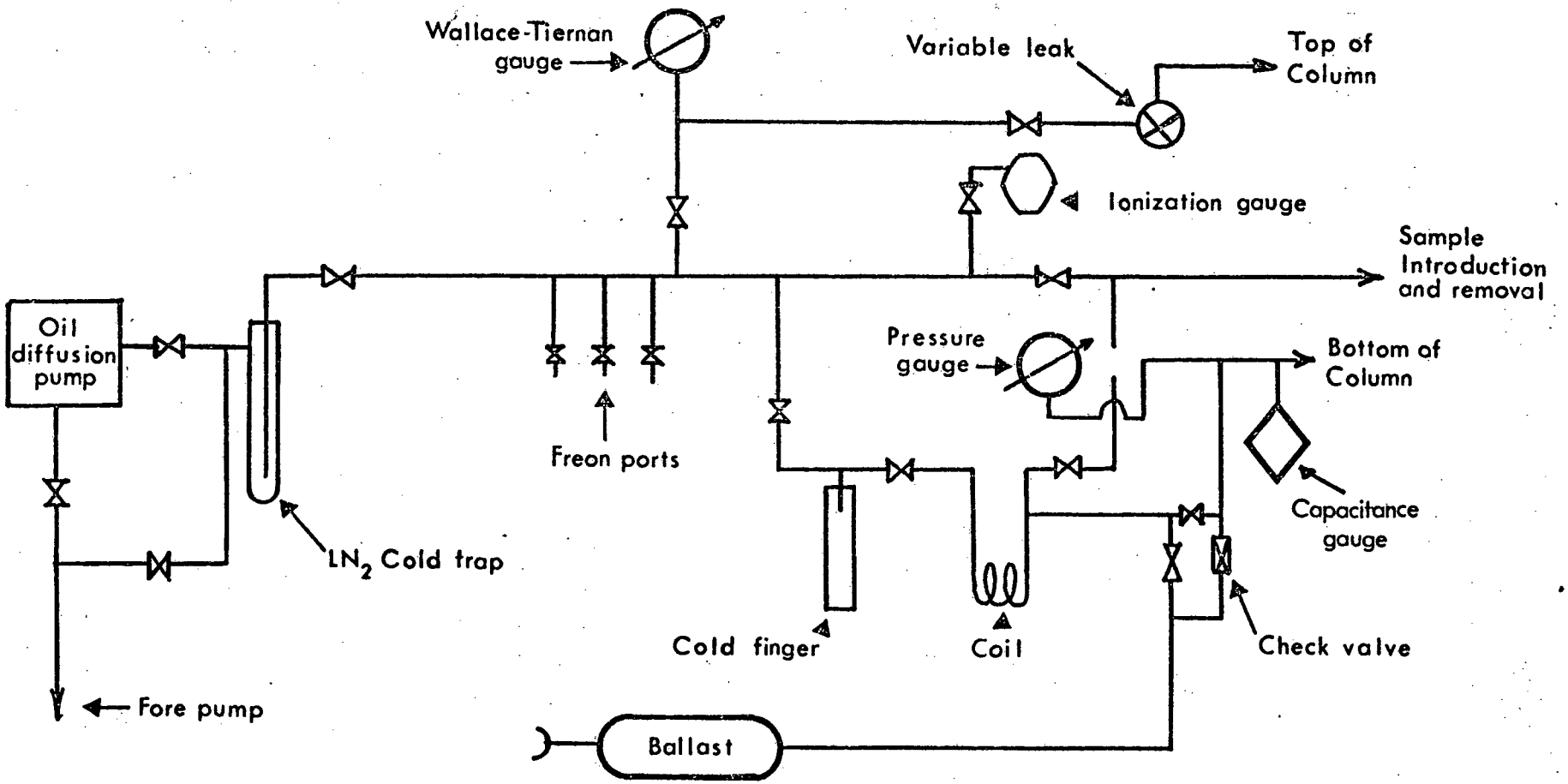

Figure 6. Vacuum System for Distillation Column.

little modification from its original state, except for the addition of the capacitance gauge on the boiler sampling line. The modification to the boiler is shown in Figure 7; the addition of the well allowed placement of the platinum resistance probe.

The liquid nitrogen level in the dewar surrounding the column's helium jacket was maintained using a Veeco Instruments Model VLN 30 Liquid Nitrogen Level Controller. The controller used with two sensor leads and a 3 way solenoid, comprise a system (see Figure 8) which can hold a liquid nitrogen level between two predetermined points. When the level of liquid nitrogen falls below the low sensor the three way solenoid is activated and a liquid nitrogen holding tank (Union Carbide's Model OC-50) is pressurized. The dewar is filled until the level reaches the high sensor. Upon achieving the required level the holding tank is vented to the atmosphere. A vacuum system to maintain a high vacuum in the Helium jacket of the column was fabricated primarily in stainless steel. The system, which is a one-inch vacuum pumping station, employs a Consolidated Vacuum Corporation Type VMF 21 oil diffusion pump and a Vacuum Instrument Corporations BT-20 liquid nitrogen bucket cold trap. The configuration of the system is shown in Figure 9. The valves are Veeco Instruments bellows sealed valves. Vacuum readings are obtained using a Model TG-7 thermocouple gauge in conjunction with a Model RG-81 Ionization Gauge Controller and Model RG-75 Ionization Gauge Tube, manufactured by Veeco Instruments Inc.

C) Combustion Train

The isotopic analysis of the $^{13}C/^{12}C$ ratio is most easily performed on samples of carbon dioxide. We therefore needed to develop a process

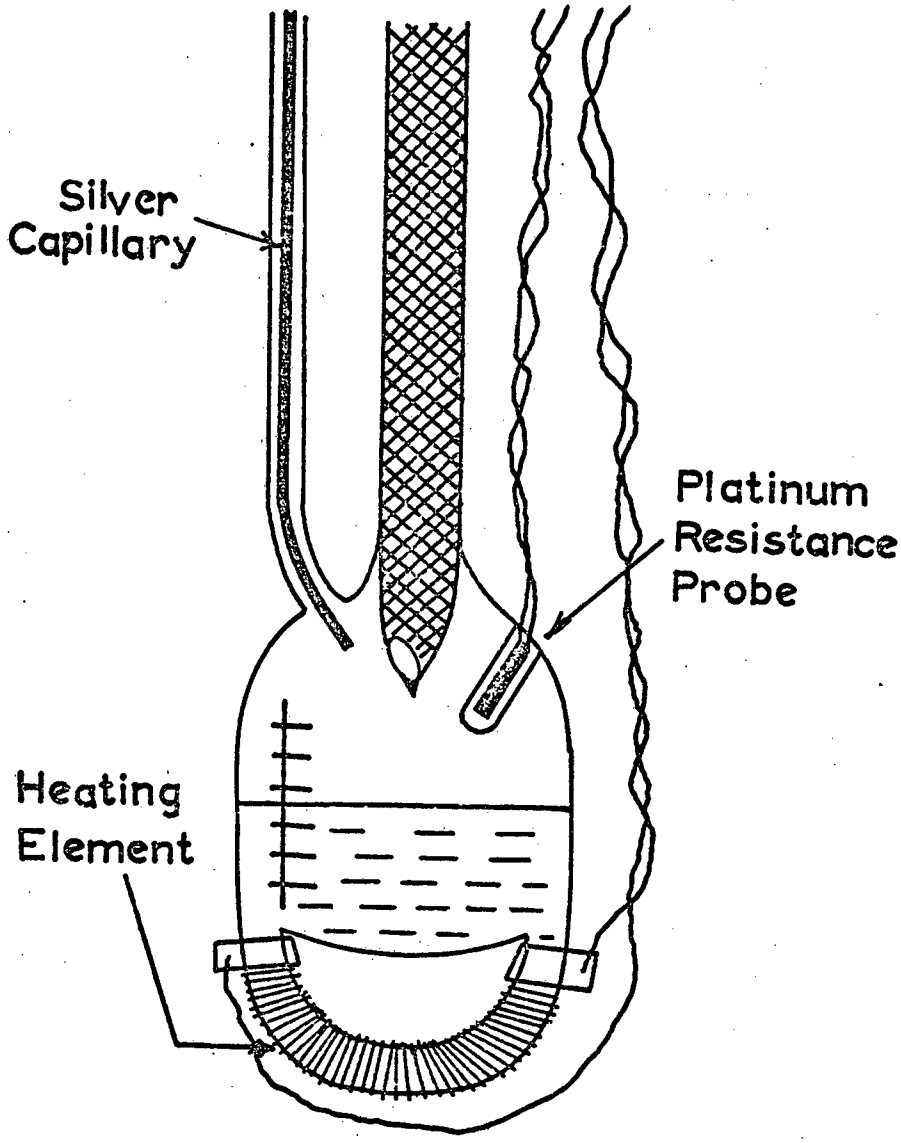

Figure 7. Modified Boiler

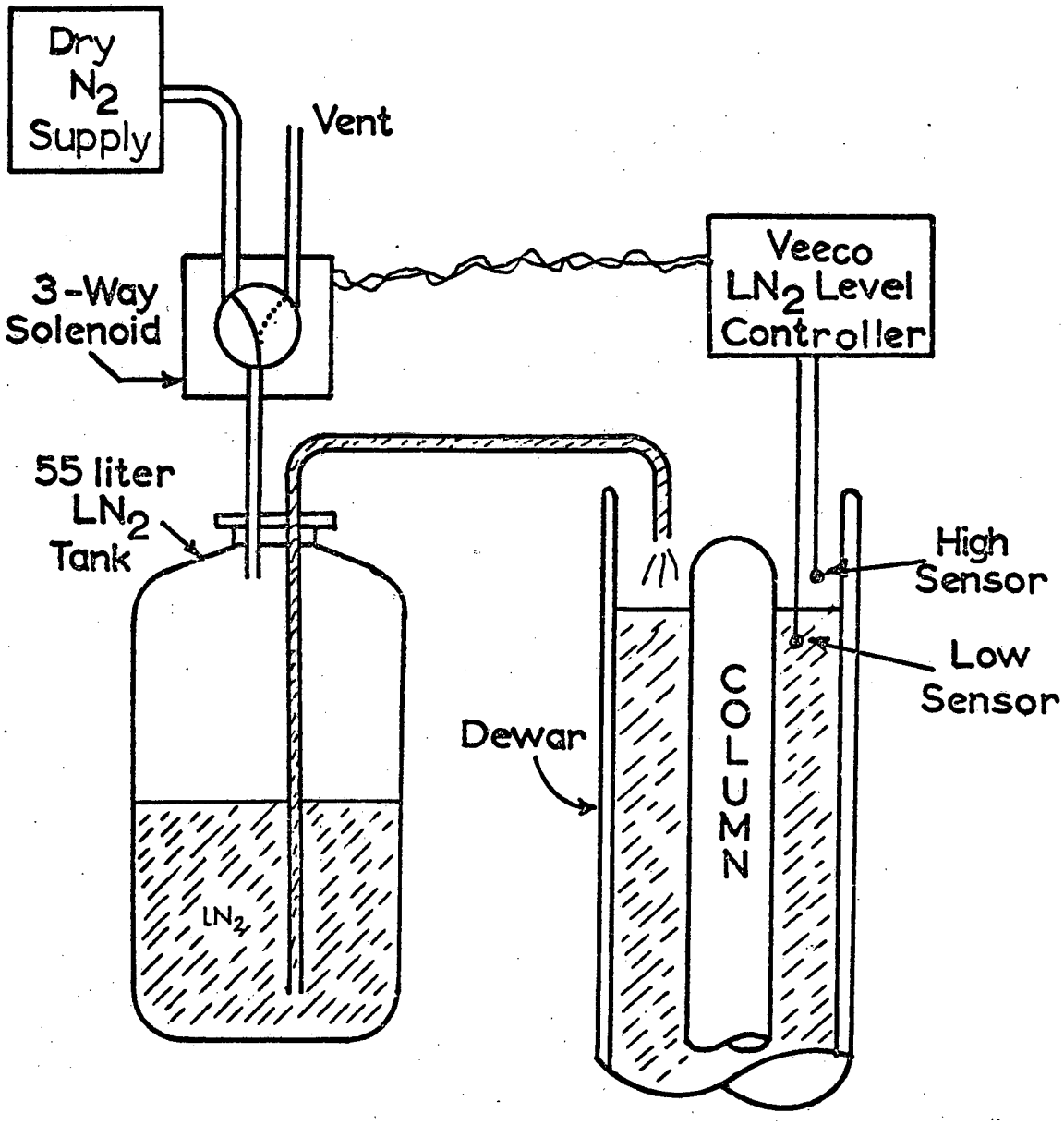

Figure 8. LN_2-Level Control for Distillation Dewar.

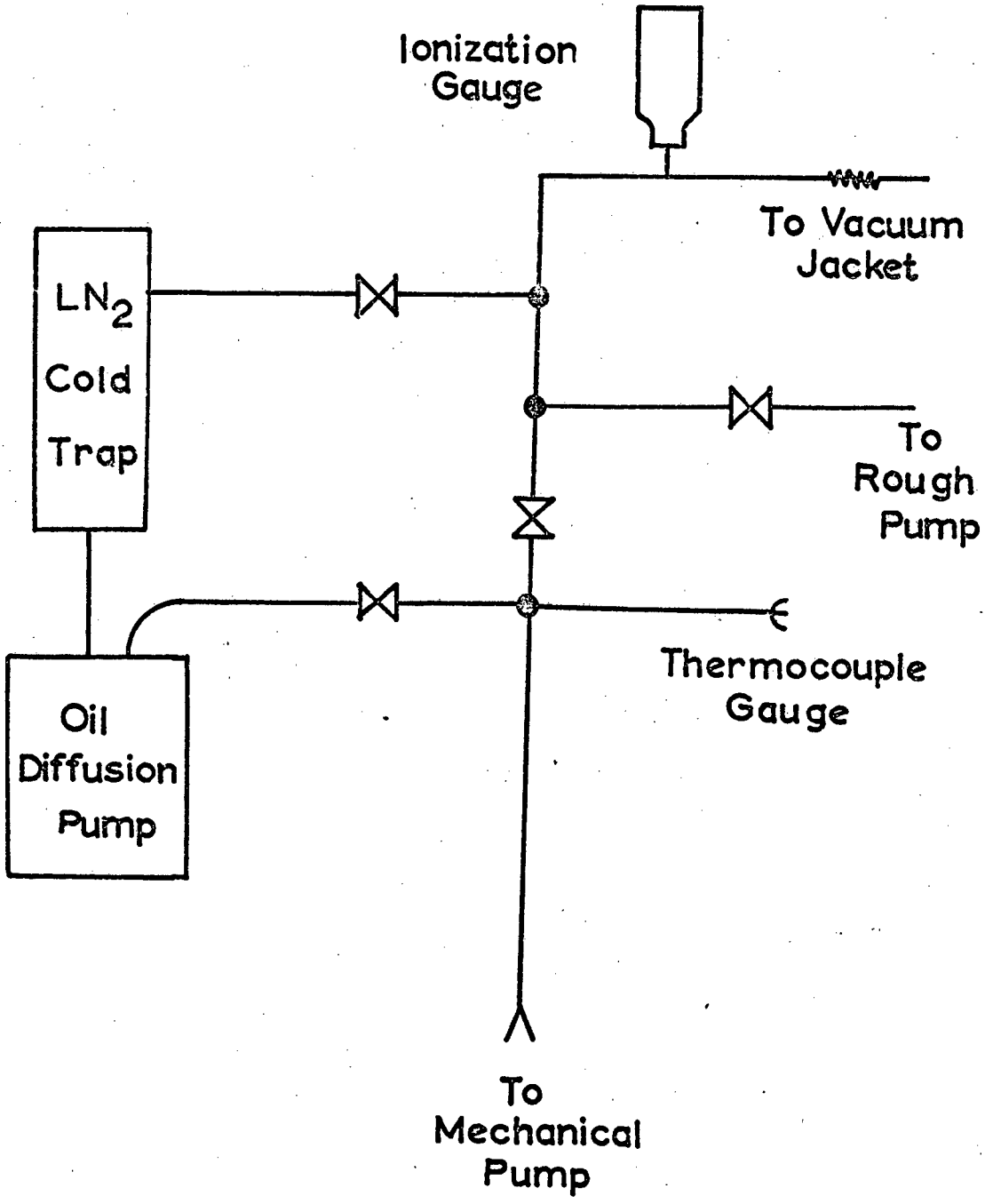

Figure 9. Vacuum System for the Vacuum Jacket.

for the oxidation of $CClF_3$ with sufficiently high yield so as to make a correction for $^{13}C/^{12}C$ isotope effect unnecessary. It was decided that a 95% conversion of $CClF_3$ to CO_2 would limit the error due to possible carbon isotope fractionation during the chemical conversion to a maximum of -0.05%, an error we found acceptable.

The train consists of three sections (see Figure 3). The first section is a 55 centimeters long quartz tube, 10 mm in outside diameter. The tube is packed alternately with platinum gauze and crushed quartz. It is heated by two Lindberg-Hevi Duty ovens. The ovens are capable of maintaining temperatures of 1200°C. to within $\pm$ 5°C of an average value. This section of the train is maintained at approximately 1050°C, at which temperature $CClF_3$ is decomposed to CO_2, fluorine (which is converted to SiF_4), and inorganic chlorine(which passes through this section). The second section of the train is a 10 mm O.D. pyrex tube which is packed with silver wool. This 20 cm length of tubing is maintained at 300° $\pm$ 5°C by an oven home-fabricated specifically for this use. The silver wool section is used to remove inorganic chlorine products of combustion. The final section is a pyrex U-tube filled with silica gel, built in to remove moisture, the presence of which Prof. Ma had suggested would catalize the combustion. After preliminary investigations it was deemed unnecessary to inject any moisture into the system when the combustion temperature is above 1000°C.

Oxygen used in the train is obtained from a tank and purified by passing the stream through a concentrated H_2SO_4 bubble tower, a Drierite absorption tube, and finally an Ascarite absorption tube. After leaving the purifier the stream is divided into two legs. One passes through the sample inlet area, thereby driving the sample into the oven, the other leg bypasses this area and floods the oven with oxygen.

The combustion product, CO_2, thus obtained contained a small amount (usually less than one percent) of uncombusted freon plus traces (less than 0.05%) of yet undetermined impurities. The carbon dioxide samples were then purified by processing them through a home-made gas-chromatograph. A schematic flow diagram is shown in Figure 10. A description follows.

The preparative gas chromatograph consists of 5 primary areas. These are, the carrier gas system, the sample introduction system, the chromatographic columns, the detecting system and the collection system.

The carrier gas, helium, is taken from the tank and passed through a drying tube to remove moisture. The gas line is then split and each of the resulting lines is passed through one of a pair of matched needle-valves. One of the metered lines runs directly to the reference chromatographic column while the other passes along to the sample introduction system.

The sample introduction system works in either of two modes. A sample may be introduced through a septum port using a syringe or the sample may be introduced from a stainless steel crude sample holder, which can be evacuated. When the sample holder is used provisions have been made for purging any air trapped in the holder connectors.

The chromatographic columns are contained in their own insulated oven. The temperature of the oven may be regulated from room temperature to 350°C. Presently the system is being used at 300°C. The present columns are approximately 6' in length and a quarter inch in diameter. They contain alumina. The columns are easily replaced due to the use of Swagelok bulkhead fittings.

The detecting system consists of a Gow Mac thermistor thermal-

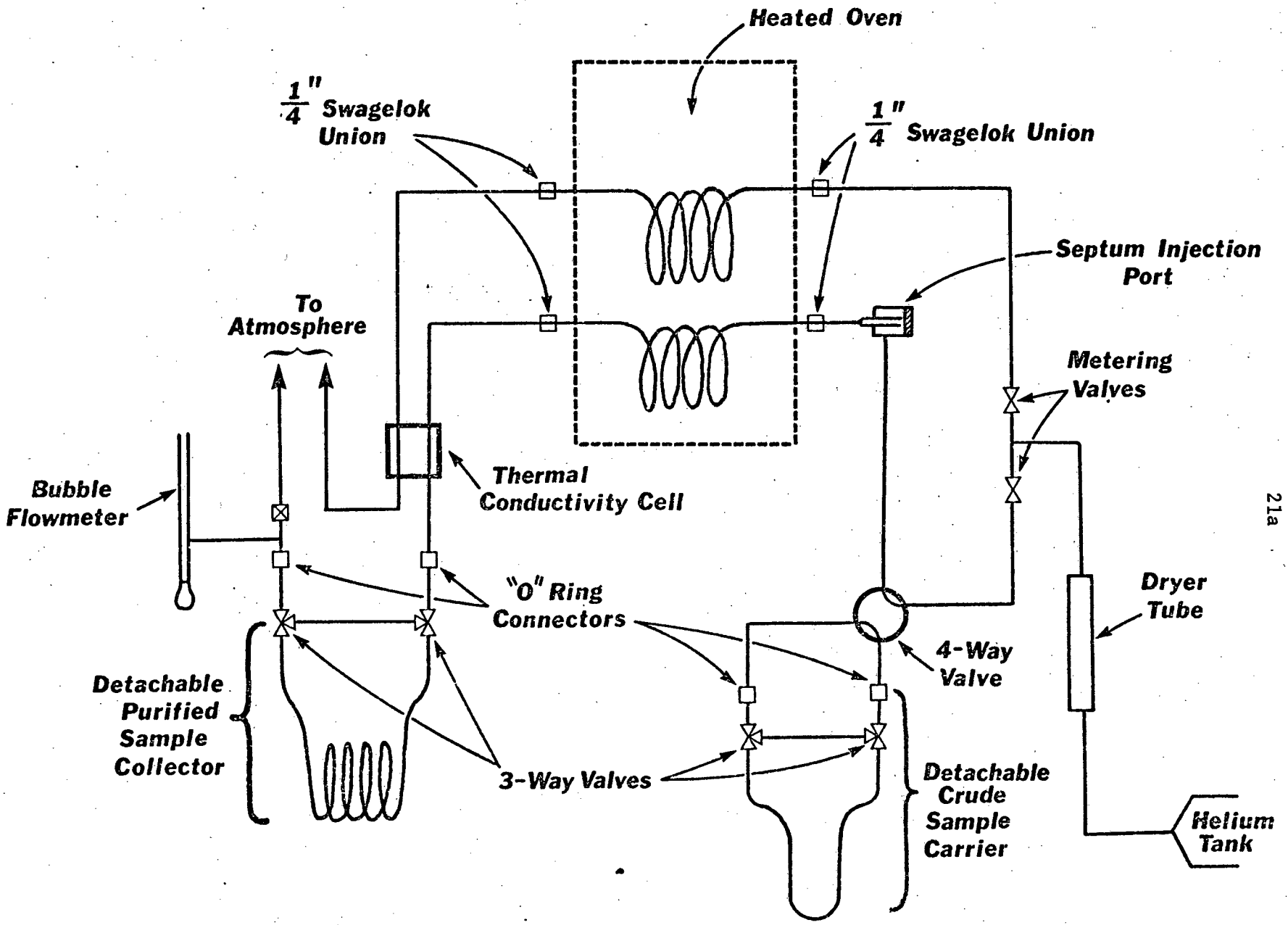

Figure 10. Preparative G/C for Carbon Dioxide

conductivity cell, and a Gow Mac power supply control unit. This combination allows for the switching of attenuation and polarity, adjustment of offset voltage and delivers a constant current. The peaks are recorded on a standard chart recorder.

The collection system is primarily another detachable stainless steel holder. The use of 3 way valves allows the operator of the chromatograph to either allow the effluent to pass to the atmosphere or it may be directed through the holder. The holder is immersed in liquid nitrogen. The CO_2 passing through the holder is readily deposited on its walls. After the product has been collected the coils are kept immersed in the liquid nitrogen while the holder is connected to a vacuum system. After the non-condensible helium in the holder has been evacuated the coils are allowed to heat up and the product is transferred to a glass sample holder for analysis.

Initially, standard freon samples were combusted and purified and these samples were analysed chromatographically both before and after combustion. Results were compared with data concerning the elution times of various freons (see Section II-3-A).

II-2. Precision Measurement of the Vapor Pressure of $CClF_3$

It was found that published data[21] on the vapor pressure of $CClF_3$ were inconsistent. In addition there was no assurance of the accuracy of the temperatures reported by various investigators. It was decided that

a consistent set of vapor pressure data be assembled. To this end samples of $CClF_3$ were chromatographically purified (see section II-3-A). All impurities in the sample were less than 1 ppm.

The manometry was accomplished in a cryostated differential manometer in the laboratory of Prof. Jacob Bigeleisen at the University of Rochester. The cryostat[22] is capable of setting and maintaining cryogenic temperatures to within $\pm$ 0.001°C for several hours. The differential manometry is accomplished by the use of differential capacitance gauges, which are capable of measuring differences of up to 50 torr to $\pm$ 0.1 millitorr. The vapor phase volume in the cryostated sample holder-manometer system is negligible as compared to the amount of liquid in the sample holder. The absolute pressure of the $CClF_3$ was measured to within $\pm$ 1 millitorr by use of a Texas Instruments quartz spiral gauge. Vapor pressure data was obtained from 139.3°K to 191.7°K. The results were fitted by the method of least squares to a four term equation: For $CClF_3$ this equation was:

$$\log_{10}P \text{ (torr)} = \frac{-631.075}{T(^{\circ}K)} + 2.85930 + 0.028664T - 0.000059338T^2 \quad (16)$$

The single largest deviation in Equation 16 from an experimental point is 0.006 out of 1.552 in $\log_{10}P$. The results are plotted in Figure 11.

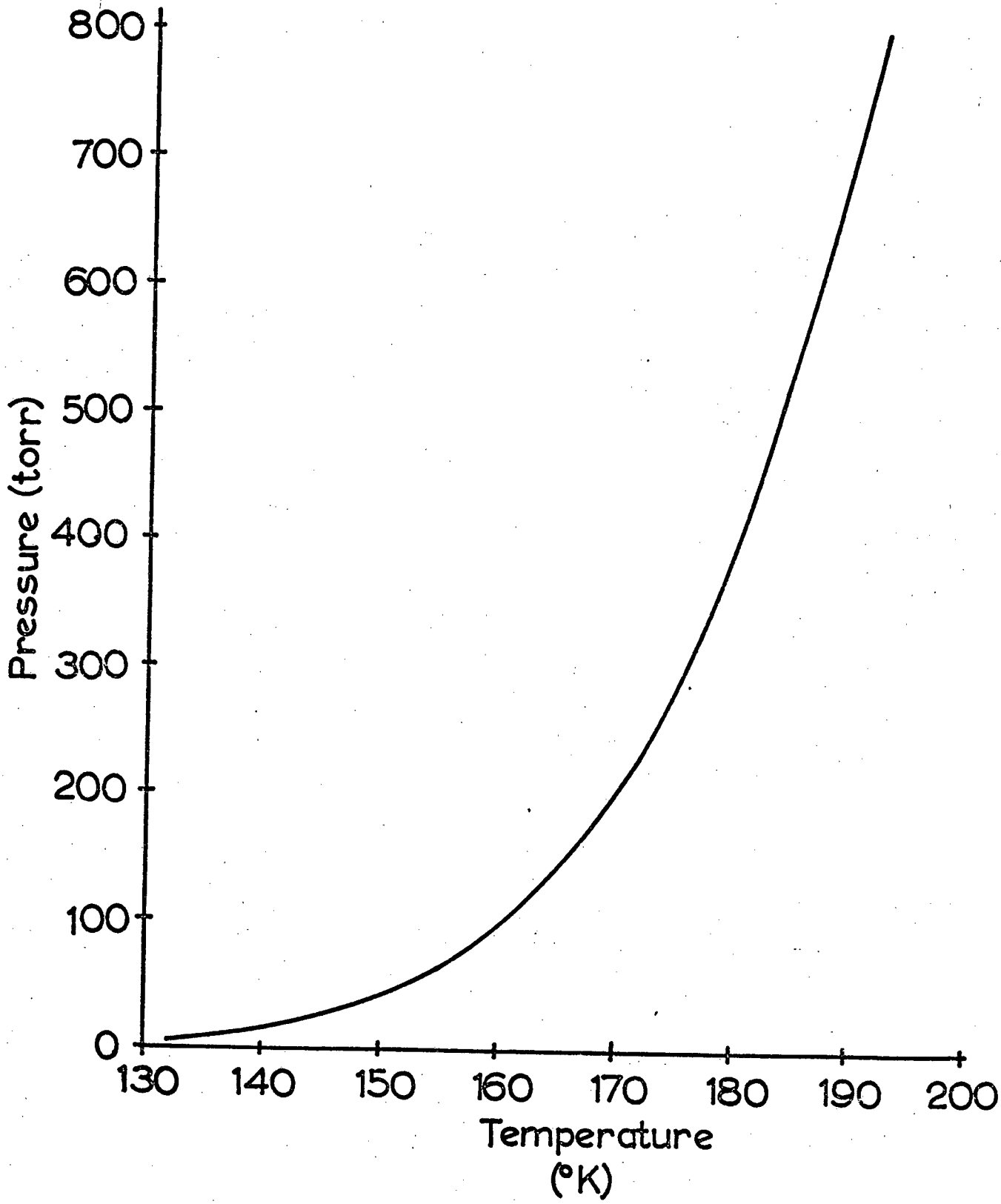

Figure 11. Vapor Pressure Data for Freon-13.

II-3. Experimental Procedure

A. Purification of $CClF_3$

Using the preparative gas chromatograph described in section II-1-A twenty purification runs were performed on 1/30 of a mole aliquots of $CClF_3$ supplied by Matheson Gas Products. Each run consisted of three primary parts. Part one was the introduction of the sample. Part two consisted of the elution of the freon and the division of the effluent into "cuts". Finally each cut was analysed for impurities and combined with other cuts of similar purity.

The chromatographic column was charged with the $CClF_3$ in the following manner. The short coil of the chromatographic column (see Figure 2) was immersed in liquid nitrogen. As soon as it was sufficiently cold the sample of $CClF_3$ was introduced from the vacuum line. The pressure of the sample in this vacuum line was recorded before introduction, and provides a measure of the amount of $CClF_3$ used, since the line's volume was known. As soon as the $CClF_3$ sample was frozen into the beginning of the short alumina column the liquid nitrogen was replaced with an ice bath. The short alumina column was maintained at ice bath temperature throughout the run whereas the long column was kept at room temperature. Helium carrier gas flow was maintained constant throughout the run.

The thermalconductivity detector indicated the small impurity peaks which preceeded the main $CClF_3$ peak and the start of the main peak. The dual pyrex coil effluent collector system allowed one coil to be used for collection while the other coil was emptied of a previous fraction. The fractions were taken with respect to time and the amount of material visible in the collector. The elution times for different fractions

varied from 15 to 60 minutes. Each fraction was stored in a separate high vacuum bulb to be analysed.

In order to combine the cuts of the product of the chromatographic runs into a sample of sufficiently high purity it was necessary to 1) qualitatively identify all the impurities and 2) to quantitatively determine each impurity using the Perkin-Elmer gas chromatograph.

The $CClF_3$ supplied by Matheson Gas Products had a minimum purity of 99.0% (mol) the impurities are other halocarbons and air. Retention times were obtained using a 6' x 1/8" O.D. stainless steel column filled with 5.7 grams of Al_2O_3 (Fisher A-540), at 150°C with a helium flow rate of 3.5 cc/sec for CCl_3F (Freon-11), CCl_2F_2 (Freon-12), $CClF_3$ (Freon-13) and CF_4 (Freon-14) using the flame ionization detector. The retention times relative to CF_4 are given in Table II. The chromatograph of the $CClF_3$ showed the presence of two impurities, CCl_2F_2 and CF_4.

The impurities were quantitatively determined. Running chromatographs of samples of known composition established the sensitivity of the flame ionization detector towards the various Freons. These relative sensitivities are shown in Table II. for Freon 12, 13 and 14.

TABLE II

	Relative Sensitivity With Respect to: Freon 12	Freon 13	Freon 14	Relative Retention Time
Freon-12	1	2.23	412	3.1
Freon-13	0.43	1	177	1.5
Freon-14	0.00243	0.00566	1	1.0

After analysis all fractions whose level for any impurity was less than 10^{-6} were combined and stored as material to be used in the distillation.

B. Distillation

The following paragraphs will outline the preparation for, and execution of a distillation run on the Biegeleisen column.

Approximately two days prior to a distillation run all diffusion pumps (on the service line and on the helium jacket line) are started up and liquid nitrogen traps filled. Up to this point the vacuum lines have been kept under rough vacuum. On the night before the distillation the UC-55 liquid nitrogen holding tank is filled to capacity. The aging of this liquid nitrogen was found to be necessary due to the fact that the liquid nitrogen is shipped at higher pressure than is maintained in our tanks, therefore time must be allowed for it to come to thermal equilibrium in its new environment. With these things accomplished the column is left on automatic until the morning of the distillation.

On the morning of the distillation certain preparations are made, these include preparation of the $CClF_3$ sample and cooling of the distillation column. In order to prepare the sample for introduction to the column it is first frozen (using liquid nitrogen) into the cold finger shown in Figure 6. As soon as approximately 1/4 mole (which includes an excess over the amount actually needed for the distillation) of $CClF_3$ is frozen into the cold finger, the liquid nitrogen is removed and replaced with a dry ice-acetone slurry. This maintains the pressure in the cold finger (which is isolated by closing the two adjacent valves at approximately one atmosphere. It was found that the closer everything involved in the distillation could be kept to the actual

distillation temperature, the more smoothly things ran. At this point the LN_2 level controller for the dewar surrounding the helium jacket was turned on to automatic and was filled. Temperature within the boiler was monitored and as it approached the target temperature for the distillation the next phase of the distillation procedure, the charging of the column, was started.

From its construction, it can be seen that in the absence of conducting gas within the vacuum jacket the packed section of the column is cooled by the liquid nitrogen by conduction (from near the condenser area). It follows, thereby, that a temperature gradient is established as the column is cooled, with the boiler area being the warmest area, the condenser area the coldest. In order to charge and wet the column packing properly, this gradient was employed. It allowed the charge of $CClF_3$ to freeze and liquify on the packing rather than condense into the boiler. The charging procedure is given in the next paragraph.

In a very loose sense of the word one can look at this charging procedure as isothermal. As soon as the temperature probe in the boiler was at the proper temperature (that temperature selected for this particular run) the valve on the column side of the cold finger and the needle valve leading to the top of the column were opened. As the $CClF_3$ entered the column it either froze or condensed on the coldest section of the column (that near the condenser). As additional $CClF_3$ entered the column it warmed the area it was condensing on and this "wet area" can be thought of as having moved down the column towards the boiler, i.e., the column was warmed to a uniform temperature. During this time the amount of $CClF_3$ entering the column was adjusted using the needle valve in order to keep the indication of temperature (pressure and probe

readings) constant. As the gradient was destroyed by the entering $CClF_3$ the boiler starts to fill with the charge and as soon as the level was approximately 1/8" to 1/4" below the tip of the packed section the column was sealed and the heater current started. This is the start of the reflux and was time zero for our own time measurement. At this point the pressure is already stabilized and the column practically is at equilibrium due to the "isothermal" charging. Pressure throughout the charging was recorded using the output of the Setra Systems capacitance gauge. At this point the sampling phase began.

Sampling of the condenser begins as soon as possible after time zero, usually 10 to 15 minutes. Samples are withdrawn from the top through a variable leak into a small manifold of known volume (ca. 75 ml) and whose pressure can be read by use of a Wallace-Tiernan pressure gauge. Approximately 5×10^{-3} moles of $CClF_3$ are withdrawn for each sample. A sample was usually withdrawn over a period of approximately three to five minutes. In order to see the build up of the isotopic gradient samples were taken every 15 minutes for an hour, then every 20 minutes for an hour, every half hour for an hour and then hourly up to approximately 6 hours after time zero. Pressure and temperature measurements were noted during the extraction of each sample.

Samples of the boiler were taken at least twice each run. The sample was taken by filling the service manifold with sample withdrawn from the boiler through the capillary leading to the boiler.

All samples were stored in 60 ml high vacuum glass gas sample holders manufactured by Eck and Krebs Scientific Glassware.

All samples were now ready for combustion, which is outlined in the next section.

In order to apply the theory of K. Cohen to the kinetics of the distillation it is necessary to determine the amount of $CClF_3$ held up in the column. The procedure developed to determine this holdup is essentially a two stage shut-down of the column. After the last samples are removed from the column during regular operation, the line connecting the boiler to the service vacuum line is opened in order to allow the $CClF_3$ in the boiler to be distilled out. The heater current is increased to compensate for this loss of material, thereby maintaining pressure in the column at the same constant level. As soon as the boiler is emptied the column is sealed and the heater current is shut off. The liquid nitrogen level controller maintaining the level in the dewar surrounding the column is shut off and the liquid nitrogen is allowed to boil off. After the dewar is emptied the column heater is turned on again and all the material in the column is collected in a high vacuum stainless steel weighing vessel. The vessel is weighed, its empty weight of 126.02 grams subtracted and thereby the amount of $CClF_3$ held up in the column is known.

The holdup in the condenser was determined in a separate series of experiments. The manifold of known volume leading to the column was filled with a known pressure of $CClF_3$. The charge was allowed to slowly enter the column until the first drop appeared at the condenser tip. The remaining pressure in the manifold was then noted. By applying the ideal gas laws the amount of $CClF_3$ that entered the condenser before the first drop was observed was obtained, and this amount was considered to be equal to the condenser holdup.

C. Combustion and Purification.

In order to facilitate isotopic analysis the $CClF_3$ samples taken from the column were combusted to carbon dioxide. After combustion the resulting carbon dioxide was purified by gas chromatography in order to remove any substance which might be harmful to the mass spectrometer used for the analysis. The following paragraphs give the procedure used in combusting and purifying the samples. The apparatus used are shown in Figures 2 and 10 and are described in sections II-1-A and II-1-B.

Each sample was transferred from its holder into a manifold of known volume, and its pressure was measured using a Wallace Tiernan pressure gauge. The sample was now transferred to the combustion sample trap by freezing the sample into the trap at liquid nitrogen temperature. Oxygen was allowed to flow through the oven for 5 minutes using the bypass stopcock. At this point the liquid nitrogen was removed from around the combustion-sample trap and oxygen was allowed to flow both through the bypass and to sweep through the sample trap for ten minutes. At the end of the ten minute period the oxygen flow was halted and five minutes of pump down time were allowed, followed by two minutes of Helium flow to remove any traces of sample from the system. Another ten minute pump-down period was allowed at this point. In all cases the flow rate of gases entering the ovens was .05 liters/min. The sample was clearly visible at this time in the collector coils. The sample was now removed and its pressure in a known volume recorded. This was compared to its precombustion value. The sample was now ready for purification.

At this point the sample was transferred to the inlet side of the purification gas chromatograph. Using a flow rate of 20 cc/min. at 300°C and an alumina column the carbon dioxide was purified. Elution of

impurity peaks followed and these fractions were discarded. At the appearance of carbon dioxide the valves were switched to allow collection of the sample. The sample pressure was now measured in a known volume. This sample was now ready for isotopic analysis.

D. Mass-Spectrometry.

Isotopic analysis was carried out on each sample on a Consolidated Engineering Corporation's Model 21-201 Mass Spectrometer. The model 21-201 is of the Nier type of construction. The feature which makes this particular model very attractive for isotopic analysis is the fact that it is a dual collector instrument (see figure 12). In this mass spectrometer gas molecules enter at low pressure (approx. 10^{-6} torr), are ionized, accelerated into a magnetic field. In the magnetic field all these particles follow paths which are arcs of circles with heavier particles traveling paths with a larger radius than lighter particles. After passing through the magnetic field each mass (or more correctly mass/charge) is focused at a different point. The model 21-201's dual collector allows the beam impinging on one of its collectors to be compared with the beam falling on its other collector. This allows simultaneous recording of the number of ions hitting each collector.

A model 201-21 was generously made available at Brookhaven National Laboratory in the laboratory of Dr. L. Friedman.

Prior to each isotopic analysis a standard carbon-dioxide sample was introduced into the inlet system. With the ion accelerating voltage set at 1200 volts the magnetic field was scanned and recorded using the number two collector (narrow slit). Upon detecting the mass 44 and 45 peaks the field was varied to place

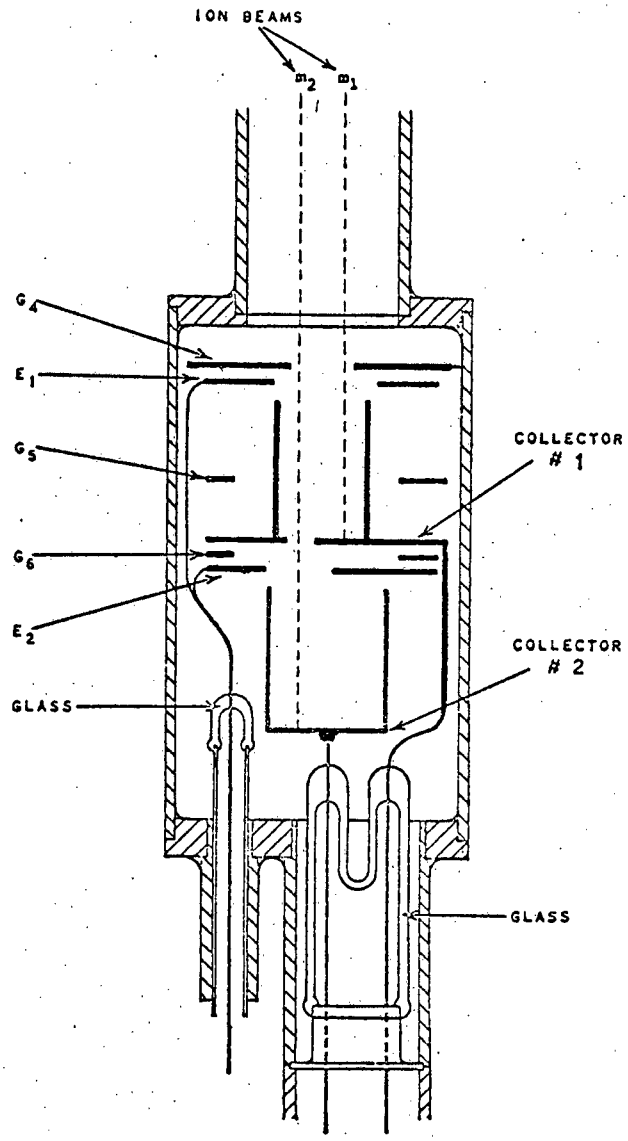

Figure 12. Dual Collector used in the Model 21-201 Mass Spectrometer.

Ion beams enter from top. The higher mass m_1 reaches Collector #2. The lower mass impinges on Collector #1. (Each collector has a box-like shield.) G_5 and G_6 are grounded shields to prevent electrical leakage between E_1 or E_2 and Collector #1. E_1 and E_2 operate at -45 volts with respect to ground and act as suppressors of secondary electrons released by ion bombardment from the collectors. Their slits are large enough so that they intercept no ions.

the 45 peak on the number two collector. The peak was placed directly on the collector by using the ion accelerating voltage as a fine adjust. With mass 45 on the number two collector the number one collector collected masses 42.6 to 46.5. In order to get more accurate data all samples were run at constant pressure. Amplifiers were zeroed and checked periodically throughout each session. Adequate time was allowed for pump out in order to avoid memory of previous samples.

III. DATA REDUCTION.

Cohen's theory[11] of transient kinetics of a square cascade was applied to the data from the mass-spectrometric analysis of the samples from the condenser and boiler in order to determine the relative vapor pressures of the isotopic species. A modification of the theory of long-time kinetics was developed, and a paper describing the results of this modification is pending publication in the proceedings of the International Conference on the Chemistry and Physics of Stable Isotopes, which was held in Romania in 1973. A preprint of this paper is attached as an appendix of this thesis. The modified theory was used to map the kinetics parameters, A and B, in the ranges of overall separation and relative, condenser to column, holdups needed for the reduction of the present data. The following section, Section III-1, contains an outline of the modified Cohen's theory of long-time kinetics. Section III-2 will then outline a method of application of Cohen's theory to the present problem, and Section III-3 will contain a complete set of sample calculations pertaining to one particular run.

III-1. Cohen's Theory.

The transient behavior of a square, counter-current, cascade of close-separation stages during start-up period was theoretically analyzed by K. Cohen[11] in relation to the fractionation of uranium-235. A consideration of the material balance of desired substance between the product stage and the s-th stage under conditions of constant flows leads[11] to a partial differential equation:

$$\lambda \frac{\partial N}{\partial t} = \frac{\partial^2 N}{\partial s^2} - \epsilon \frac{\partial}{\partial s}\left[\Psi N + N (1 - N) \right] \qquad (17)$$

where $N = N(s,t)$ is the average mole fraction of the desired substance in the input streams for the s-th stage (cf: Figure 13), counted toward the product end starting from the feed point in the cascade, at time t from the start-up of the cascade. Other quantities used in Eqn. (17), all being dimensionless, are:

$\epsilon = \alpha - 1$, where α is the "head-to-tail" separation factor. This use of α is different from Cohen's, in that the latter is the "head" or "tail" separation factor. This α is twice Cohen's α [12,19,20,23]

$\lambda = 2h$, where h is the holdup per stage per unit flow, or the average process time per stage.

$\Psi = \frac{2P}{\epsilon L}$, where P is the production rate, or the rate of withdrawal of product at the product-end of the column, and L is the total interstage flow rate at the stage s. In a square distillation cascade under total reflux, L is also equal to twice the boil-up rate.

When the mole fraction of the desired substance is negligibly small compared to unity, Eqn. (17) becomes linear:

$$\lambda \frac{\partial N}{\partial t} = \frac{\partial^2 N}{\partial s^2} - \epsilon (1 + \Psi) \frac{\partial N}{\partial s} \qquad (18)$$

This would be the case in preliminary fractionation processes of isotopes, such as ^{235}U, D, ^{13}C and ^{15}N. Cohen solved the equation under the following initial and boundary conditions:

At $t = 0$; $N(s, t = 0) = N_o$ at all s

At $s = 0$ (feed point); $N(0,t) = N_o$ at all t

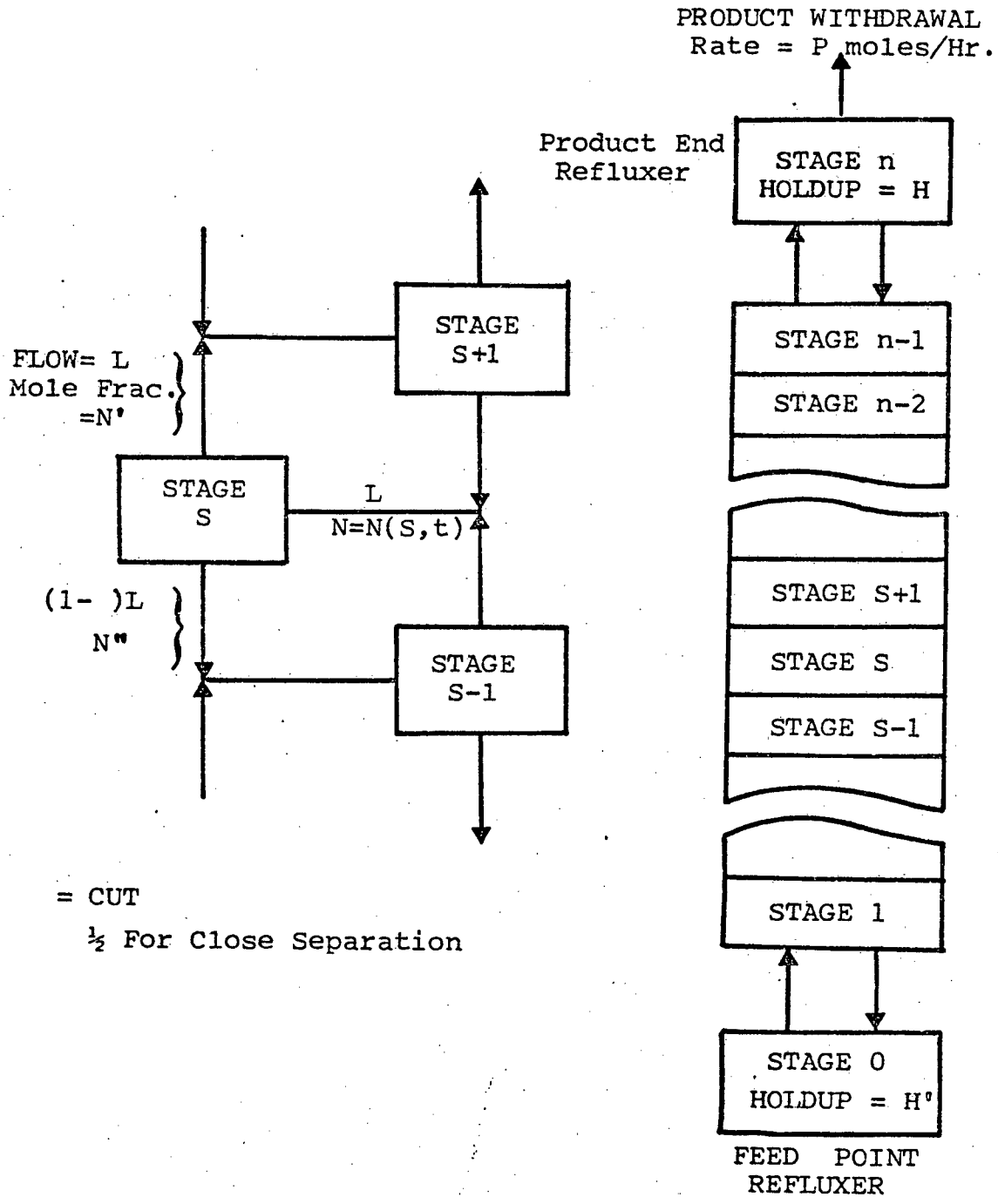

Figure 13. Square Cascade

At s = n (product end); P = 0 at all t
Holdup in refluxer = H

Such a solution is of general interest due to two reasons. First, in large-scale production, one seeks to minimize the initial start-up period during which the system is operated under total reflux. Second, observations of the transient behavior can be used for evaluating such separation system constants as the number of theoretical plates and the separation factor[11].

Short-Time Kinetics

The solution, at $t<\lambda n^2/10$ is of the form[11]

$$q(t) \equiv \frac{N(t)}{N_0} = 1 + 2\epsilon\sqrt{\frac{t}{\pi\lambda}}\, M\left(-\tfrac{1}{2},3/2,-\frac{\epsilon^2 t}{4}\right) + \frac{\epsilon^2 t}{2} \qquad (19)$$

He tabulated the value of the confluent hypergeometric function M (-1/2, 3/2, - x) for the value of x between 0.0 and 4.0 in the steps of x = 0.2. The function M defined as

$$M\left(-\tfrac{1}{2},3/2,-x\right) = \tfrac{1}{2}e^{-x} + \tfrac{1}{2}(x+\tfrac{1}{2})\sqrt{\frac{\pi}{\lambda}}\,\mathrm{erf}\sqrt{x} \qquad (20)$$

has been more finely mapped. The result is tabulated in Table III. It has been found from Table III that under the present experimental conditions at $\epsilon \lesssim 0.01$, the approximation of $M \simeq 1$ is satisfactory at all values of t at which Equation (19) is applicable. Furthermore, the term of t in Equation (19) is negligible compared to the term of $\sqrt{t}$. Thus, Equation (19) becomes

$$\frac{N(t)}{N_o} = 1 + \frac{2\epsilon}{\pi\lambda}\sqrt{t}$$

THE CONFLUENT HYPERGEOMETRIC FUNCTION M(-1/2,3/2,-X)

	0.00	0.01	0.02	0.03	0.04	0.05	0.06	0.07	0.08	0.09
0.00	1.000	1.003	1.007	1.010	1.013	1.017	1.020	1.023	1.026	1.030
0.10	1.033	1.036	1.040	1.043	1.046	1.049	1.052	1.056	1.059	1.062
0.20	1.065	1.069	1.072	1.075	1.078	1.081	1.084	1.088	1.091	1.094
0.30	1.097	1.100	1.103	1.107	1.110	1.113	1.116	1.119	1.122	1.125
0.40	1.128	1.131	1.134	1.138	1.141	1.144	1.147	1.150	1.153	1.156
0.50	1.159	1.162	1.165	1.168	1.171	1.174	1.177	1.180	1.183	1.186
0.60	1.189	1.192	1.195	1.198	1.201	1.204	1.207	1.210	1.213	1.216
0.70	1.218	1.221	1.224	1.227	1.230	1.233	1.236	1.239	1.242	1.245
0.80	1.248	1.250	1.253	1.256	1.259	1.262	1.265	1.268	1.270	1.273
0.90	1.276	1.279	1.282	1.285	1.287	1.290	1.293	1.296	1.299	1.301
1.00	1.304	1.307	1.310	1.313	1.315	1.318	1.321	1.324	1.326	1.329
1.10	1.332	1.335	1.337	1.340	1.343	1.345	1.348	1.351	1.354	1.356
1.20	1.359	1.362	1.364	1.367	1.370	1.372	1.375	1.378	1.381	1.383
1.30	1.386	1.388	1.391	1.394	1.396	1.399	1.402	1.404	1.407	1.410
1.40	1.412	1.415	1.417	1.420	1.423	1.425	1.428	1.430	1.433	1.436
1.50	1.438	1.441	1.443	1.446	1.449	1.451	1.454	1.456	1.459	1.461
1.60	1.464	1.466	1.469	1.472	1.474	1.477	1.479	1.482	1.484	1.487
1.70	1.489	1.492	1.494	1.497	1.499	1.502	1.504	1.507	1.509	1.512
1.80	1.514	1.517	1.519	1.522	1.524	1.526	1.529	1.531	1.534	1.536
1.90	1.539	1.541	1.544	1.546	1.548	1.551	1.553	1.556	1.558	1.561
2.00	1.563	1.565	1.568	1.570	1.573	1.575	1.577	1.580	1.582	1.585
2.10	1.587	1.589	1.592	1.594	1.596	1.599	1.601	1.604	1.606	1.608
2.20	1.611	1.613	1.615	1.618	1.620	1.622	1.625	1.627	1.629	1.632
2.30	1.634	1.636	1.639	1.641	1.643	1.646	1.648	1.650	1.653	1.655
2.40	1.657	1.659	1.662	1.664	1.666	1.669	1.671	1.673	1.675	1.678
2.50	1.680	1.682	1.684	1.687	1.689	1.691	1.693	1.696	1.698	1.700
2.60	1.702	1.705	1.707	1.709	1.711	1.714	1.716	1.718	1.720	1.723
2.70	1.725	1.727	1.729	1.731	1.734	1.736	1.738	1.740	1.742	1.745
2.80	1.747	1.749	1.751	1.753	1.756	1.758	1.760	1.762	1.764	1.766
2.90	1.769	1.771	1.773	1.775	1.777	1.779	1.782	1.784	1.786	1.788
3.00	1.790	1.792	1.794	1.797	1.799	1.801	1.803	1.805	1.807	1.809
3.10	1.811	1.814	1.816	1.818	1.820	1.822	1.824	1.826	1.828	1.830
3.20	1.832	1.835	1.837	1.839	1.841	1.843	1.845	1.847	1.849	1.851
3.30	1.853	1.855	1.858	1.860	1.862	1.864	1.866	1.868	1.870	1.872
3.40	1.874	1.876	1.878	1.880	1.882	1.884	1.886	1.888	1.890	1.892
3.50	1.894	1.897	1.899	1.901	1.903	1.905	1.907	1.909	1.911	1.913
3.60	1.915	1.917	1.919	1.921	1.923	1.925	1.927	1.929	1.931	1.933
3.70	1.935	1.937	1.939	1.941	1.943	1.945	1.947	1.949	1.951	1.953
3.80	1.955	1.957	1.959	1.961	1.963	1.965	1.966	1.968	1.970	1.972
3.90	1.974	1.976	1.978	1.980	1.982	1.984	1.986	1.988	1.990	1.992
4.00	1.994	1.996	1.998	2.000	2.002	2.004	2.005	2.007	2.009	2.011

TABLE III

or

$$\frac{N(t)}{N_o} = 1 + \frac{2\sqrt{\epsilon^2 n}}{\sqrt{\pi}} \sqrt{\frac{L/2}{H_{col}}} \sqrt{t} \qquad (21)$$

where $$H_{col} = nhL \qquad (22)$$

A plot of $N(t)/N_o$ against $\sqrt{t}$ should give a straight line with a slope which is equal to

$$\text{Slope} = \frac{2\sqrt{\epsilon^2 n}}{\sqrt{\pi}} \sqrt{\frac{\text{Boil-up rate}}{\text{Column holdup}}} \qquad (23)$$

Long-Time Kinetics

The solution, at $t > n^2/10$, is of the form (17)

$$q(t) = e^{\epsilon n} - (e^{\epsilon n} - 1)\, A(\epsilon n, K/\lambda n) \exp - \left[\frac{B(\epsilon n, K/\lambda n)\, t}{\lambda n^2}\right] \qquad (24)$$

where A and B are related to the smallest root of a transcendental equation, which will be discussed later. Cohen gave tables of A and B for $K/\lambda n$ between 0.0 and 0.5 in steps of 0.1 and for ϵn between 0.0 and 1.2 in steps of 0.1. It was found highly desirable to extend and refine Cohen's table beyond the limits for ϵn in both the positive and negative directions. Also, it was felt useful to extend the time limit to the region below $t = \lambda n^2/10$ by adding a higher term of expansion to Equation (24).

Cohen's solution, Equation (24), can be modified into

$$\frac{N - N_o}{N_\infty - N_o} = 1 - A_1 e^{-B_1 \tau} - A_2 e^{-B_2 \tau} \qquad (25)$$

where $N_\infty = e^{\epsilon n}$ is the overall separation at steady state, and $\tau = t/\lambda n^2$ is the reduced time, or the time measured in the unit of average process time divided by the number of stages. A_1 and B_1 are Cohen's A and B, respectively. The last term in Eqn. (25) represents the next higher term in the approximation.

The long-time kinetics parameters A_2 and B_2, as well as A_1 and B_1, are explicit functions of solutions of transcendental equations and parametrically dependent on the quantities $K/\lambda n$ and ϵn. The transcendental equations were numerically solved, and A_i and B_i were tabulated for $K/\lambda n$ from 0.00 to 0.50 in steps of 0.05 and for ϵn from -3.0 to +3.0 in steps of 0.1. Details of the solution and calculations of these parameters are found in the Appendix. It has since been decided that the last term of Equation (25) is negligible for the present study. An even finer mapping of A_1 and B_1 in the small local ranges of $K/\lambda n$ and ϵn has been made for application in the present work. The results are tabulated in Table IV.

According to Equation (25) using the first two terms on the right-hand side, a plot of $\ln (q_\infty - q)/(q_\infty - 1)$ against the time t, where $q_\infty = \exp(\epsilon n)$, would yield a straight line with

$$\text{Intercept} = \ln A \qquad (26)$$

and

$$-(\text{Slope}) = \frac{B}{\lambda n^2}$$

		A_1 and B_1 at Holdup Ratio K/λn of									
n		0.008	0.009	0.010	0.011	0.012	0.013	0.014	0.015	0.016	0.017
0.020	A=	0.8186	0.8194	0.8202	0.8209	0.8217	0.8225	0.8232	0.8240	0.8247	0.8255
	B=	2.4086	2.4038	2.3990	2.3943	2.3895	2.3848	2.3801	2.3754	2.3707	2.3660
0.021	A=	0.8187	0.8195	0.8203	0.8210	0.8218	0.8225	0.8233	0.8240	0.8248	0.8255
	B=	2.4076	2.4028	2.3981	2.3933	2.3886	2.3838	2.3791	2.3744	2.3697	2.3650
0.022	A=	0.8188	0.8196	0.8203	0.8211	0.8219	0.8226	0.8234	0.8241	0.8249	0.8256
	B=	2.4066	2.4019	2.3971	2.3923	2.3876	2.3828	2.3781	2.3734	2.3687	2.3641
0.023	A=	0.8189	0.8197	0.8204	0.8212	0.8220	0.8227	0.8235	0.8242	0.8250	0.8257
	B=	2.4057	2.4009	2.3961	2.3913	2.3866	2.3819	2.3772	2.3725	2.3678	2.3631
0.024	A=	0.8190	0.8197	0.8205	0.8213	0.8220	0.8228	0.8235	0.8243	0.8250	0.8258
	B=	2.4047	2.3999	2.3951	2.3904	2.3856	2.3809	2.3762	2.3715	2.3668	2.3621
0.025	A=	0.8191	0.8198	0.8206	0.8214	0.8221	0.8229	0.8236	0.8244	0.8251	0.8259
	B=	2.4037	2.3989	2.3941	2.3894	2.3846	2.3799	2.3752	2.3705	2.3658	2.3611
0.026	A=	0.8191	0.8199	0.8207	0.8214	0.8222	0.8230	0.8237	0.8245	0.8252	0.8259
	B=	2.4027	2.3979	2.3932	2.3884	2.3837	2.3789	2.3742	2.3695	2.3648	2.3602
0.027	A=	0.8192	0.8200	0.8208	0.8215	0.8223	0.8230	0.8238	0.8245	0.8253	0.8260
	B=	2.4017	2.3969	2.3922	2.3874	2.3827	2.3780	2.3732	2.3685	2.3639	2.3592
0.028	A=	0.8193	0.8201	0.8209	0.8216	0.8224	0.8231	0.8239	0.8246	0.8254	0.8261
	B=	2.4007	2.3960	2.3912	2.3864	2.3817	2.3770	2.3723	2.3676	2.3629	2.3582
0.029	A=	0.8194	0.8202	0.8209	0.8217	0.8225	0.8232	0.8240	0.8247	0.8255	0.8262
	B=	2.3998	2.3950	2.3902	2.3855	2.3807	2.3760	2.3713	2.3666	2.3619	2.3572
0.030	A=	0.8195	0.8203	0.8210	0.8218	0.8225	0.8233	0.8241	0.8248	0.8255	0.8263
	B=	2.3988	2.3940	2.3892	2.3845	2.3797	2.3750	2.3703	2.3656	2.3609	2.3563
0.031	A=	0.8196	0.8203	0.8211	0.8219	0.8226	0.8234	0.8241	0.8249	0.8256	0.8264
	B=	2.3978	2.3930	2.3882	2.3835	2.3788	2.3740	2.3693	2.3646	2.3600	2.3553
0.032	A=	0.8197	0.8204	0.8212	0.8220	0.8227	0.8235	0.8242	0.8250	0.8257	0.8264
	B=	2.3968	2.3920	2.3873	2.3825	2.3778	2.3731	2.3684	2.3637	2.3590	2.3543
0.033	A=	0.8197	0.8205	0.8213	0.8220	0.8228	0.8236	0.8243	0.8250	0.8258	0.8265
	B=	2.3958	2.3910	2.3863	2.3815	2.3768	2.3721	2.3674	2.3627	2.3580	2.3534
0.034	A=	0.8198	0.8206	0.8214	0.8221	0.8229	0.8236	0.8244	0.8251	0.8259	0.8266
	B=	2.3948	2.3901	2.3853	2.3806	2.3758	2.3711	2.3664	2.3617	2.3570	2.3524

TABLE IV.

		A_1 and B_1 at Holdup Ratio $K/\lambda n$ of									
ϵn		0.008	0.009	0.010	0.011	0.012	0.013	0.014	0.015	0.016	0.017
0.035	A=	0.8199	0.8207	0.8214	0.8222	0.8230	0.8237	0.8245	0.8252	0.8260	0.8267
	B=	2.3939	2.3891	2.3843	2.3796	2.3748	2.3701	2.3654	2.3607	2.3561	2.3514
0.036	A=	0.8200	0.8208	0.8215	0.8223	0.8230	0.8238	0.8246	0.8253	0.8260	0.8268
	B=	2.3929	2.3881	2.3833	2.3786	2.3739	2.3692	2.3645	2.3598	2.3551	2.3504
0.037	A=	0.8201	0.8209	0.8216	0.8224	0.8231	0.8239	0.8246	0.8254	0.8261	0.8269
	B=	2.3919	2.3871	2.3824	2.3776	2.3729	2.3682	2.3635	2.3588	2.3541	2.3495
0.038	A=	0.8202	0.8209	0.8217	0.8225	0.8232	0.8240	0.8247	0.8255	0.8262	0.8269
	B=	2.3909	2.3861	2.3814	2.3766	2.3719	2.3672	2.3625	2.3578	2.3532	2.3485
0.039	A=	0.8203	0.8210	0.8218	0.8225	0.8233	0.8241	0.8248	0.8255	0.8263	0.8270
	B=	2.3899	2.3852	2.3804	2.3757	2.3709	2.3662	2.3615	2.3568	2.3522	2.3475
0.040	A=	0.8203	0.8211	0.8219	0.8226	0.8234	0.8241	0.8249	0.8256	0.8264	0.8271
	B=	2.3890	2.3842	2.3794	2.3747	2.3700	2.3653	2.3606	2.3559	2.3512	2.3466
0.041	A=	0.8204	0.8212	0.8220	0.8227	0.8235	0.8242	0.8250	0.8257	0.8265	0.8272
	B=	2.3880	2.3832	2.3785	2.3737	2.3690	2.3643	2.3596	2.3549	2.3502	2.3456
0.042	A=	0.8205	0.8213	0.8220	0.8228	0.8236	0.8243	0.8251	0.8258	0.8265	0.8273
	B=	2.3870	2.3822	2.3775	2.3727	2.3680	2.3633	2.3586	2.3539	2.3493	2.3446
0.043	A=	0.8206	0.8214	0.8221	0.8229	0.8236	0.8244	0.8251	0.8259	0.8266	0.8274
	B=	2.3860	2.3812	2.3765	2.3718	2.3670	2.3623	2.3576	2.3530	2.3483	2.3436
0.044	A=	0.8207	0.8214	0.8222	0.8230	0.8237	0.8245	0.8252	0.8260	0.8267	0.8274
	B=	2.3850	2.3803	2.3755	2.3708	2.3661	2.3614	2.3567	2.3520	2.3473	2.3427
0.045	A=	0.8208	0.8215	0.8223	0.8230	0.8238	0.8246	0.8253	0.8260	0.8268	0.8275
	B=	2.3841	2.3793	2.3745	2.3698	2.3651	2.3604	2.3557	2.3510	2.3464	2.3417
0.046	A=	0.8208	0.8216	0.8224	0.8231	0.8239	0.8246	0.8254	0.8261	0.8269	0.8276
	B=	2.3831	2.3783	2.3736	2.3688	2.3641	2.3594	2.3547	2.3500	2.3454	2.3407
0.047	A=	0.8209	0.8217	0.8225	0.8232	0.8240	0.8247	0.8255	0.8262	0.8270	0.8277
	B=	2.3821	2.3773	2.3726	2.3679	2.3631	2.3584	2.3537	2.3491	2.3444	2.3398
0.048	A=	0.8210	0.8218	0.8225	0.8233	0.8241	0.8248	0.8256	0.8263	0.8270	0.8278
	B=	2.3811	2.3764	2.3716	2.3669	2.3622	2.3575	2.3528	2.3481	2.3434	2.3388
0.049	A=	0.8211	0.8219	0.8226	0.8234	0.8241	0.8249	0.8256	0.8264	0.8271	0.8279
	B=	2.3801	2.3754	2.3706	2.3659	2.3612	2.3565	2.3518	2.3471	2.3425	2.3378

TABLE IV. (continued)

ϵn		A_1 and B_1 at Holdup Ratio $K/\lambda n$ of									
		0.008	0.009	0.010	0.011	0.012	0.013	0.014	0.015	0.016	0.017
0.050	A=	0.8212	0.8219	0.8227	0.8235	0.8242	0.8250	0.8257	0.8265	0.8272	0.8279
	B=	2.3792	2.3744	2.3697	2.3649	2.3602	2.3555	2.3508	2.3462	2.3415	2.3369
0.051	A=	0.8213	0.8220	0.8228	0.8236	0.8243	0.8251	0.8258	0.8265	0.8273	0.8280
	B=	2.3782	2.3734	2.3687	2.3640	2.3592	2.3545	2.3499	2.3452	2.3405	2.3359
0.052	A=	0.8214	0.8221	0.8229	0.8236	0.8244	0.8251	0.8259	0.8266	0.8274	0.8281
	B=	2.3772	2.3725	2.3677	2.3630	2.3583	2.3536	2.3489	2.3442	2.3396	2.3349
0.053	A=	0.8214	0.8222	0.8230	0.8237	0.8245	0.8252	0.8260	0.8267	0.8274	0.8282
	B=	2.3762	2.3715	2.3667	2.3620	2.3573	2.3526	2.3479	2.3433	2.3386	2.3340
0.054	A=	0.8215	0.8223	0.8230	0.8238	0.8246	0.8253	0.8261	0.8268	0.8275	0.8283
	B=	2.3753	2.3705	2.3658	2.3610	2.3563	2.3516	2.3470	2.3423	2.3376	2.3330
0.055	A=	0.8216	0.8224	0.8231	0.8239	0.8246	0.8254	0.8261	0.8269	0.8276	0.8283
	B=	2.3743	2.3695	2.3648	2.3601	2.3554	2.3507	2.3460	2.3413	2.3367	2.3320
0.056	A=	0.8217	0.8225	0.8232	0.8240	0.8247	0.8255	0.8262	0.8270	0.8277	0.8284
	B=	2.3733	2.3686	2.3638	2.3591	2.3544	2.3497	2.3450	2.3403	2.3357	2.3311
0.057	A=	0.8218	0.8225	0.8233	0.8241	0.8248	0.8256	0.8263	0.8270	0.8278	0.8285
	B=	2.3723	2.3676	2.3628	2.3581	2.3534	2.3487	2.3440	2.3394	2.3347	2.3301
0.058	A=	0.8219	0.8226	0.8234	0.8241	0.8249	0.8256	0.8264	0.8271	0.8279	0.8286
	B=	2.3714	2.3666	2.3619	2.3572	2.3524	2.3478	2.3431	2.3384	2.3338	2.3291
0.059	A=	0.8219	0.8227	0.8235	0.8242	0.8250	0.8257	0.8265	0.8272	0.8279	0.8287
	B=	2.3704	2.3656	2.3609	2.3562	2.3515	2.3468	2.3421	2.3374	2.3328	2.3282

TABLE IV. (continued)

$$= \frac{B\ (L/2)}{n\ H_{col}} \tag{27}$$

Then,

$$n = - \frac{(\text{Boil-up rate})\ B}{(\text{Column holdup})\ (\text{slope})} \tag{28}$$

III-2. Outline of Method of Data Reduction.

For each run the mass-spectrometric data were processed in the following manner.

The raw mass-spectrometric data of the 45/44 relative peak ratio represents the atom ratio, R, of ^{13}C to ^{12}C contained in the CO_2 samples. The overall separation between the top and bottom of the column, q(t), is given by

$$q(t) = \frac{N(t)}{N_{bottom}} = \frac{N(t)}{N_o} \tag{29}$$

where

$$N = \frac{R}{R + 1} \tag{30}$$

Theoretically, the various quantities of the long and short time kinetics are inter-related in many ways, as summarized in Figure 14, and these relationships may be used to check and double-check calculations of various quantities concerned. However, it turned out that only one or two proints lie within the time range of $t < \lambda n^2/10$ in all distillation runs carried out in this study. Therefore, the short-time kinetics was abandoned as a check for the calculated ϵ and n. Thus, only long-time kinetics was employed, according to which the slope of the plot was used to compute n and then ϵ .

Thus, from the isotopic ratio of $^{13}C/^{12}C$, R, of a condenser sample,

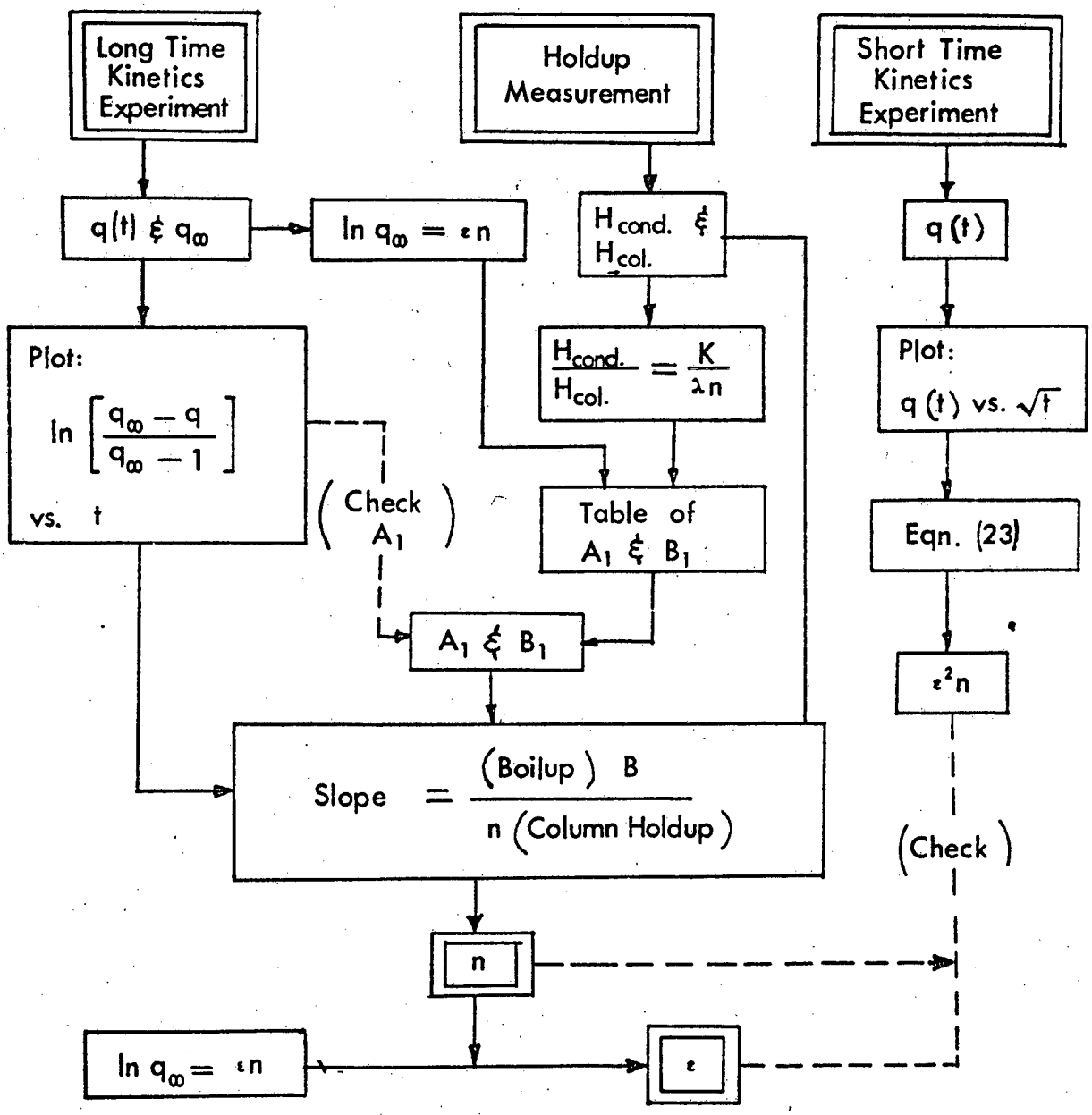

Figure 14. Flow Chart of Data Reduction

and the isotopic ratio of $^{13}C/^{12}C$, R_o, of a boiler sample, N was calculated by Equation (30). Then, q was calculated from Equation (29), and $\ln (q_\infty - q)/(q_\infty - 1)$ was plotted as a function of time t. The plots were fit to a linear function of t, using equal weights for all points: The possible error in the plotted quantity due to uncertainties of $\pm 2.2 \times 10^{-5}$ in the isotopic ratio measurements are of the order of 0.014 and do not vary significantly from point to point. The errors on the least-squares fit parameters, the slope and the intercept, were estimated based on the root-mean-square error of the actual scatter of the experimental points around the best-fit line[24]. The points with largest deviations were eliminated until the estimate of error on the slope became about 10% of the absolute magnitude of the slope or less. It was found that the values of the slope is rather insensitive to decisions to retain or discard points, while the intercept is very sensitive to such decisions. Therefore, the slope would lead to relatively objective evaluation of n and ϵ, in spite of the somewhat arbitrary decision that had to be made on the experimental points. It was also found that the intercept of the long-time kinetics plot, which is equal to $\ln A_1$, is too sensitive to relatively small uncertainties in the time zero. Thus, for instance, referring to Table XVII, the intercept for Run FR-01 is -0.4385. The intercept for all runs, according to the A_1 value arrived at from ϵn, $K/\lambda n$ and Table IV, should have been about - 0.195. The latter value of intercept could have been obtained if the time zero were set only 15 minutes earlier than the time zero actually used.

III-3. Sample Calculation.

The Run FR-03 will be used in this illustration. Referring to Tables VII and XVII, the validity limit of the short and long-time kinetics is

$$t = \frac{\lambda n^2}{10} = \frac{n}{10}\,\frac{H_{col}}{(L/2)} = \frac{n}{10}\,\frac{\text{Column holdup}}{\text{Boilup rate}}$$

$$= \frac{47}{10}\,\frac{5.64}{1.198} = 22 \text{ Minutes}$$

With the time zero used in this run, therefore the only point that falls within the range of short-time kinetics is the one at 20 minutes. The short-time kinetics will not be used.

Average R of three boiler samples = 0.010904

$$\therefore \text{Average N of boiler} = \frac{0.010904}{1 + 0.010904} = 0.010786$$

For Condenser Sample #5;

$$N = \frac{0.011350}{1 + 0.011350} = 0.011223$$

$$q = \frac{0.011223}{0.010786} = 1.040$$

$$q_\infty = 1.0460$$

$$\therefore y \quad \ln \frac{q_\infty - q}{q_\infty - 1} = -2.1032$$

The linear least squares fit (LSF) yields

$$\text{Slope} = -0.01067 \pm 0.00163$$

$$\text{Intercept} = -1.206 \pm 0.294$$

The y-values calculated from these LSV parameters are compared to the experimental values under the column "First LSF" in Table V. Since the RMSE of the above slope is much more than 10% of the absolute magnitude of the slope, the experimental points Nos. 1, 6, 8 and 11 were removed, and the linear LSF was carried out on the remaining eight points. The second LSF yielded

$$\text{Slope} = -0.082 \pm 0.0007$$

$$\text{Intercept} = -1.330 \pm 0.123$$

and the column in Table V headed by "Second LSF". In Figure 18, the experimental y is plotted against time, and the solid line is drawn according to the slope and intercept of the second LSF.

Now,

$$\epsilon n = \ln q_\infty = \ln 1.0460 = 0.045$$

$$K/\lambda n = \frac{\text{condenser holdup}}{\text{column holdup}} = \frac{0.064 \text{ gram}}{5.64 \text{ gram}} = 0.0113$$

From Table IV,

$$A_1 = 0.8232 \quad \text{and} \quad B_1 = 2.3684$$

$$\therefore n = \frac{(1.198)(2.3684)}{(5.74)\ (0.0082)} = 60.3$$

The error on n is taken as being due to that on the slope of the linear LSF only, and, therefore,

$$\sigma_n = 60.3 \frac{0.0007}{0.0082} = 5.1$$

TABLE V

Sample Calculation for Run FR-03

Point No.	y_o* (experimental)	First LSF		Second LSF	
		y (Calc'd)	y_o-y	y (Calc'd)	y_o-y
1	-0.9218	-1.4193	0.4975	-	-
2	-1.4262	-1.5899	0.1638	-1.6246	0.1984
3	-1.6870	-1.7819	0.0949	-1.7721	0.0851
4	-2.1359	-1.9632	-0.1727	-1.9115	-0.2244
5	-2.1032	-2.1232	0.0200	-2.0344	-0.0688
6	-2.9344	-2.3365	-0.5979	-	-
7	-2.1527	-2.5498	0.3971	-2.3622	0.2095
8	-3.5916	-2.8697	-0.7219	-	-
9	-3.1391	-3.1897	0.0506	-2.8540	0.2851
10	-3.3974	-3.8296	0.4322	-3.3457	0.0517
11	-5.5375	-4.4695	-1.0680	-	-
12	-4.1512	-4.2460	0.0948	-4.2882	0.1370

* $y = \ln (q_\infty - q)/(q_\infty - 1)$

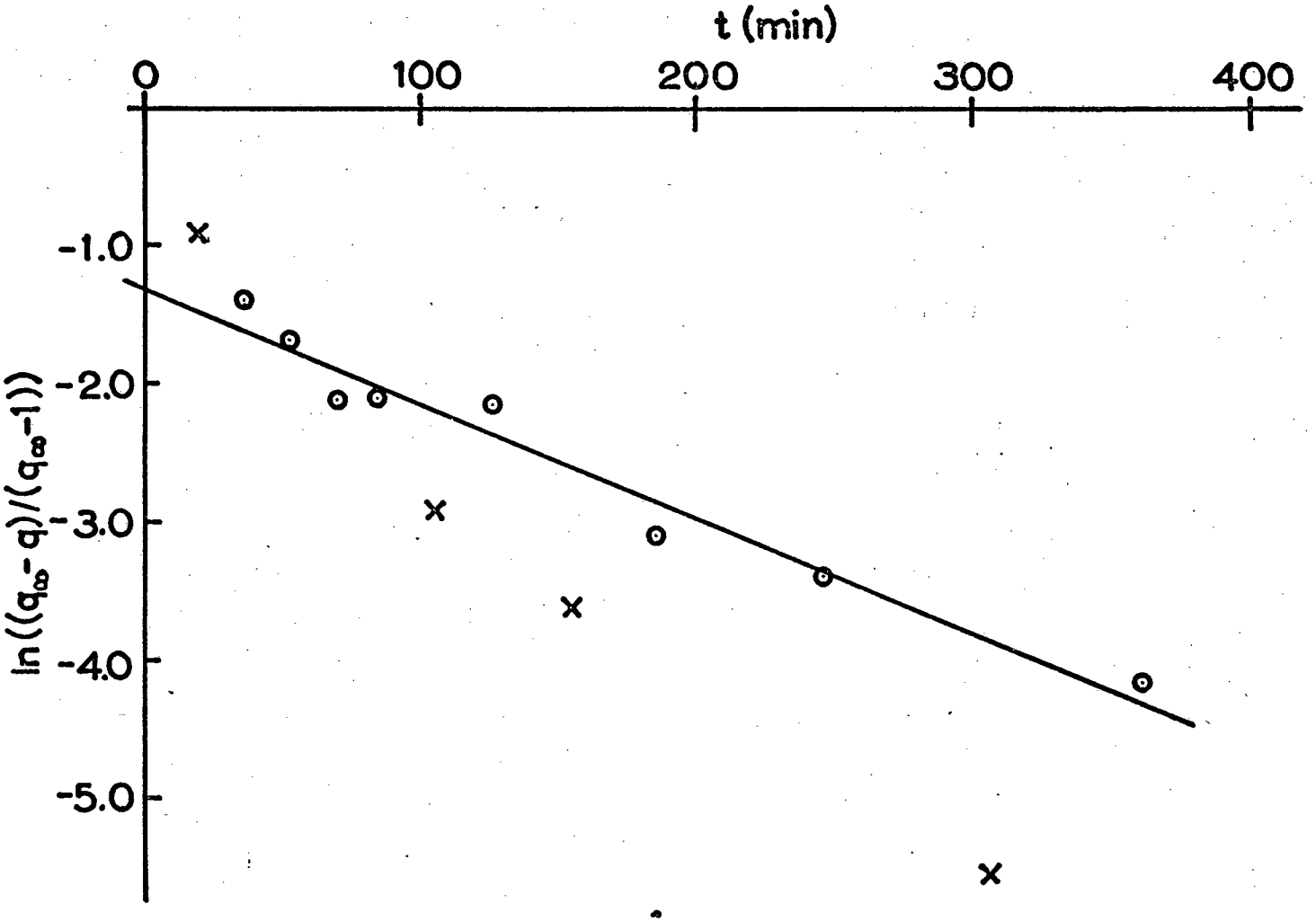

Figure 18. Long Time Kinetics Plot of Run FR-03.

Then,

$$\epsilon = \frac{\epsilon n}{n} = \frac{0.045}{60.3} = 0.75 \times 10^{-3}$$

and $$\sigma_\epsilon = 0.75 \frac{0.0007}{0.0082} = 0.06 \times 10^{-3}$$

Thus,

$$\alpha \equiv \frac{P'}{P} \cong \frac{\text{Vapor pressure of } {}^{12}C \text{ species}}{\text{Vapor pressure of } {}^{13}C \text{ species}}$$

$$= \frac{1}{1+\epsilon} = \frac{1}{1 + 0.00075} = 0.99925$$

The uncertainty on $T \ln (P'/P)$ used later in the LSF to fit the separation factors to the formula $T \ln (P'/P) = A/T^2 - B/T$, was obtained as

$$\epsilon = T\sigma_{\ln\alpha} = T\sigma_{\ln(1+\epsilon)} \quad T\sigma_\epsilon$$

$$= (175.9) \times (6 \times 10^{-5}) = 0.0105$$

IV. RESULTS

Results of these experimental data and calculations are tabulated in Tables VI to XVII, one table for each distillation run. Calculations of ϵ and n are summarized in Table XVIII. The final results on α are found in Table XIX.

The entries in Tables VI to XVII are self-explanatory. In Table XVIII, the "pressure from WT gauge" was read from the Wallace-Tiernan differential pressure gauge, and the "T(^{o}K) from pressure" was obtained by using Equation (16) and the capacitance gauge reading. The "T(^{o}K) from PRT reading" is read from the platinum resistance thermometer, and the resistance reading was converted to the absolute temperature by using a calibration traceable to the National Bureau of Standards. The least-squares fit formula for the calibration is

$$T(^{o}K) = \frac{-0.59608}{R\ (ohm)} + 31.028 + 2.2279R$$

$$+ 0.2432 \times 10^{-2} R^{2} - 0.49494 \times 10^{-5} R^{3} \qquad (31)$$

The discrepancy between two temperature readings is an indication of reliability of Wallace-Tiernan gauge, which is excellent. The last column of Table XVIII is an indication of degree of wetness of column packing.

The data of Tables VI to XVII have been plotted in Figures 15 to 17, and 19 to 27. Each graph shows all the experimental points taken during a run, but those points that were retained in the final least-squares fit in the long-time kinetics have been indicated by the circled dots, while those that were not retained have been shown as a cross. The line through the plot corresponds to the least-squared line of the linear long-time kinetics.

TABLE VI. Data for Run FR-01.

N_{BOILER} = 0.01080 Epsilon x n = 0.042

$N_{INFINITY}$ = 0.01127 $Q_{INFINITY}$ = 1.0436

Column Holdup = 4.95 grams Boil up Rate = 1.389 grams/min.

$N_{READING}$	$Q_{READING}$	Long-Time	Time
0.010935	1.012	-0.3363	7
0.011004	1.018	-0.5639	23
0.011120	1.029	-1.1337	38
0.011154	1.032	-1.3898	53
0.011151	1.032	-1.3650	67
0.011192	1.036	-1.7828	83
0.011184	1.035	-1.6774	98
0.011255	1.042	-3.3444	113
0.011255	1.042	-3.3444	133
0.011255	1.042	-3.3444	154
0.011260	1.042	-3.6915	173
0.011269	1.043	-5.0778	203
0.011252	1.042	-3.1817	233
0.011270	1.043	-5.4832	293
0.011270	1.043	-5.4832	353

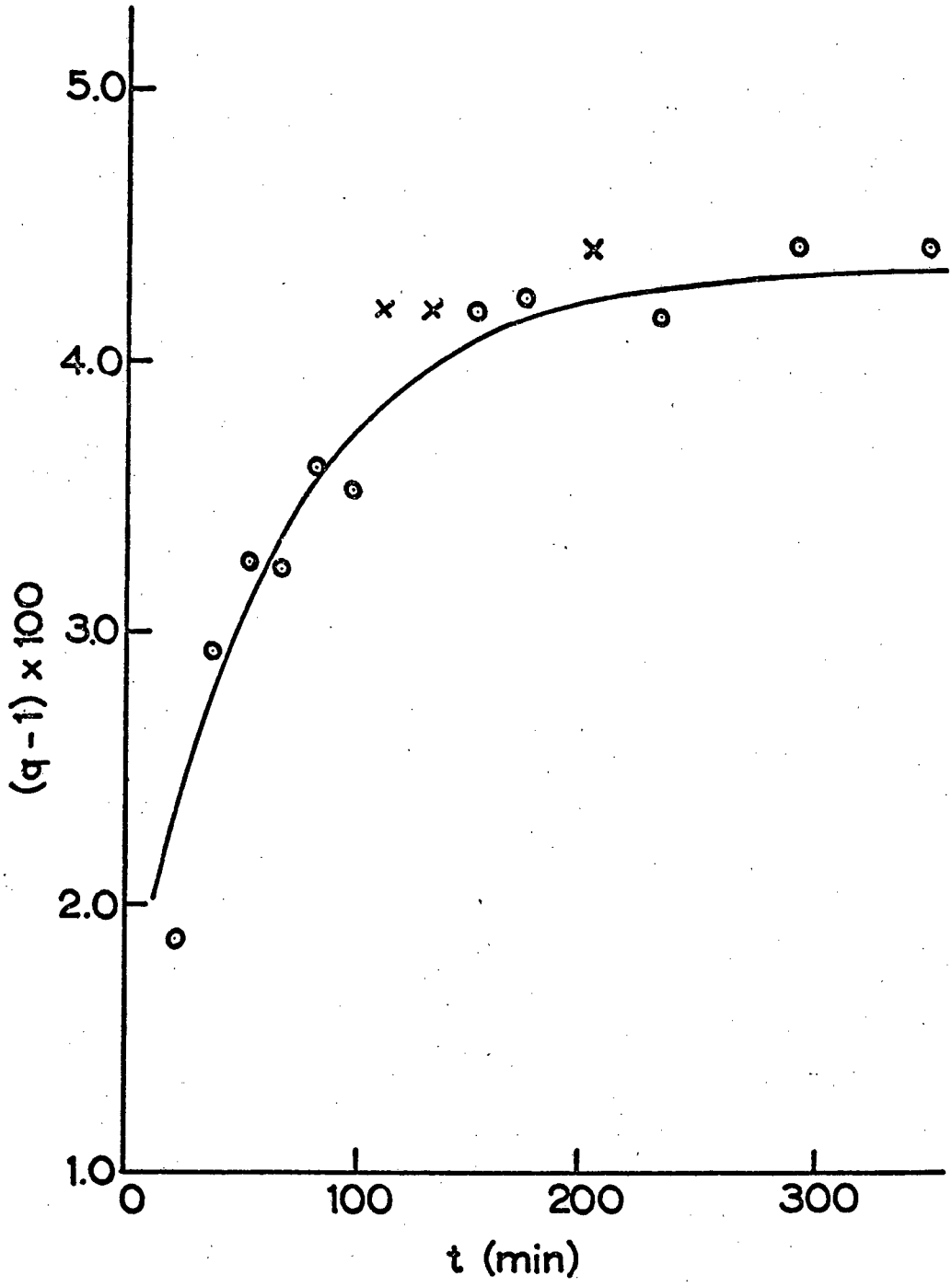

Figure 15. Separation as a Function of Time; Run FR-01.

TABLE VII. Data for Run FR-02

N_{BOILER} = 0.010705 Epsilon x n = 0.045

$N_{INFINITY}$ = 0.011272 $Q_{INFINITY}$ = 1.053

Column Holdup = 5.05 grams Boilup Rate = 1.198 grams/min.

$N_{READING}$	$Q_{READING}$	Long-Time	Time
0.011057	1.033	-0.9725	24
0.011150	1.042	-1.5415	44
0.011166	1.043	-1.6796	58
0.011191	1.045	-1.9550	73
0.011214	1.048	-2.2843	92
0.011235	1.050	-2.7509	111
0.011235	1.050	-2.7509	131
0.011232	1.049	-2.6728	162
0.011250	1.051	-3.2706	191
0.011270	1.053	-5.6662	256

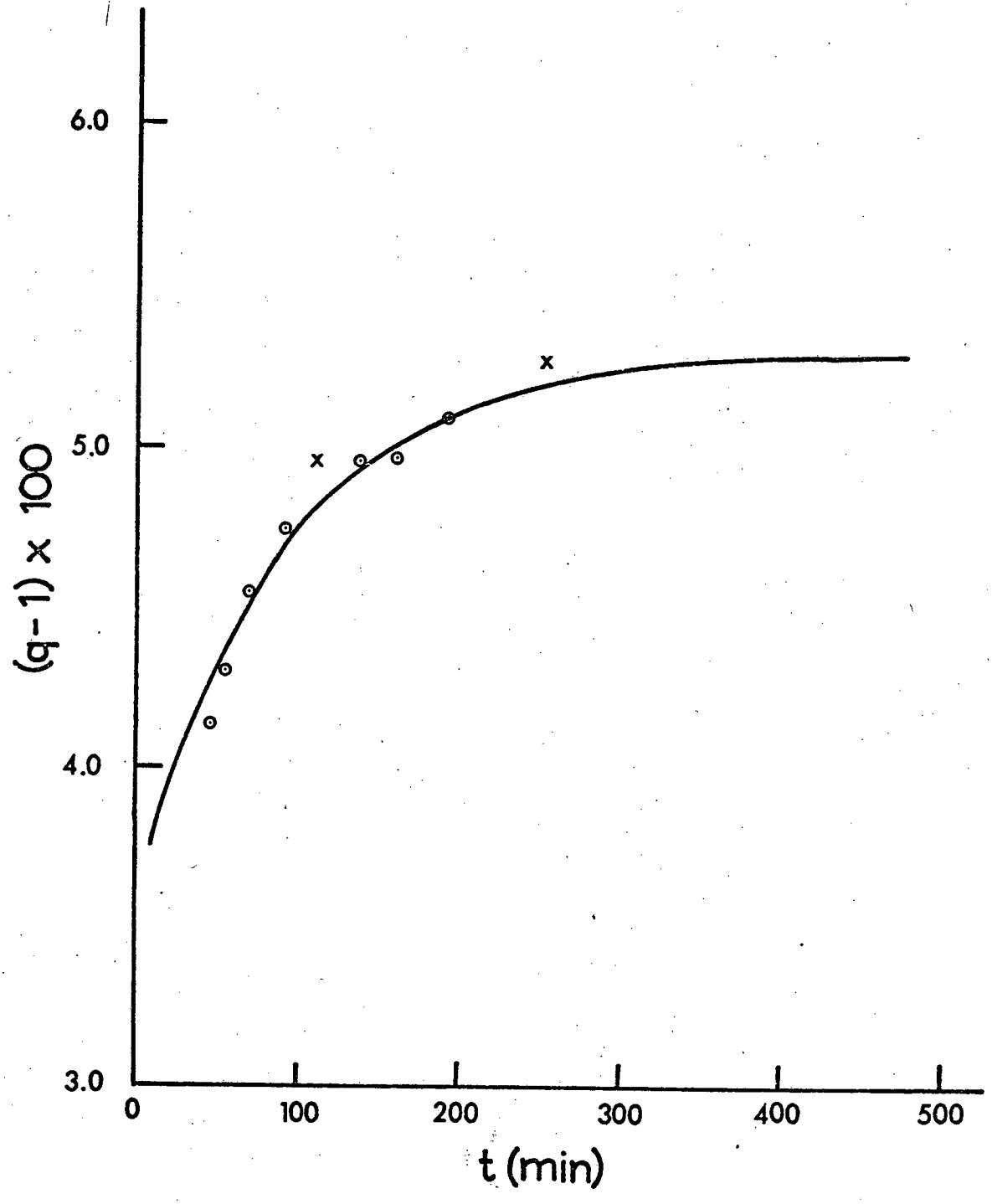

Figure 16. Separation as a Function of Time; Run FR-02.

TABLE VIII. Data for Run FR-03

N_{BOILER} = 0.010787 Epsilon x n = 0.045

$N_{INFINITY}$ = 0.011283 $Q_{INFINITY}$ = 1.046

Column Holdup = 5.74 grams Boilup Rate = 1.198 grams/min.

$N_{READING}$	$Q_{READING}$	Long-Time	Time
0.011086	1.028	-0.9218	20
0.011164	1.035	-1.4262	36
0.011191	1.038	-1.6870	54
0.011225	1.041	-2.1359	71
0.011223	1.040	-2.1032	86
0.011257	1.044	-2.9344	106
0.011226	1.041	-2.1527	126
0.011270	1.045	-3.5916	156
0.011262	1.044	-3.1391	186
0.011267	1.044	-3.3974	246
0.011281	1.046	-5.5375	306
0.011275	1.045	-4.1512	361

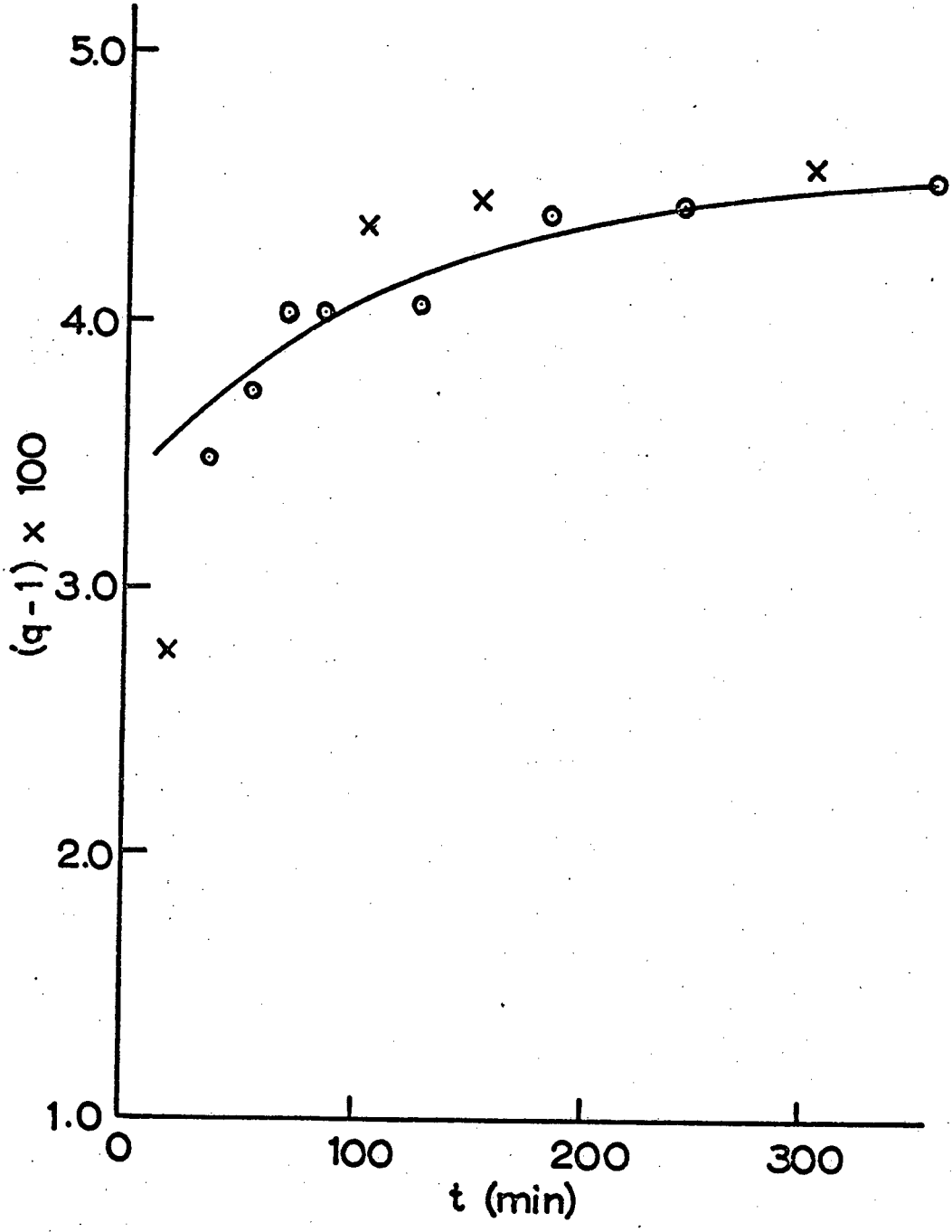

Figure 17. Separation as a Function of Time; Run FR-03.

TABLE IX. Data for Run FR-04

N_{BOILER} = 0.010857 Epsilon x n = 0.042

$N_{INFINITY}$ = 0.011318 $Q_{INFINITY}$ = 1.042

Column Holdup = 4.30 grams Boil up Rate = 0.937 grams/min.

$N_{READING}$	$Q_{READING}$	Long-Time	Time
0.010993	1.012	-0.3483	16
0.011112	1.023	-0.8047	32
0.011182	1.030	-1.2150	46
0.011199	1.031	-1.3526	61
0.011251	1.036	-1.9226	84
0.011218	1.033	-1.5219	102
0.011217	1.033	-1.5122	123
0.011231	1.034	-1.6681	152
0.011316	1.042	-1.6681	152

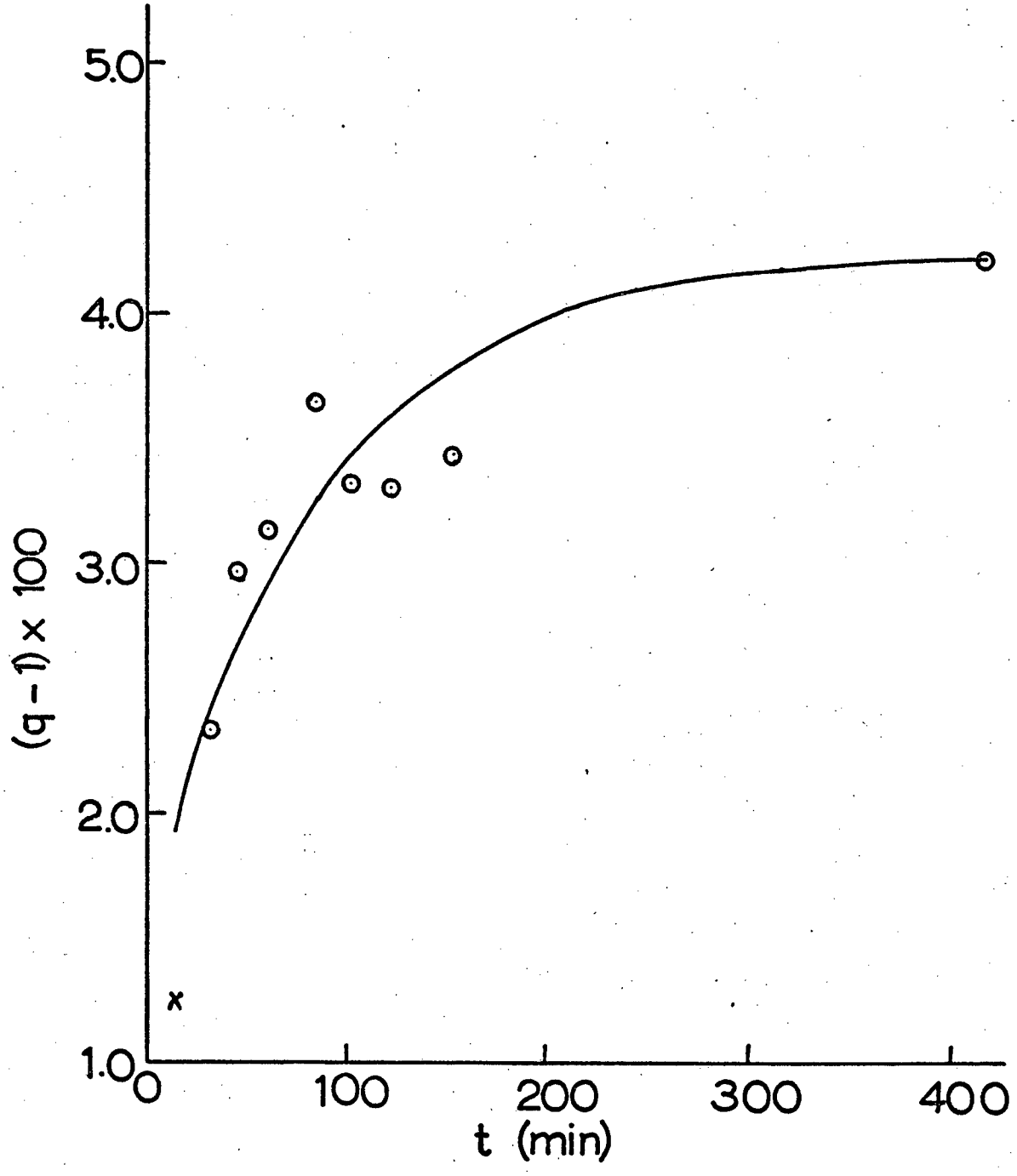

Figure 19. Separation as a Function of Time; Run FR-04.

TABLE X. Data for Run FR-05

N_{BOILER} = 0.010647 Epsilon x n = 0.053

$N_{INFINITY}$ = 0.011226 $Q_{INFINITY}$ = 1.054

Column Holdup = 7.00 grams Boilup Rate = 1.490 grams/min.

$N_{READING}$	$Q_{READING}$	Long-Time	Time
0.010996	1.033	-0.9234	27
0.011030	1.036	-1.0847	42
0.011031	1.036	-1.0898	57
0.011043	1.037	-1.1520	72
0.011125	1.045	-1.7485	115
0.011133	1.046	-1.8294	145
0.011224	1.054	-5.6879	175
0.011184	1.050	-2.6456	210
0.011182	1.050	-2.5766	270
0.011174	1.049	-2.4130	380

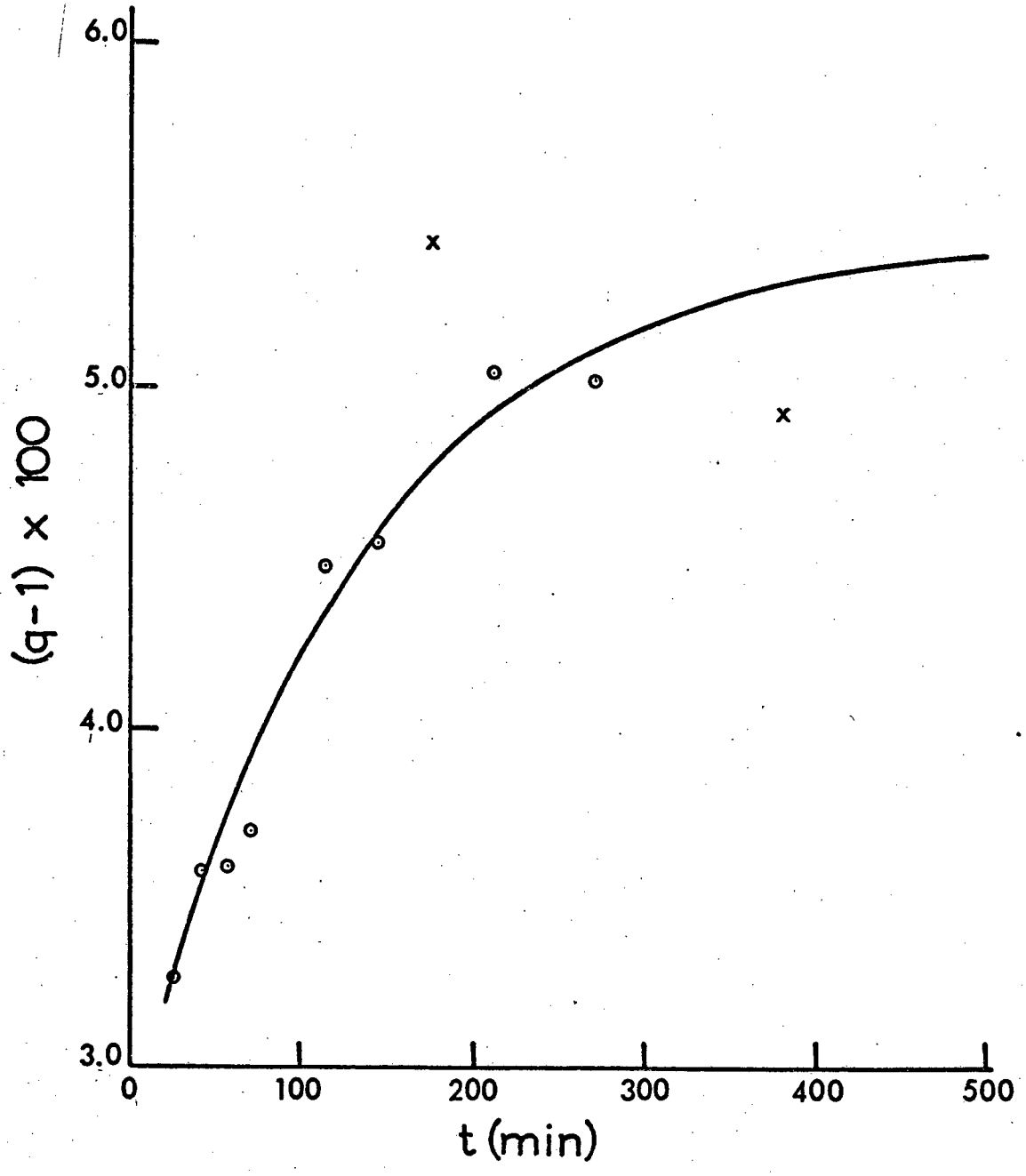

Figure 20. Separation as a Function of Time; Run FR-05.

TABLE XI. Data for Run FR-06

N_{BOILER} = 0.010632 Epsilon x n = 0.046

$N_{INFINITY}$ = 0.011130 $Q_{INFINITY}$ = 1.047

Column Holdup = 5.74 grams Boilup Rate = 1.449 grams/min.

$N_{READING}$	$Q_{READING}$	Long-Time	Time
0.010905	1.026	-0.7936	12
0.010913	1.026	-0.8291	26
0.011009	1.035	-1.4196	43
0.011034	1.038	-1.6469	57
0.011079	1.042	-2.2805	97
0.011122	1.046	-4.1519	117
0.011083	1.042	-2.3606	147
0.011121	1.046	-4.0335	178
0.011076	1.042	-2.2245	243
0.011115	1.045	-3.5236	303
0.011128	1.047	-5.5382	362

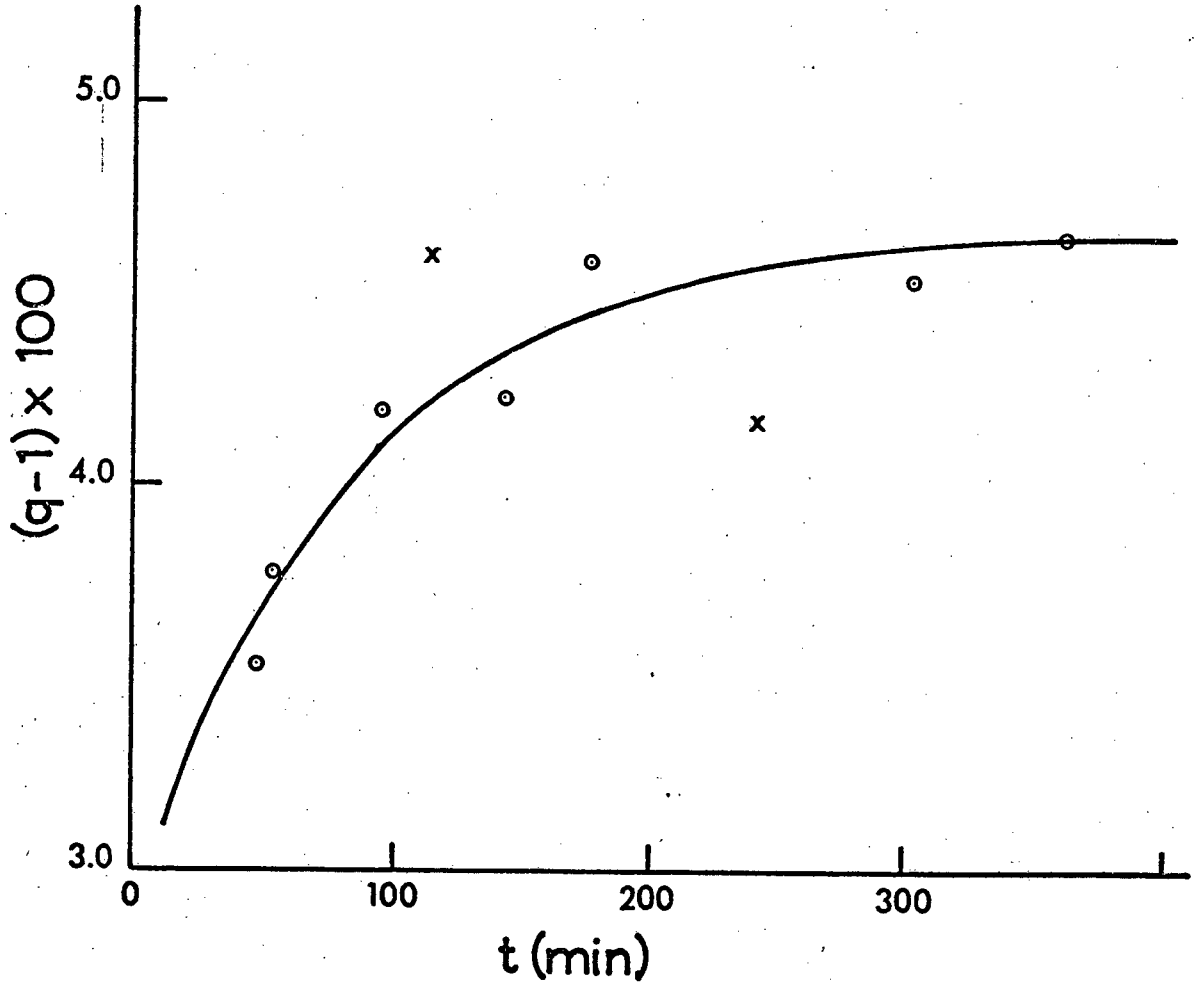

Figure 21. Separation as a Function of Time; Run FR-06.

TABLE XII. Data for Run FR-07

N_{BOILER} = 0.011381 Epsilon x n = 0.029

$N_{INFINITY}$ = 0.011711 $Q_{INFINITY}$ = 0.029

Column Holdup = 4.90 grams Boil up Rate = 1.490 grams/min.

$N_{READING}$	$Q_{READING}$	Long-Time	Time
0.011389	1.001	-0.0232	9
0.011518	1.012	-0.5341	24
0.011619	1.021	-1.2792	39
0.011639	1.023	-1.5184	55
0.011704	1.028	-3.8766	68
0.011708	1.029	-4.7239	84
0.011708	1.029	-4.7239	103
0.011707	1.029	-4.4362	123
0.011707	1.029	-4.4362	143
0.011708	1.029	-4.7239	163
0.011707	1.029	-4.4362	193
0.011709	1.029	-5.1293	223
0.011706	1.029	-4.2130	253
0.011707	1.029	-4.4362	283
0.011708	1.029	-4.7239	353
0.011701	1.028	-3.5188	413

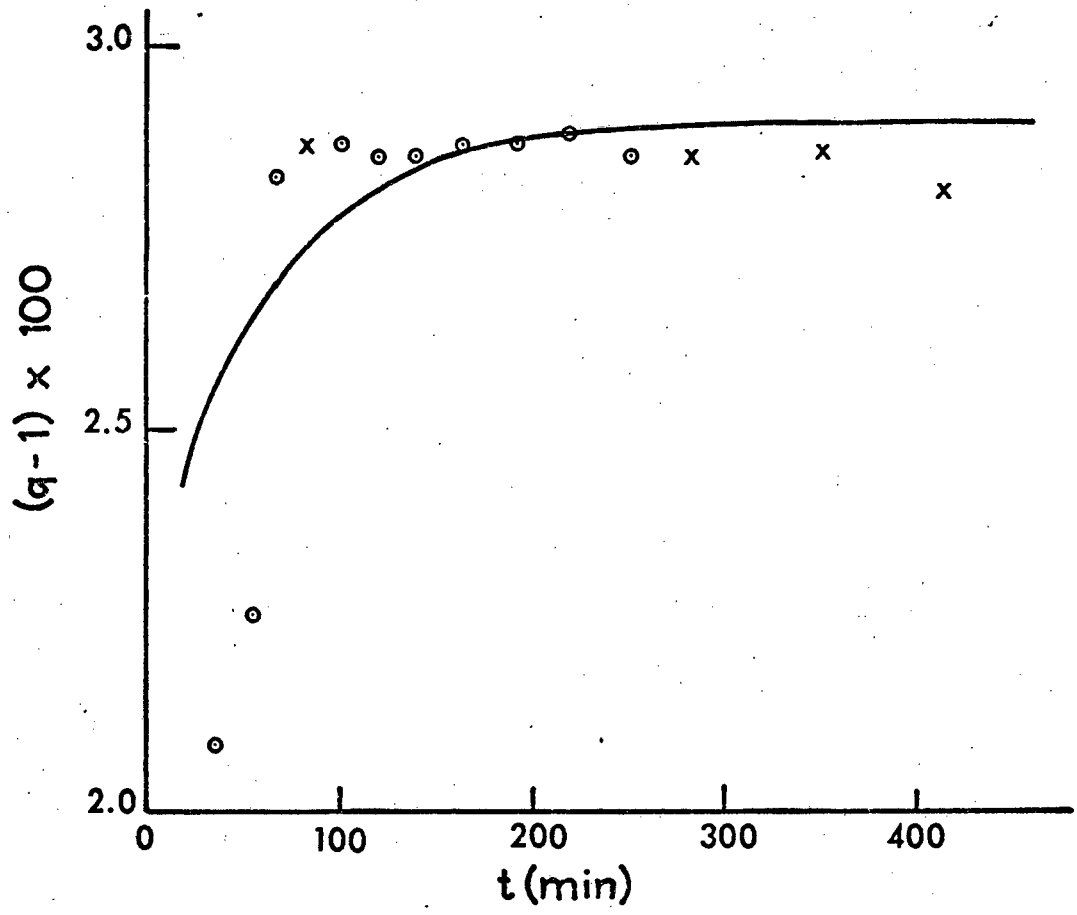

Figure 22. Separation as a Function of Time; Run FR-07.

TABLE XIII. Data for Run FR-08

N_{BOILER} = 0.011276 Epsilon x n = 0.039

$N_{INFINITY}$ = 0.011727 $Q_{INFINITY}$ = 1.040

Column Holdup = 5.85 grams Boil up Rate = 1.108 grams/min.

$N_{READING}$	$Q_{READING}$	Long-Time	Time
0.011414	1.012	-0.3663	8
0.011572	1.026	-1.0658	23
0.011681	1.036	-2.2845	68
0.011669	1.035	-2.0572	83
0.011702	1.038	-2.9155	98
0.011702	1.038	-2.9155	113
0.011703	1.038	-2.9563	127
0.011703	1.038	-2.9563	157
0.011716	1.039	-3.7371	187
0.011715	1.039	-3.6499	218
0.011714	1.039	-3.5698	248
0.011717	1.039	-3.8326	308
0.011722	1.040	-4.5236	367
0.011725	1.040	-5.4399	450

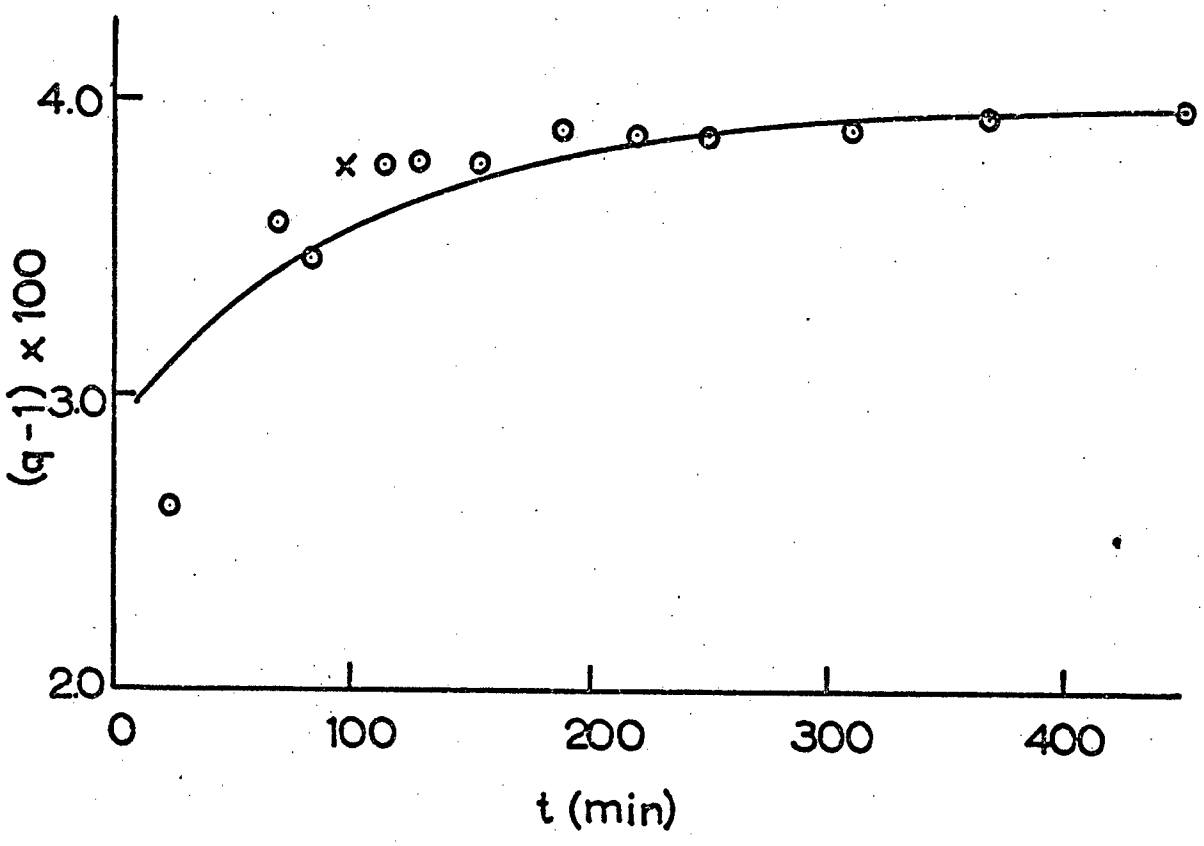

Figure 23. Separation as a Function of Time; Run FR-08.

TABLE XIV. Data for Run FR-09

N_{BOILER} = 0.011146 Epsilon x n = 0.054

$N_{INFINITY}$ = 0.011759 $Q_{INFINITY}$ = 1.055

Column Holdup = 6.24 grams Boil up Rate = 2.297 grams/min.

$N_{READING}$	$Q_{READING}$	Long-Time	Time
0.011336	1.017	-0.3704	11
0.011451	1.027	-0.6887	27
0.011561	1.037	-1.1282	49
0.011655	1.046	-1.7687	70
0.011655	1.046	-1.7687	92
0.011723	1.052	-2.8307	112
0.011722	1.052	-2.8037	135
0.011713	1.051	-2.5914	257
0.011757	1.055	-5.7525	317
0.011757	1.055	-5.7525	410

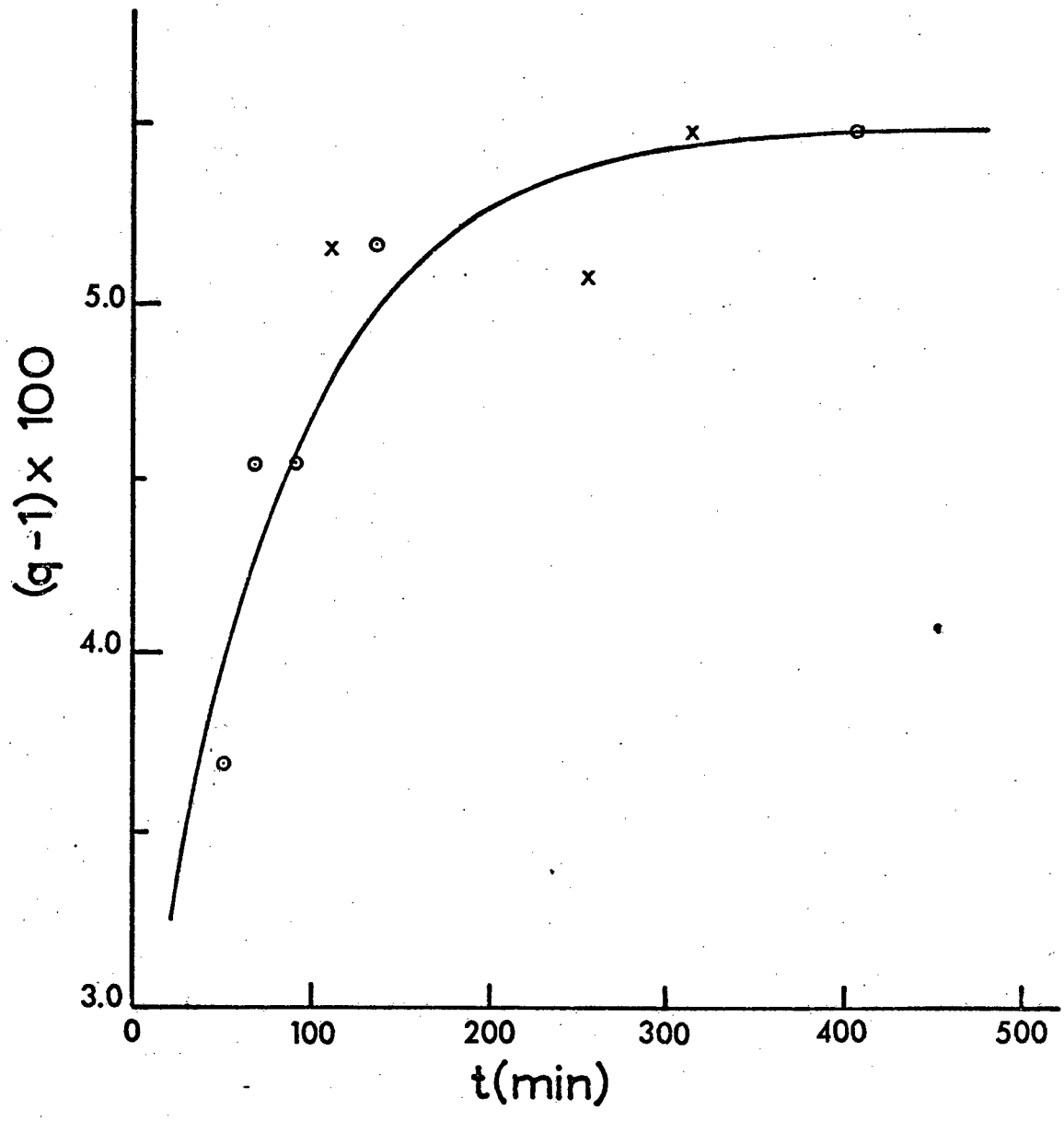

Figure 24. Separation as a Function of Time; Run FR-09.

TABLE XV. Data for Run FR-10

N_{BOILER} = 0.011184 Epsilon x n = 0.041

$N_{INFINITY}$ = 0.011649 $Q_{INFINITY}$ = 1.042

Column Holdup = 7.24 grams Boilup Rate = 2.695 grams/min.

$N_{READING}$	$Q_{READING}$	Long-Time	Time
0.011407	1.020	-0.6550	14
0.011423	1.021	-0.7220	35
0.011509	1.029	-1.2017	54
0.011604	1.038	-2.3360	73
0.011524	1.030	-1.3124	98
0.011606	1.038	-2.3804	123
0.011614	1.038	-2.5811	147
0.011615	1.038	-2.6094	171
0.011621	1.039	-2.8322	235
0.011647	1.041	-5.4724	300

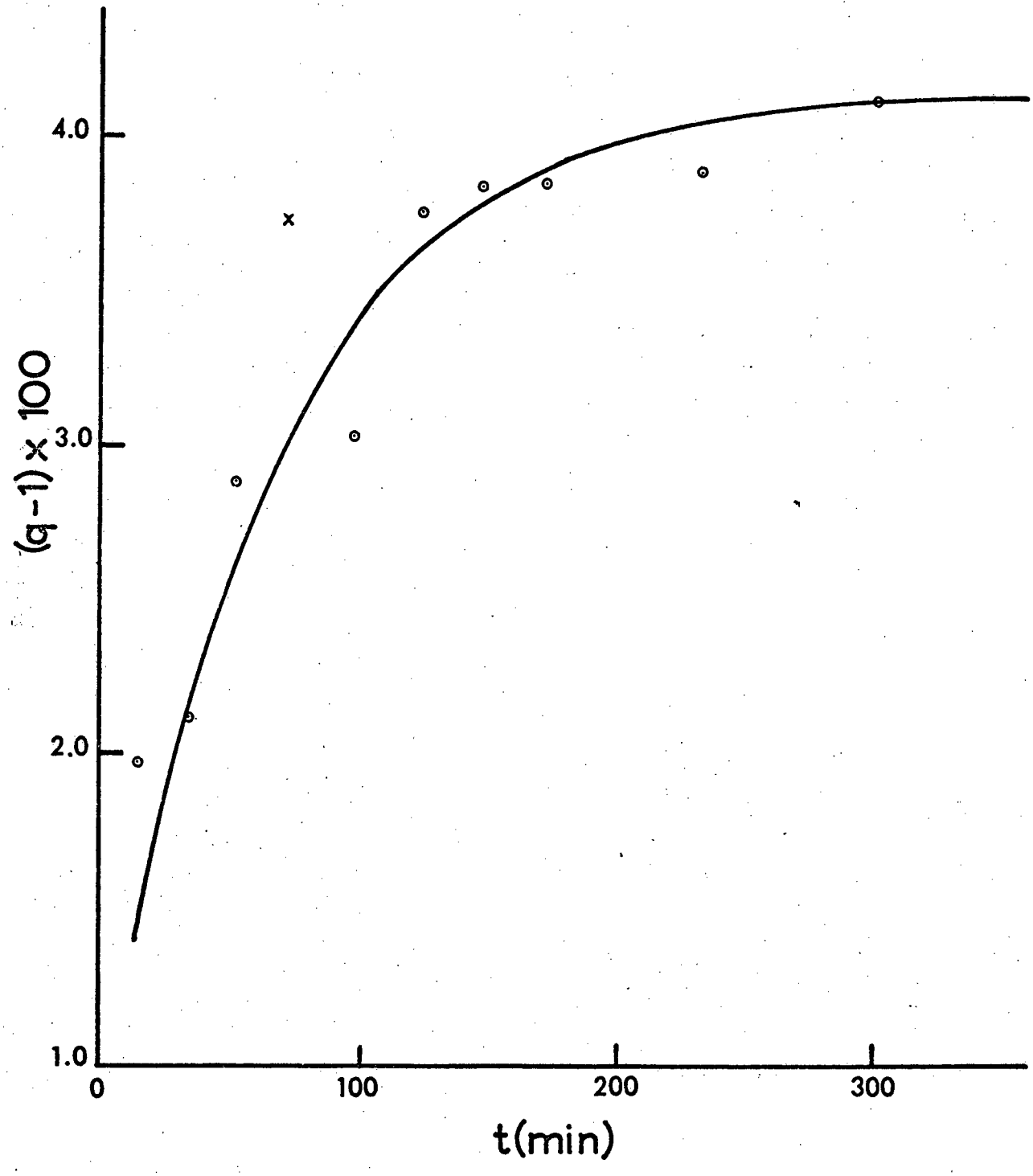

Figure 25. Separation as a Function of Time; Run FR-10.

TABLE XVI. Data for Run FR-11

N_{BOILER} = 0.011519 Epsilon x n = 0.035

$N_{INFINITY}$ = 0.011930 $Q_{INFINITY}$ = 1.036

Column Holdup = 5.44 grams Boil up Rate = 2.373 grams/min.

$N_{READING}$	$Q_{READING}$	Long-Time	Time
0.011588	1.006	-0.1848	17
0.011770	1.022	-0.9431	46
0.011825	1.027	-1.3702	61
0.011861	1.030	-1.7802	81
0.011888	1.032	-2.2817	101
0.011914	1.034	-3.2704	121
0.011916	1.035	-3.4042	168
0.011908	1.034	-2.9521	211
0.011928	1.036	-5.3485	256
0.011907	1.034	-2.8650	306

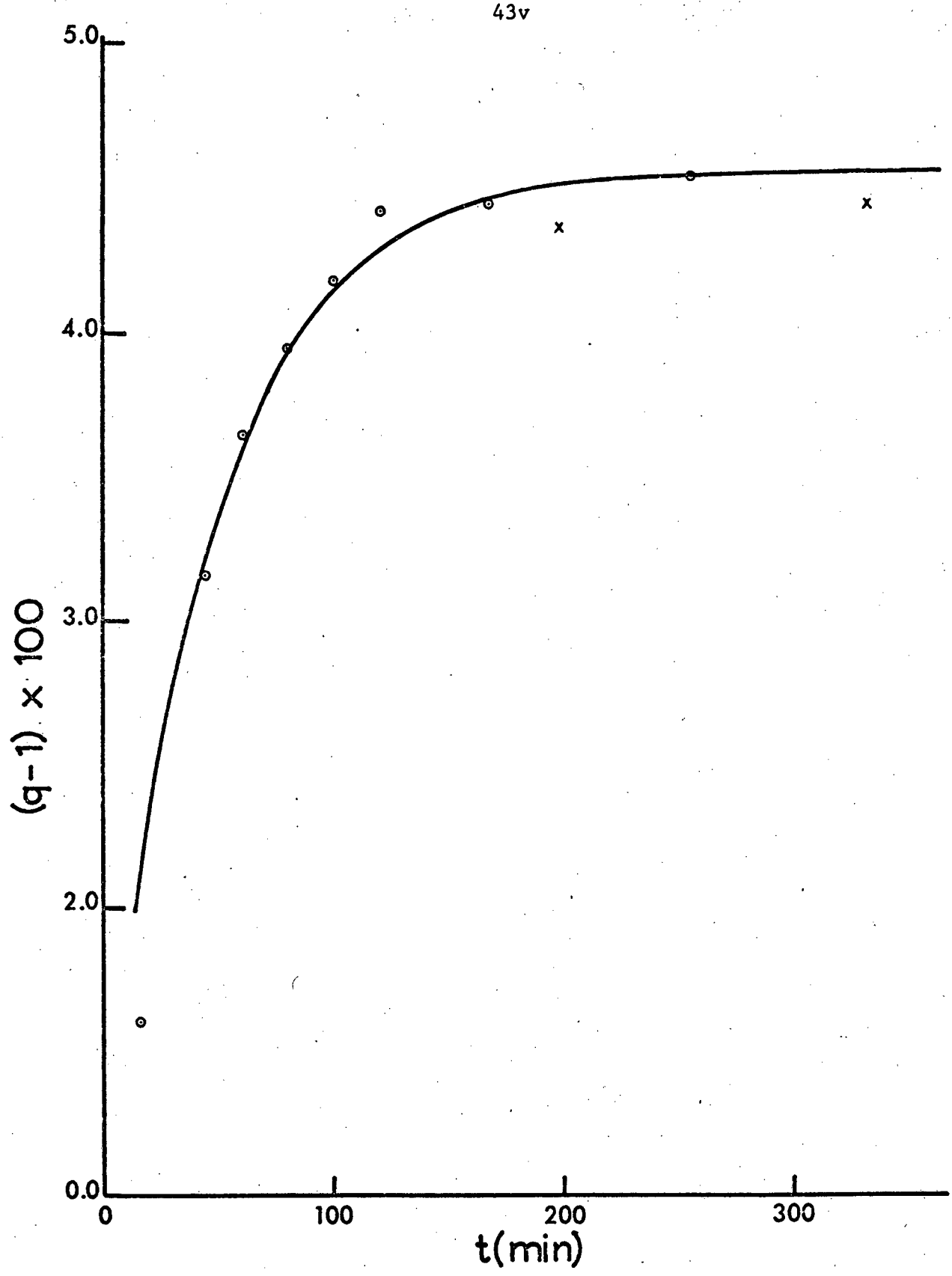

Figure 26. Separation as a Function of Time; Run FR-11.

TABLE XVII. Data for Run FR-12

N_{BOILER} = 0.011539 Epsilon x n = 0.043

$N_{INFINITY}$ = 0.012043 $Q_{INFINITY}$ = 1.044

Column Holdup = 5.74 grams Boilup Rate = 2.048 grams/min.

$N_{READING}$	$Q_{READING}$	Long-Time	Time
0.011595	1.005	-0.1187	27
0.011699	1.014	-0.3814	42
0.011961	1.037	-1.8172	77
0.012024	1.042	-3.2519	117
0.012008	1.041	-2.6644	162
0.012017	1.041	-2.9523	209
0.012036	1.043	-4.3021	247
0.012041	1.044	-5.5517	319

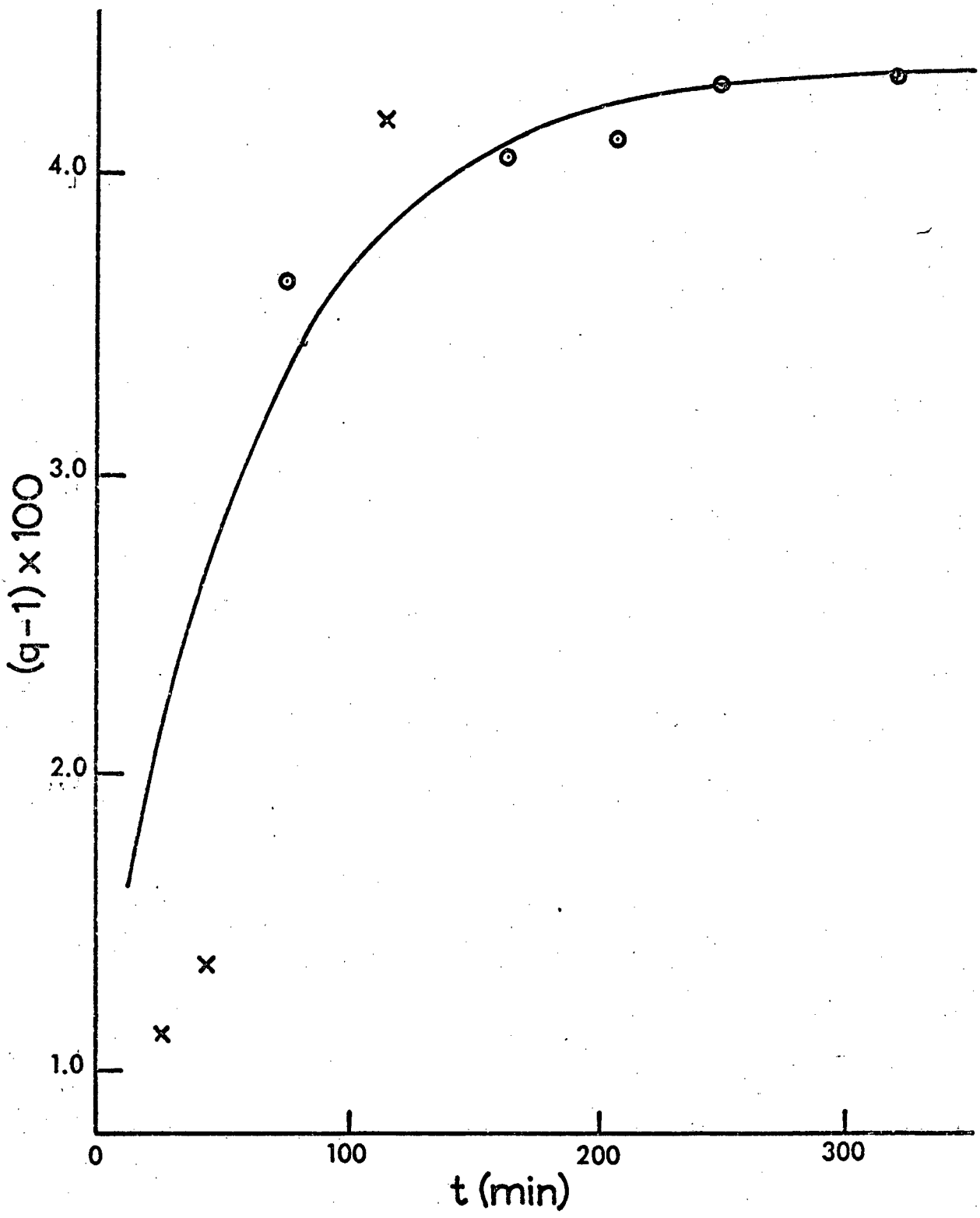

Figure 27. Separation as a Function of Time; Run FR-12.

V. DISCUSSION

The results tabulated in Table XIX were least-squares fit to a functional form

$$T \ln\alpha = \frac{A}{T} - B \tag{32}$$

where A and B are the least-squares parameters, and 1/T is the independent variable.

$$\text{Here, } \alpha \equiv \frac{P'}{P} \equiv \frac{\text{Vapor pressure of } {}^{12}\text{C species}}{\text{Vapor pressure of } {}^{13}\text{C species}} = \frac{1}{1+\epsilon} \tag{33}$$

Equation (32) is directly obtainable from Bigeleisen's vapor pressure formula, Equation (11). Each point of Table XIX is weighted according to

$$w_i = \frac{1}{\sigma_i^2} = \left(T_i \frac{1}{\sigma_{\epsilon i}}\right)^2 \tag{34}$$

where w_i is the weight of the i-th point in Table XIX, σ_i is an error on the i-th value of $T \ln\alpha$, which is equal to $T_i \sigma_{\epsilon i}$, in which $\sigma_{\epsilon i}$ is the error on the i-th ϵ as given in Table XVIII. The procedure led to

$$A = 1.5 \pm 14.1 \tag{35}$$

$$B = -0.159 \pm 0.076 \tag{36}$$

The errors reported in Equation (35) and (36) are based on the actual scatter of the experimental points around the LSF line[24], and include not only the statistical errors but also all accidental errors if any. Errors on A and B, as predicted by propagation of error starting with the errors on ϵ of Table XIX are $\pm$ 12.8 and 0.068. The latter errors, called internal deviations, are comparable in magnitudes with the deviations of Equations (35) and (36), called external deviations, indicating that there are no particularly bad experimental points and

TABLE XVIII

Summary of Calculation of ϵ and n

Run Nos.	P(torr) from W-T Gauge	T(°K) from Pressure	T(°K) from PRT-reading ohms	T(°K) from PRT-reading °K	Column Holdup (gram)	Boilup rate (g/min)	K/λn	εn
4	189± 12	169.1±0.7	58.7±0.2	169.2±0.4	4.30	0.937	0.0149	0.042
3	300± 3	175.9±0.2	61.4±0.1	175.9±0.2	5.74	1.198	0.0112	0.045
8	304± 8	176.1±0.3	61.4±0.1	175.9±0.2	5.85	1.108	0.0110	0.039
2	405± 52	180.7±2.1	63.5±0.5	181.1±0.2	5.05	1.198	0.0127	0.051
1	505± 4	184.4±0.2	64.9±0.1	184.5±0.3	4.95	1.389	0.0129	0.043
6	521± 30	184.9±1.0	65.4±0.2	185.8±0.5	5.74	1.449	0.0111	0.046
7	563± 6	186.3±0.1	65.9±0.1	187.0±0.2	4.90	1.490	0.0131	0.029
5	604± 8	187.5±0.2	66.2±0.2	187.8±0.5	7.00	1.490	0.0091	0.053
9	993±121	196.9±2.0	69.6±0.1	196.9±0.3	6.24	2.297	0.0103	0.054
10	1073± 77	198.4±1.4	70.5±0.2	198.7±0.5	7.24	2.695	0.0088	0.041
12	1171± 50	200.2±0.9	71.3±0.1	200.7±0.3	5.74	2.048	0.0111	0.043
11	1524±155	205.9±2.3	73.8±0.1	206.9±0.3	5.44	2.373	0.0118	0.035

TABLE XVIII (continued)

Summary of Calculation of ϵ and n

Run Nos.	A	B	Negative of Slope of Long-Time Kinetics (min^{-1})	Negative of Intercept of Long-Time Kinetics (Dimensionless)	Results of Long-Time Kinetics n	Results of Long-Time Kinetics $\epsilon \times 10^3$	Holdup per stage(g)
4	0.8257	2.3544	0.0115 ± 0.0011	0.47 ± 0.19	44.7 ± 4.3	0.93 ± 0.09	0.109
3	0.8232	2.3684	0.0082 ± 0.0007	1.33 ± 0.12	60.3 ± 5.1	0.75 ± 0.06	0.092
8	0.8225	2.3757	0.0096 ± 0.0011	1.29 ± 0.23	46.9 ± 5.4	0.83 ± 0.10	0.125
2	0.8250	2.3559	0.0110 ± 0.012	1.12 ± 0.14	50.8 ± 5.5	1.00 ± 0.11	0.099
1	0.8243	2.3628	0.0153 ± 0.0012	0.44 ± 0.20	43.3 ± 3.4	0.99 ± 0.08	0.114
6	0.8232	2.3683	0.0116 ± 0.0019	0.96 ± 0.35	51.5 ± 8.4	0.89 ± 0.15	0.111
7	0.8233	2.3755	0.0163 ± 0.0046	1.52 ± 0.66	44.3 ± 12.5	0.65 ± 0.18	0.111
5	0.8223	2.3710	0.0077 ± 0.0008	0.73 ± 0.11	65.5 ± 6.8	0.81 ± 0.08	0.107
9	0.8235	2.3642	0.0127 ± 0.0010	0.66 ± 0.18	68.5 ± 5.4	0.79 ± 0.06	0.091
10	0.8211	2.3841	0.0150 ± 0.0019	0.23 ± 0.30	59.2 ± 7.5	0.69 ± 0.09	0.122
12	0.8230	2.3713	0.0157 ± 0.0025	0.28 ± 0.54	53.9 ± 8.6	0.80 ± 0.13	0.106
11	0.8228	2.3758	0.0212 ± 0.0015	0.66 ± 0.19	48.9 ± 3.5	0.72 ± 0.05	0.111

TABLE XIX.

Separation Factor $\alpha(^{12}C/^{13}C)$ as a Function of Temperature

Temperature (^{o}K)	$(\alpha-1)\ x10^{3}$
169.1	-0.93 $\pm$0.09
175.9	-0.75 $\pm$0.06
176.1	-0.83 $\pm$0.10
180.7	-1.00 $\pm$0.11
184.4	-0.99 $\pm$0.08
184.9	-0.89 $\pm$0.15
186.3	-0.65 $\pm$0.18
187.5	-0.81 $\pm$0.08
196.9	-0.79 $\pm$0.06
198.4	-0.69 $\pm$0.09
200.2	-0.80 $\pm$0.13
205.9	-0.72 $\pm$0.05

that the form of the LSF function of Equation (32) is a reasonable one.

These parameters would indicate, if the liquid $CClF_3$ remained liquid with the same density and liquid-external forces, that the magnitude of inverse vapor pressure isotope effect slowly decreases with decreasing temperature until $T \simeq 10^{o}K$, at which point there would be no isotope effect. However, one should not give too much quantitative significance to these values of A and B, since the deviations are too large. Thus, if A were 15 instead of 1.5, the cross-over temperature at which the vpie vanishes would have been $100^{o}K$ rather than $10^{o}K$. Again, if for instance the value of $(\alpha - 1)$ at $175.9^{o}K$ were -0.72×10^{-3}, the slope would have been 4.2 ± 15.2 and the intercept would have been -0.173 ± 0.081. These large uncertainties are all caused by the small value of carbon isotope effect.

The values of A and B of Equation (35) and (36) are of the right order of magnitude, however. Bigeleisen, Cragg and Jeevanandam[12] reported that, for liquid methane $^{13}C/^{12}C$, $A = 93.8 \pm 6.1$ and $B = 0.535 \pm 0.06$. This experimental value of A for methane is much larger than the present value of A for $CClF_3$, this marked reduction in A is expected due to the larger molecular weight and larger moments of intetia of $CClF_3$. Based on experimental data on the interatomic distances $R_{CF} = 1.328$ A and $r_{CCl} = 1.751\ A^{o}$ and the tetrahedral angles for $CClF_3$, one obtains $I_A = I_B = 150.590$ and $I_C = 89.347$ for $^{12}C^{35}ClF_3$, in units of millidynes per angstrom per atomic mass unit. The molecular weights of $^{12}C^{35}ClF_3$ and $^{13}C^{35}ClF_3$ are 103.964 and 104.967, respectively. If one assumes that all translational and rotational vibrations of molecule in the liquid are independent and uncoupled harmonic oscillations, then Equation (12) would become

$$A = \frac{1.4385}{24\ (5.88852 \times 10^{-7})} \times \left[3\, f_t \left(\frac{1}{M'} - \frac{1}{M} \right) + f_{Rx} \left(\frac{1}{I'_x} - \frac{1}{I_x} \right) + f_{Ry} \left(\frac{1}{I'_y} - \frac{1}{I_y} \right) + f_{Rz} \left(1 / I'_z - 1 / I_z \right) \right] \qquad (37)$$

where the factor 1.4385 is equal to hc/k, $(5.88852 \times 10^{-7})^{-1}$ is the conversion factor between the eigenvalues of secular equation in units of mdyne $\cdot$ $\mathring{A}^{-1}$ $\cdot$ $(amu)^{-1}$ and the eigenvalues in units of cm^{-2}; f_T is the translational force constant; M' and M are molecular weights of the light and heavy isotopic molecules; f_{Rx}, f_{Ry}, and f_{Rz} are the rotational force constants for hindered rotations around the three principal axes; I_x, I_y, and I_z are the moments of inertia. Thus, assuming $f_T \sim 0.06$ mdyne $\cdot \mathring{A}^{-1}$ and $f_R \sim 0.05$ mdyne $\cdot$ $\mathring{A}^{-1}$, substitution of these molecular constants of $^{12}C^{35}ClF_3$ and $^{13}C^{35}ClF_3$ yields

$$A \text{ for } \frac{P'(^{12}C^{35}ClF_3)}{P\ (^{13}C^{35}ClF_3)} \simeq 1.73 \ {}^{o}K \qquad (38)$$

Thus, the value of A reported in Equation (35) is of the right order of magnitude. It is due to the smallness of A/T^2 term, whose magnitude is of the order of 10^{-5} at T 200°K, that caused the very flat, temperature insensitive behavior of vpie in this investigation of carbon isotope effects in $CClF_3$.

Possible effects due to the existence of stable isotopes of chlorine in $CClF_3$ has been evaluated as follows. The naturally occurring chlorine is 75.53% ($\equiv$ a)^{35}Cl and 24.47% ($\equiv$ b)^{37}Cl. Therefore, $CClF_3$ contains four isotopic species; $^{12}C^{35}ClF_3$, $^{13}C^{35}ClF_3$, $^{12}C^{37}ClF_3$ and $^{13}C^{37}ClF_3$. Let us assume that these isotopic species, at the time of their synthesis, had

distributed themselves according to the equilibrium constant for

$$^{12}C^{37}ClF_3 + {}^{13}C^{35}ClF_3 \rightleftharpoons {}^{12}C^{35}ClF_3 + {}^{13}C^{37}ClF_3 \qquad (39)$$

The equilibrium constant is

$$\ln K = \ln \frac{s}{s'} f \left[\frac{^{12}C^{35}ClF_3}{^{13}C^{35}ClF_3}\right] - \ln \frac{s}{s'} f \left[\frac{^{12}C^{37}ClF_3}{^{13}C^{37}ClF_3}\right] \qquad (40)$$

According to Bigeleisen's first rule of the mean[25], this K is unity to the extent of validity of the first quantum correction. Thus, ^{35}Cl, or ^{37}Cl, has no preference for ^{12}C or ^{13}C as a partner in the $CClF_3$ molecule. The atom fraction of ^{35}Cl, or of ^{37}Cl, in ^{12}C species is equal to the atom fraction of ^{35}Cl (or of ^{37}Cl) in ^{13}C species. If the mole fractions of $^{12}C^{35}ClF_3$, $^{13}C^{35}ClF_3$, $^{12}C^{37}ClF_3$ and $^{13}C^{37}ClF_3$ are denoted by (1-x-y-z), x, y and z, respectively, we have

$$\frac{y}{1-x-z} = b$$

$$\frac{z}{x+z} = b$$

$$\frac{x}{1-y-z} = a$$

$$\frac{z}{y+z} = a$$

One of these four equations is redundant, the solution is uniquely determined as

$$\left.\begin{aligned} x_1^{\,o} &= \text{Mole fraction } {}^{12}C^{35}ClF_3 = (1-a)(1-b) \\ x_2^{\,o} &= \text{Mole fraction } {}^{13}C^{35}ClF_3 = a\,(1-b) \\ x_3^{\,o} &= \text{Mole fraction } {}^{12}C^{37}ClF_3 = (1-a)\,b \\ x_4^{\,o} &= \text{Mole fraction } {}^{13}C^{37}ClF_3 = ab \end{aligned}\right\} \qquad (41)$$

Now, assume that, in each stage of the distillation column having n theoretical plates, the three heaviest isotopic species each fractionates against ${}^{12}C^{35}ClF_3$ without any exchange of isotopes between them. Set

$$\alpha\left(\frac{{}^{12}C^{35}ClF_3}{{}^{13}C^{35}ClF_3}\right) \equiv \alpha_2 \qquad (42)$$

$$\alpha\left(\frac{{}^{12}C^{35}ClF_3}{{}^{12}C^{37}ClF_3}\right) \equiv \alpha_3 \qquad (43)$$

and

$$\alpha\left(\frac{{}^{12}C^{35}ClF_3}{{}^{13}C^{37}ClF_3}\right) \equiv \alpha_4 \qquad (44)$$

Assuming that the boiler composition stays at the natural enrichment, the n stages of cascade will then lead to the following overall steady state separations:

$$q_2 \equiv \frac{(x_2 \,/\, x_1)}{(x_2^{o} \,/\, x_1^{o})} = \alpha_2^{n} \simeq 1 + n\,\epsilon_2 \qquad (45)$$

$$q_3 \equiv \frac{(x_3/x_1)}{(x_3^o/x_1^o)} = \alpha_3^n \simeq 1 + n\epsilon_3 \tag{46}$$

$$q_4 \equiv \frac{(x_4/x_1)}{(x_4^o/x_1^o)} = \alpha_4^n \simeq 1 + n\epsilon_4 \tag{47}$$

We are interested in the atom fraction of ^{13}C in the condenser:

$$x_2 + x_4 = \left(\frac{x_1}{x_1^o}\right) a\alpha_2^n \left[(1 - b) + \frac{\alpha_4}{\alpha_2}\right]^n$$

as opposed to the atom fraction of ^{12}C in the condenser;

$$x_1 + x_4 = \left(\frac{x_1}{x_1^o}\right) (1 - a) \left[(1 - b) + b\alpha_3^n\right]$$

Thus, the atom ratio of ^{13}C to ^{12}C in the condenser is

$$R_c \equiv \frac{x_2 + x_4}{x_1 + x_3} = \frac{a}{1-a} \alpha_2^n \left[\frac{1 + (b/(1-b))(\alpha_4/\alpha_2)^n}{1 + (b/(1-b))(\alpha_3^n)}\right]$$

$$\simeq \frac{a}{1-a} \alpha_2^n \left\{1 + \frac{b}{1-b}\left[\frac{\alpha_4}{\alpha_2} - \alpha_3^n\right]\right\}$$

$$\simeq \frac{a}{1 - a} \alpha_2^n \left[1 + \frac{nb}{1-b}(\epsilon_4 - \epsilon_2 - \epsilon_3)\right] \tag{48}$$

But, the atom ratio of ^{13}C to ^{12}C in the boiler is

$$R_b = \frac{x_2^o + x_4^o}{x_1^o + x_3^o} = \frac{a}{1-a} \tag{49}$$

Therefore, the overall separation of ^{13}C vs ^{12}C between the condenser and boiler is

$$Q \equiv \frac{R_c}{R_b} = \alpha_2^n \left[1 + \frac{nb}{1-b}\left[\epsilon_4 - \epsilon_2 - \epsilon_3\right]\right] \tag{50}$$

On the other hand,

$$\epsilon_2 \simeq \ln\alpha_2 = \frac{A_2}{T^2} - \frac{B_2}{T}$$

$$\epsilon_3 \simeq \ln\alpha_3 = \frac{A_3}{T^2} - \frac{B_3}{T} \tag{51}$$

$$\epsilon_4 \simeq \ln\alpha_4 = \frac{A_4}{T^2} - \frac{B_4}{T}$$

where

$$A_4 \simeq A_2 + A_3 \tag{52}$$

according to the first-order sum rule under the assumption of negligible external-internal interaction. In any case, the terms of A/T^2 are small. Similarly the relation

$$B_4 \simeq B_2 + B_3 \tag{53}$$

is not a bad first-order approximation, according to the zero-point energy approximation[26] and under the assumption of negligible external-internal interaction, although the second-order deviation from such rules have been explicitly investigated[27] and have been associated with not-so-negligible external-internal interactions in the case of D/H substitutions in ethylene.

Under these assumptions, Equation (50) thus predicts

$$Q \simeq \alpha_2^n \quad , \tag{54}$$

which implies that the presence of chlorine isotopes in CCl_3F would have no effects on the fractionation of carbon isotopes, according to this first-order approximation. Any effect of chlorine isotopes thus must come from the higher-order deviation which would lead to

$$\epsilon_4 \neq \epsilon_2 + \epsilon_3 \, . \tag{55}$$

Since 1/T of the present study varies only between 4.85×10^{-3} and 5.92×10^{-3}, the reciprocal of an appropriate temperature T_{av}, taken within the range of the experimental temperatures, may be factored out of the Bigeleisen's first-order relation,

$$\ln \alpha = \frac{A}{T^2} - \frac{B}{T} \quad ,$$

In this case, the functional form for the least-squares fitting of the data of Table XVIII becomes

$$\ln \alpha = \frac{A'}{T} - B' . \tag{56}$$

The fit of the data to this form yields

$$A' = 0.173 \pm 0.098, \tag{57}$$

and

$$B' = (0.11 \pm 0.53) \times 10^{-3} \, . \tag{58}$$

Based on the standard deviations of these LSF constants, there seems to be no obvious advantage for either one of the two functional forms.

VI. CONCLUSION

The vapor pressure isotope effect between the vapor pressure of $^{12}CC1F_3$, P', and the vapor pressure of $^{13}CC1F_3$, P, between the temperatures of 169° and 206°K, may be expressed as

$$\ln \frac{P'}{P} = \frac{(1.5 \pm 14.1)}{T^2} - \frac{(0.159 \pm 0.076)}{T} , \quad (59)$$

or

$$\ln \frac{P'}{P} = \frac{(0.173 \pm 0.098)}{T} - (0.11 \pm 0.53) \times 10^{-3}. \quad (60)$$

To the first-order approximation, the presence of chlorine isotopes would not affect the fractionation of carbon isotopes.

VII. RECOMMENDATION

In order to investigate the possible effects of chlorine isotopes to the separation of carbon isotopes in $CClF_3$, it would be necessary to carry out a precision differential manometry of vapor pressure differences among the four isotopic specie of $CClF_3$ in a precision cryostat[22] of the type Prof. Bigeleisen has at University of Rochester, which is under construction in Prof. Ishida's laboratory. It would be necessary to synthesize the isotopic $CClF_3$ with sufficiently high isotopic purity to insure significant difference in vapor pressures and to minimize corrections for the isotopic impurities in the specimen. This procedure is highly recommended over the distillation studies, because the expected small isotope effects may be quantitatively measured only through the high precision cryostatic technique.

VIII. ACKNOWLEDGEMENT

I wish to extend my thanks to:

* The United States Energy Research and Development Administration, whose research contract with Professor T. Ishida made this research possible.

* Dr. Lou Friedman and Mr. Pete Irsa of Brookhaven National Laboratory for the use of their excellent mass spectrometry laboratory and their indulgence in teaching me the use of their equipment.

* Professor Jacob Bigeleisen of the University of Rochester for letting us use his precision cryostat for the determination of the vapor pressure of $CClF_3$.

* The graduate and undergraduate research students of Professor T. Ishida for immeasurable assistance in this research.

* My father for his assistance in the physical preparation of this thesis.

* Mr. Ottmar Safferling for his construction, maintenance and repair of the considerable amount of glass equipment used in this research.

* Professors H. Finston and P.G. Mennitt for their excellent guidance as thesis committee members.

* Lastly, but most importantly, Professor T. Ishida for his outstanding guidance, patience and devotion to excellence.

IX. REFERENCES

1) Report to United States Atomic Energy Commission, LA-4391, "A Carbon-13 Production Plant Using Carbon Monoxide Distillation", D.E. Armstrong, A.C. Briesmeister, B.B. McInteer, R.M. Potter. (1970).

2) J.P. Agrawal, Separation Science, 6 (6), 819 (1971). J.P. Agrawal, Ibid., 6 (6), 831 (1971). A.R. Gupta and T.I. Taylor, Annual Progress Report to U.S.A.E.C., CU-15-62 (1962).
Madhav R. Ghate and T.I. Taylor, Annual Progress Report to U.S.A.E.C., CU-755-6 (1969).
Madhav R. Ghate and T.I. Taylor, Ibid., CU-755-7 (1970).

3) R.A. Schwind, Chem. Prog. Eng., 50, 75 (1969); AEC Report MLM-1886, Mound Laboratory, Feb. 1972.

4) C.A. Hutchinson, D.W. Stewart, H.C. Urey, J. Chem. Phys., 8, 532 (1940).

5) J.S. Drury, L.L. Brown, A.A. Palko, AEC Report ORNL 4306 (1968).

6. M.R.Ghate, T.I. Taylor, Annual Progress Report to U.S. A.E.C., COO-3263 (1973).

7) K. Clausius and G. Dickel, Naturwiss, 26, 546 (1938).

8) J. Bigeleisen and M.G. Mayer, J. Chem. Phys.,15, 261 (1947).

9) C & E News, 53, #19 17 (1975).

10) J. Bigeleisen, J. Chem. Phys.,34, 1485, 261 (1947).

11) K. Cohen, "The Theory of Isotope Separation as Applied to the Large Scale Production of ^{235}U", McGraw Hill Book Co., N.Y. (1951).

12) J. Bigeleisen, C.B. Cragg, M. Jeevanandam, J. Chem. Phys., 47, 4335 (1967).

13) P. Baertschi, W. Kuhn and H. Kuhn, Nature, 171, 1018 (1953).

14) M. Wolfsberg, J. Chem. Phys., 60, 15 (1963).

15) A.E.C. Report, NYO-4266-1, T. Ishida, (1972).
A.E.C. Report, COO-3127-1, T. Ishida, (1973).

16) J. Bigeleisen, Advan. Chem. Ser., 89, 1 (1969).

17) C.J. Rodden, Ed., "Analytical Chemistry of the Manhattan Project", McGraw Hill Book Co., New York (1950)

IX. REFERENCES (continued)

18) J. Bigeleisen, Private Communication.

19) J. Bigeleisen, S.V. Ribnikar, J. Chem. Phys.,35, 1297 (1961).

20) J. Bigeleisen, M.J. Stern, A. Van Hook, J. Chem. Phys., 38, 497 (1963).

21) For instance, F. Albright and J.J. Martin, Ind. Eng. Chem., 44, 188 (1952); also, Handbook of Chemistry and Physics, 53rd Edition, P. D151 (1972).

22) J. Bigeleisen, F. P. Brooks, T. Ishida and S.V. Ribnikar, Rev. Sci. Instr., 39, 353 (1968).

23) M. Benedict and T.H. Pigford, "Nuclear Chemical Engineering", McGraw Hill Book Co., Inc., New York (1957).

24) M.E. Rose, Phys. Rev.,91, 610 (1953).

25) J. Bigeleisen, J. Chem. Phys., 23, 2264 (1955).

26) J. Bigeleisen and P. Goldstein, Z. Naturfirsch, 18, 205 (1963).

27) M.J. Stern, A. Van Hook and M. Wolfsberg, J. Chem. Phys., 39, 3179 (1963).

APPENDIX I

Kinetics of A Square Cascade of Close-Separation Stages Under Total Reflux*

by Takanobu Ishida and Henry Wieck
Brooklyn College of
The City University of New York
Brooklyn, New York 11210

Abstract

To facilitate the determination of the separation factor and the number of theoretical stages of a square cascade of close-separation stages from measurements of its long-time kinetics under total reflux, extensive tables of kinetics parameters have been produced in accordance with K. Cohen's theory. Cohen's treatment has been extended in several ways. The kinetics parameters of the first transient term have been finely mapped, and the ranges of various parameters have been extended to include large overall separations as well as the stripping section. The second transient term of the long-time kinetics has been evaluated, and a possible application of this correction term has been suggested in relation to the experimental determination of the column parameters. Under comparable conditions a steady concentration profile, along the column, is attained faster in the stripping section than in the enriching section. A distinction between the enriching and stripping section is important in using the transient theory for the evaluation of the cascade characteristics under ordinary laboratory conditions.

* Research supported by the U.S. Atomic Energy Commission under Contract No. AT(11-1)-3127.

The transient behavior of a square, counter-current, cascade of close-separation stages during start-up period was theoretically analyzed by K.Cohen(1)in relation to the fractionation of uranium-235. A consideration of the material balance of desired substance between the product stage and the s-th stage under conditions of constant flows leads(1) to a partial differential equation:

$$\lambda \frac{\partial N}{\partial t} = \frac{\partial^2 N}{\partial s^2} - \epsilon \frac{\partial}{\partial s}\left[\Psi N + N\,(1 - N)\right] \qquad (1)$$

where N = N(s,t) is the average mole fraction of the desired substance in the input streams for the s-th stage (cf: Figure 1), counted toward the product end starting from the feed point in the cascade, at time t from the start-up of the cascade. Other quantities used in Eqn. (1), all being dimensionless, are:

$\epsilon = \alpha - 1$, where α is the "head-to-tail" separation factor. This use of α is different from Cohen's, in that the latter is the "head" or "tail" separation factor. This α is twice Cohen's α (2,3).

$\lambda = 2h$, where h is the holdup per stage per unit flow, or the average process time per stage.

$\Psi = \frac{2P}{\epsilon L}$, where P is the production rate, or the rate of withdrawal of product at the product-end of the column, and L is the total interstage flow rate at the stage s. In a square cascade, L is independent of s. In a square distillation cascade under total reflux, L is also equal to twice the boil-up rate.

When the mole fraction of the desired substance is negligibly small compared to unity, Eqn. (1) becomes linear:

$$\lambda \frac{\partial N}{\partial t} = \frac{\partial^2 N}{\partial s^2} - \epsilon (1 + \Psi) \frac{\partial N}{\partial s} \qquad (2)$$

This would be the case in preliminary fractionation processes of isotopes, such as ^{235}U, D, ^{13}C and ^{15}N. Cohen solved the equation under the following initial and boundary conditions:

At t = 0;	$N(s, t = 0) = N_o$	at all s
At s = 0 (feed point);	$N(0, t) = N_o$	at all t
At s = n (product end);	P = 0	at all t
	Holdup in refluxer = H	

Such a solution is of general interest due to two reasons. First, in large-scale production, one seeks to minimize the initial start-up period during which the system is operated under total reflux. Second, observations of the transient behavior can be used for evaluating such separation system constants as the number of theoretical plates and the separation factor(1). The theory of transient column behavior is of primary importance in both applications. The present study is a part of our effort to extend limits of the validity of Cohen's theory.

The solution , at $t > \lambda n^2/10$, is of the form (1)

$$\frac{N(n,t)}{N_o} = e^{\epsilon n} - (e^{\epsilon n} - 1)\, A(\epsilon n, K/\lambda n) \exp\left[- \frac{B(\epsilon n, K/\lambda n)\, t}{\lambda n^2}\right] \qquad (3)$$

where A and B are related to the smallest root of a transcendental equation, which will be discussed later. Cohen gave tables of A and B for $K/\lambda n$ between 0.0 and 0.5 in steps of 0.1 and for ϵn between 0.0 and 1.2 in steps of 0.1. It is highly desirable to extend and refine Cohen's table beyond the limits for ϵn in both the positive and negative directions. We also felt that it is useful to extend the time limit to the region below $t = \lambda n^2/10$ by adding a higher

term of expansion to Eqn. (3).

MATHEMATICAL PROCEDURE

Cohen's solution can be transformed into

$$\frac{N - N_o}{N_\infty - N_o} = 1 - A_1 e^{-B_1 \tau} - A_2 e^{-B_2 \tau} \qquad (4)$$

where $N_\infty = e^{\epsilon n}$ is the overall separation at steady state, and $\tau = t/\lambda n^2$ is the reduced time, or the time measured in the unit of average process time divided by the number of stages. A_1 and B_1 are Cohen's A and B, respectively. The last term in Eqn. (4) represents the next higher term in the approximation.

Both B_1 and B_2 are defined as

$$B \equiv a^2 + x^2, \qquad (5)$$

where $a \equiv \epsilon n$, and x is either the smallest positive root x_1 or the second smallest positive root x_2 of the equation,

$$\tan x = \frac{x}{c + b x^2}, \qquad (6)$$

in which $b \equiv K/\lambda n = H/Lhn$, $K \equiv 2H/L$, and $c \equiv a^2 b + a$. In

the special case of $c > 1$, an imaginary root exists, in which case $B_1 = a^2 - x_o^2$, where x_o is the only root of the equation,

$$\tanh x = \frac{x}{c - b x^2} . \qquad (7)$$

All the cases have been summarized in Table I. It is to be noted that the case of $c < 1$ includes all negative values of c. Cohen's table covers the cases of $0 \leq c \leq 1.92$ for B_1. The case of $a = b = 0$ represents a singular point, where $B_1 = (\pi/2)^2$, although this has no physical meaning. The ranges of x_1 and x_2 for all conceivable cases have been tabulated in Table II.

Table I. Summary of Formula for B_1 and B_2

$c = a^2b + a$	B_1	B_2
< 1	$a^2 + x_1^2$	$a^2 + x_2^2$
$= 1$	a^2	$a^2 + x_1^2$
> 1	$a^2 - x_o^2$	$a^2 + x_1^2$

The pre-exponential coefficients A_1 and A_2 are both related to B_1 and B_2, respectively, by

$$A_i = \frac{2a}{B_i\,(e^{2a} - 1)\left[\, b + \frac{1}{2} + \frac{C_i\,(C_i + 1)}{2\,(B_i - a^2)} \right]} \qquad (8)$$

where

$$C_i \equiv - b\,B_i - a^2 .$$

Singularities exist as follows: When $c = a^2 b + a = 1$,

$$A_1 = \frac{2}{a\,(e^{2a} - 1)\,(b + \frac{1}{3})} , \qquad (9)$$

while A_2 is nonsingular. When $a = 0$,

$$A_i = \frac{1}{B_i \left[\, b + \frac{1}{2} + \frac{C_i\,(C_i + 1)}{2B_i} \right]} \qquad (10)$$

A pair of computer subroutine programs were written, one for calculations of A_1 and B_1, and the other for A_2 and B_2. Each subroutine takes a and b as input from a calling program, and returns a pair of numbers A_i and B_i. The root of the transcendental Eqn. (6) is obtained by using Newton's linear iterative algorithm. All precautions were taken to avoid accidental crossover to an undesired branch of the function during the iterative process.

RESULTS AND DISCUSSION

Numerical results for A_1 and B_1 have been tabulated in Table III for $K/\lambda n$ from 0.00 to 0.50 in steps of 0.05, and for ϵn from -3.0 to +3.0 in steps of 0.1. Similar tabulation is presented for A_2 and B_2 in Table IV. It is seen that the present values of A_1 and B_1 are in complete agreement with Cohen's, wherever the comparison is possible.

In Figures 2 and 3, values of A_1 and B_1, respectively, have been plotted against ϵn, at various values of $K/\lambda n$, the ratio of the holdup in the product refluxer to the total holdup in the column. The negative ϵn represents the stripping section. In reference to Eqn. (4), the contribution of the first transient term, $A_1 e^{-B_1 \tau}$, to the fractional equilibrium attainment, $(N - N_o)/(N_\infty - N_o)$, has been plotted in Figure 4 as a function of the reduced time τ for the case of no refluxer holdup. The line for $\epsilon n = 0$ has been included only for reference purposes. For the same reduced time, the stripping section attains its steady state much faster than the enriching section. However, the graph does not by any means imply that, within the stripping section, the equilibrium time in the longer column is shorter. The equilibrium time in the stripping section does in fact increase with the number of plates since $t = \lambda n^2 \tau$, although

the rate of increase is much slower than that in the enriching section.

Plots of A_2, B_2, and $A_2 e^{-B_2 \tau}$ are presented in Figures 5, 6, and 7, respectively. The most striking difference from the previous graphs is the complete reversal of trends of A as a function of ϵn and of $K/\lambda n$. Not only does A_2 decrease with increasing ϵn, but also decreases with increasing holdup ratio, while A_1 increases with increasing ϵn and $K/\lambda n$. Although the magnitude of A_2 is smaller than A_1, it is evident that the second transient term becomes relatively significant at smaller values of ϵn and $K/\lambda n$. It is noted from Figure 6 that, compared to the first transient term, the second term is damped much faster, so that the second term in general is important at small values of enrichment, holdup ratio and time. Figure 7 verifies this for $K/\lambda n = 0$. The crossing over of lines in the stripping section of Figure 7 is a result of interaction of the opposite trends of A_2 and B_2 against varying ϵn.

Finally, the relative importance of two transient terms is shown in Figure 8. It must be noted that the comparison is made at $K/\lambda n = 0$, the smallest possible value, at which the second transient term is most significant. It is thus evident that the limitation of $\tau > 0.10$ that Cohen placed for the validity of his solution, Eqn. (3), was well

founded as far as the enriching section is concerned. In the stripping section and/or at shorter time, however, the second transient term is significant.

On the other hand, the third transient term in general contributes insignificantly to $(N - N_o)/(N_\infty - N_o)$ at the reduced time much smaller than 0.1. Based on analyses of the upper and lower limits of the third smallest root of Eqn. (6), it has been found that the upper limits of the third term is of the order of 10^{-2} or smaller, even at $\tau = 0.01$ for $\epsilon n = -3$ and $K/\lambda n = 0$, the condition under which the contribution would be the greatest. Typically, for $\epsilon n = -3$ and $K/\lambda n = 0$, the upper limit is 0.05, 0.03 and 0.0002, at $\tau = 0.01$, 0.02 and 0.10, respectively. For $\epsilon n = +1$ and $K/\lambda n = 0$, the limit is 0.01, 0.06 and 0.0002, at $\tau = 0.01$, 0.02 and 0.10, respectively. It is thus fair to conclude that the inclusion of the second transient term extends the lower limit of applicability of the solution to $\tau = 0.01$ for any enriching section, and the uncertainty at this τ is at most 0.01. For the stripping section, the error may be as high as 0.05 at $\tau = 0.01$ under extreme conditions.

As an application of the subroutine programs written for calculations of A_1, B_1, A_2, and B_2, the reduced time, $\tau_{0.95}$, required for the achievement of 95 percent of the steady state value was calculated at various values of

ϵn and $K/\lambda n$. The problem is that of solving Eqn. (4) for τ, with the left-hand side equated to 0.95. It involves an iterative procedure. Results of these calculations have been plotted in Figure 9. The graph clearly shows an increasing trend in the enriching section of equilibrium time with increasing holdup in product refluxer, $K/\lambda n$, and overall separation ϵn. It should also be noted that the actual equilibrium time $t_{0.95}$ is equal to $\lambda n^2 \times \tau_{0.95}$, which in fact also increases with the length of the stripping section.

One feature in Figure 9 worth noting is the fact that the equilibrium time increases sharply with an increasing holdup ratio. This is due to the fact that, for a large holdup in the product refluxer, a large inventory of the desired isotope must be built up at the product end. The desired isotope is, by definition (cf: Eqns. (1) and (2)), the minor component, i.e., $N \ll 1$. When the minor component enriches in the liquid phase, the material holdup in the product refluxer is necessarily large. This is the case existing in most isotope separation plants. For example, in the distillation of carbon monoxide, ^{13}C (natural abundance = 1.1%) enriches in the liquid. In the exchange of nitrogen isotopes between nitric oxide and nitric acid, ^{15}N (0.37%) concentrates in the aqueous phase (4). However, the reverse situation is possible: the minor component may be

enriched in the gas phase. For instance, ^{13}C enriches in the gas phase in an exchange between hydrogen cyanide and aqueous cyanide solution(5).In a distillation, a heavy isotopic molecule may have a higher vapor pressure than the lighter molecule in a temperature range in which the vapor pressure isotope effect is "inversed". The inverse effect is favored in an isotopic molecular pair which exhibits a large isotope effect in the zero-point energy shifts of internal vibrations upon condensation(6).In these cases, the heavier isotopic species, which is the minor isotope for most of the light elements, enriches in the gas phase. Here, the holdup in the product refluxer can be made negligibly small. All other considerations being comparable, a system in which the desired isotope enriches in the gas phase has a definite advantage in that it requires a shorter start-up period.

For the determination of the separation factor and the number of theoretical plates using the long-time kinetics, one would take up to the first transient term of Eqn. (4), and obtain the best straight line through a plot of $\ell n ((N_\infty - N)/(N_\infty - N_o))$ against τ. The intercept and the slope give A_1 and B_1, respectively, both of which are functions of ϵ and n. This information, combined with experimental data on ϵn, which is $\ell n\ N_\infty$, leads to the first approximation

for ϵ and n. The second transient term in Eqn. (4) may then be added to $(N_\infty - N)/(N_\infty - N_o)$ to correct for small deviations of experimental points corresponding to small τ from the straight line. The natural logarithm of the resulting quantity would then be plotted against τ, and the second approximation for ϵ and n would be obtained accordingly.

It is worth noting that, if the desired isotope enriches in the liquid, that which is operated in an ordinary, laboratory scale, distillation column, with a large hold-up in the boiler, is a stripping section. Due to the non-symmetry of transient behavior between the enriching and stripping sections, it is incorrect to use the tables of A's and B's of the positive ϵn, when the desired minor component enriches in the liquid. On the other hand, if the minor component enriches in the vapor phase, the proper tables to use are the ones for the positive ϵn.

Such a distinction is not necessary for consideration of the transient period for an operation of production scale, because such a column is always operated as an enriching column.

ACKNOWLEDGEMENT

We wish to express our gratitude to Professor William Spindel of Yeshiva University for his stimulating discussion.

REFERENCES

1) Cohen, K., "The Theory of Isotope Separation as Applied to The Large-Scale Production of U-235," McGraw-Hill Book Co., Inc., New York, 1951.

2) Bigeleisen,J.,and S. V. Ribnikar, J. Chem. Phys. 35, 1297 (1961); J. Bigeleisen, M. J. Stern and W. A. VanHook, J. Chem. Phys. 38, 497 (1963); J. Bigeleisen, C. B. Cragg and M. Jeevanandam, J. Chem. Phys. 47, 4335 (1967).

3) Benedict,M.,and T. H. Pigford, "Nuclear Chemical Engineering," McGraw-Hill Book Co., Inc., New York (1957).

4) Spindel,W.,and T. I. Taylor, J. Chem. Phys. 24, 626 (1956).

5) Hutchison, C.A., D. W. Stewart and H. C. Urey, J. Chem. Phys. 8, 532 (1940).

6) Bigeleisen,J., J. Chem. Phys. 34, 1485 (1961); M. J. Stern, W. A. VanHook and M. Wolfsberg, ibid. 39, 3179 (1963); M. Wolfsberg, J. Chim. Phys. 60, 15 (1963).

Table II. Ranges of Roots of Equation (6)

c	b	γ *	x for $B_1 = a^2 + x^2$ **	x for $B_2 = a^2 + x^2$	Remarks
$c > 1$	$b = 0$		$< \infty$	$\left(\pi, \frac{3\pi}{2}\right)$	** When $c > 1$, $B_1 = a^2 - x^2$ where x is magnitude of imaginary root.
	$b \neq 0$		$< \sqrt{\frac{c}{b}}$		
$c = 1$			$= 0$	$\left(\pi, \frac{3\pi}{2}\right)$	
$0 < c < 1$			$\left(0, \frac{\pi}{2}\right)$	$\left(\pi, \frac{3\pi}{2}\right)$	
$c = 0$	$b = 0$		$= 0$	none	$B_1 = \left(\frac{\pi}{2}\right)^2$
	$b \neq 0$		$\left(0, \frac{\pi}{2}\right)$	$\left(\pi, \frac{3\pi}{2}\right)$	$c < 0$
$c < 0$	$b = 0$		$\left(\frac{\pi}{2}, \pi\right)$	$\left(\frac{3\pi}{2}, 2\pi\right)$	$a < 0$
	$b \neq 0$	$\gamma < \frac{\pi}{2}$	$\left(\gamma, \frac{\pi}{2}\right)$	$\left(\pi, \frac{3\pi}{2}\right)$	* $\gamma \equiv \sqrt{-c/b}$
		$\frac{\pi}{2} < \gamma < \frac{3\pi}{2}$	$\left(\frac{\pi}{2}, \gamma\right)$	$\left(\pi, \frac{3\pi}{2}\right)$	
		$\frac{3\pi}{2} < \gamma$	$\left(\frac{\pi}{2}, \pi\right)$	$\left(\frac{3\pi}{2}, \begin{matrix}\gamma \\ \text{or} \\ 2\pi\end{matrix}\right)$ ***	*** γ or 2π, whichever is smaller.

Coefficients for the First Transient Term

ϵ		A_1 and B_1 at Holdup Ratio $K/\lambda n$ of										
		0.00	0.05	0.10	0.15	0.20	0.25	0.30	0.35	0.40	0.45	0.50
-3.00	A=	0.5046	0.5686	0.6291	0.6840	0.7320	0.7730	0.8073	0.8358	0.8594	0.8788	0.8949
	B=	6.9790	6.5882	6.2005	5.8247	5.4673	5.1326	4.8227	4.5378	4.2771	4.0393	3.8224
-2.90	A=	0.5146	0.5780	0.6376	0.6914	0.7382	0.7781	0.8115	0.8392	0.8621	0.8810	0.8966
	B=	6.7752	6.3897	6.0092	5.6419	5.2937	4.9686	4.6681	4.3922	4.1401	3.9102	3.7006
-2.80	A=	0.5248	0.5875	0.6462	0.6988	0.7445	0.7833	0.8157	0.8426	0.8649	0.8832	0.8985
	B=	6.5754	6.1952	5.8218	5.4628	5.1238	4.8080	4.5166	4.2496	4.0057	3.7835	3.5810
-2.70	A=	0.5350	0.5971	0.6548	0.7063	0.7508	0.7885	0.8200	0.8461	0.8677	0.8856	0.9004
	B=	6.3795	6.0047	5.6383	5.2876	4.9574	4.6507	4.3683	4.1098	3.8740	3.6593	3.4637
-2.60	A=	0.5453	0.6068	0.6635	0.7138	0.7571	0.7938	0.8244	0.8497	0.8707	0.8880	0.9024
	B=	6.1875	5.8181	5.4587	5.1161	4.7946	4.4968	4.2231	3.9730	3.7450	3.5376	3.3487
-2.50	A=	0.5557	0.6165	0.6722	0.7213	0.7635	0.7991	0.8288	0.8534	0.8737	0.8905	0.9045
	B=	5.9993	5.6353	5.2829	4.9483	4.6354	4.3462	4.0810	3.8390	3.6187	3.4183	3.2360
-2.40	A=	0.5662	0.6262	0.6809	0.7289	0.7700	0.8045	0.8333	0.8571	0.8768	0.8931	0.9066
	B=	5.8150	5.4565	5.1109	4.7842	4.4797	4.1990	3.9420	3.7079	3.4950	3.3015	3.1256
-2.30	A=	0.5767	0.6360	0.6896	0.7365	0.7764	0.8099	0.8378	0.8608	0.8799	0.8957	0.9088
	B=	5.6346	5.2814	4.9427	4.6237	4.3274	4.0550	3.8062	3.5797	3.3740	3.1873	3.0175
-2.20	A=	0.5873	0.6458	0.6984	0.7441	0.7829	0.8154	0.8423	0.8646	0.8831	0.8984	0.9111
	B=	5.4579	5.1102	4.7782	4.4669	4.1787	3.9144	3.6734	3.4544	3.2557	3.0755	2.9117
-2.10	A=	0.5979	0.6556	0.7071	0.7517	0.7894	0.8209	0.8469	0.8685	0.8863	0.9011	0.9134
	B=	5.2850	4.9427	4.6175	4.3137	4.0334	3.7770	3.5436	3.3320	3.1401	2.9661	2.8082
-2.00	A=	0.6086	0.6655	0.7159	0.7593	0.7959	0.8263	0.8515	0.8724	0.8896	0.9038	0.9157
	B=	5.1159	4.7789	4.4604	4.1641	3.8915	3.6428	3.4170	3.2124	3.0271	2.8593	2.7071
-1.90	A=	0.6192	0.6753	0.7246	0.7668	0.8023	0.8318	0.8562	0.8763	0.8929	0.9066	0.9181
	B=	4.9504	4.6189	4.3070	4.0180	3.7530	3.5119	3.2933	3.0956	2.9168	2.7550	2.6082

Table III. (Continued)

ϵn		A_1 and B_1 at Holdup Ratio $K/\lambda n$ of										
		0.00	0.05	0.10	0.15	0.20	0.25	0.30	0.35	0.40	0.45	0.50
-1.80	A=	0.6299	0.6851	0.7333	0.7744	0.8088	0.8373	0.8608	0.8802	0.8962	0.9095	0.9206
	B=	4.7886	4.4626	4.1573	3.8754	3.6179	3.3842	3.1727	2.9817	2.8091	2.6531	2.5117
-1.70	A=	0.6406	0.6948	0.7420	0.7819	0.8152	0.8428	0.8654	0.8841	0.8995	0.9123	0.9230
	B=	4.6305	4.3099	4.0111	3.7364	3.4862	3.2596	3.0551	2.8706	2.7041	2.5537	2.4175
-1.60	A=	0.6513	0.7046	0.7506	0.7894	0.8216	0.8482	0.8701	0.8880	0.9029	0.9152	0.9255
	B=	4.4760	4.1608	3.8685	3.6008	3.3577	3.1382	2.9404	2.7623	2.6017	2.4568	2.3256
-1.50	A=	0.6619	0.7143	0.7592	0.7968	0.8280	0.8536	0.8747	0.8920	0.9063	0.9181	0.9280
	B=	4.3251	4.0154	3.7294	3.4686	3.2326	3.0199	2.8287	2.6567	2.5019	2.3623	2.2360
-1.40	A=	0.6726	0.7239	0.7677	0.8042	0.8343	0.8590	0.8793	0.8959	0.9096	0.9210	0.9305
	B=	4.1777	3.8734	3.5939	3.3398	3.1107	2.9047	2.7199	2.5540	2.4047	2.2703	2.1487
-1.30	A=	0.6831	0.7335	0.7761	0.8115	0.8406	0.8644	0.8838	0.8998	0.9130	0.9239	0.9330
	B=	4.0339	3.7350	3.4617	3.2144	2.9920	2.7926	2.6140	2.4539	2.3101	2.1807	2.0637
-1.20	A=	0.6936	0.7429	0.7844	0.8187	0.8467	0.8696	0.8883	0.9037	0.9163	0.9268	0.9355
	B=	3.8935	3.6001	3.3330	3.0923	2.8765	2.6836	2.5110	2.3566	2.2188	2.0935	1.9810
-1.10	A=	0.7041	0.7523	0.7926	0.8258	0.8528	0.8749	0.8928	0.9075	0.9196	0.9296	0.9380
	B=	3.7566	3.4686	3.2077	2.9735	2.7642	2.5775	2.4109	2.2620	2.1286	2.0087	1.9006
-1.00	A=	0.7144	0.7616	0.8008	0.8328	0.8589	0.8800	0.8972	0.9113	0.9229	0.9325	0.9405
	B=	3.6231	3.3405	3.0858	2.8580	2.6550	2.4744	2.3136	2.1700	2.0416	1.9263	1.8224
-0.90	A=	0.7247	0.7708	0.8088	0.8397	0.8648	0.8851	0.9016	0.9151	0.9261	0.9353	0.9430
	B=	3.4930	3.2158	2.9672	2.7456	2.5489	2.3742	2.2190	2.0807	1.9571	1.8462	1.7464
-0.80	A=	0.7348	0.7798	0.8167	0.8465	0.8706	0.8901	0.9059	0.9188	0.9293	0.9381	0.9454
	B=	3.3662	3.0944	2.8518	2.6365	2.4458	2.2770	2.1273	1.9940	1.8751	1.7685	1.6726
-0.70	A=	0.7448	0.7887	0.8244	0.8532	0.8764	0.8950	0.9101	0.9224	0.9325	0.9409	0.9478
	B=	3.2427	2.9763	2.7397	2.5304	2.3457	2.1826	2.0382	1.9099	1.7955	1.6931	1.6011

Table III. (Continued)

		A_1 and B_1 at Holdup Ratio $K/\lambda n$ of										
		0.00	0.05	0.10	0.15	0.20	0.25	0.30	0.35	0.40	0.45	0.50
-0.60	A=	0.7547	0.7975	0.8320	0.8598	0.8820	0.8998	0.9143	0.9260	0.9356	0.9436	0.9502
	B=	3.1225	2.8615	2.6307	2.4275	2.2487	2.0911	1.9519	1.8284	1.7184	1.6200	1.5317
-0.50	A=	0.7645	0.8061	0.8395	0.8662	0.8875	0.9046	0.9183	0.9295	0.9387	0.9462	0.9526
	B=	3.0055	2.7499	2.5249	2.3276	2.1545	2.0023	1.8682	1.7493	1.6436	1.5492	1.4644
-0.40	A=	0.7740	0.8145	0.8468	0.8725	0.8929	0.9092	0.9223	0.9329	0.9416	0.9489	0.9549
	B=	2.8916	2.6414	2.4222	2.2307	2.0632	1.9164	1.7871	1.6728	1.5713	1.4806	1.3993
-0.30	A=	0.7834	0.8228	0.8540	0.8786	0.8981	0.9137	0.9262	0.9363	0.9446	0.9514	0.9571
	B=	2.7810	2.5361	2.3226	2.1368	1.9748	1.8331	1.7086	1.5987	1.5012	1.4142	1.3363
-0.20	A=	0.7927	0.8309	0.8609	0.8846	0.9032	0.9180	0.9299	0.9395	0.9474	0.9539	0.9593
	B=	2.6734	2.4338	2.2260	2.0458	1.8892	1.7525	1.6327	1.5270	1.4334	1.3501	1.2754
-0.10	A=	0.8017	0.8387	0.8677	0.8904	0.9082	0.9223	0.9336	0.9427	0.9502	0.9563	0.9614
	B=	2.5689	2.3346	2.1324	1.9577	1.8063	1.6746	1.5592	1.4578	1.3679	1.2880	1.2165
0.00	A=	0.8106	0.8464	0.8743	0.8960	0.9130	0.9264	0.9372	0.9458	0.9529	0.9587	0.9635
	B=	2.4674	2.2384	2.0417	1.8724	1.7262	1.5992	1.4883	1.3908	1.3047	1.2281	1.1597
0.10	A=	0.8192	0.8539	0.8807	0.9015	0.9177	0.9304	0.9406	0.9488	0.9555	0.9610	0.9656
	B=	2.3689	2.1451	1.9539	1.7899	1.6487	1.5264	1.4198	1.3262	1.2436	1.1703	1.1048
0.20	A=	0.8276	0.8612	0.8869	0.9068	0.9222	0.9343	0.9439	0.9517	0.9580	0.9632	0.9675
	B=	2.2733	2.0548	1.8689	1.7101	1.5739	1.4561	1.3536	1.2638	1.1847	1.1145	1.0518
0.30	A=	0.8359	0.8683	0.8930	0.9119	0.9266	0.9380	0.9472	0.9545	0.9605	0.9654	0.9694
	B=	2.1806	1.9673	1.7867	1.6331	1.5016	1.3882	1.2898	1.2037	1.1279	1.0607	1.0008
0.40	A=	0.8438	0.8751	0.8988	0.9168	0.9308	0.9416	0.9503	0.9572	0.9628	0.9674	0.9712
	B=	2.0907	1.8826	1.7072	1.5586	1.4318	1.3228	1.2283	1.1458	1.0732	1.0089	0.9517
0.50	A=	0.8516	0.8818	0.9044	0.9216	0.9348	0.9451	0.9533	0.9598	0.9651	0.9694	0.9730
	B=	2.0036	1.8006	1.6304	1.4868	1.3646	1.2597	1.1691	1.0900	1.0205	0.9591	0.9044

Table III. (Continued)

ϵn		A_1 and B_1 at Holdup Ratio $K/\lambda n$ of										
		0.00	0.05	0.10	0.15	0.20	0.25	0.30	0.35	0.40	0.45	0.50
0.60	A=	0.8591	0.8882	0.9098	0.9262	0.9387	0.9484	0.9561	0.9623	0.9672	0.9713	0.9747
	B=	1.9193	1.7214	1.5563	1.4175	1.2998	1.1990	1.1120	1.0363	0.9698	0.9112	0.8590
0.70	A=	0.8664	0.8943	0.9150	0.9306	0.9424	0.9516	0.9589	0.9647	0.9693	0.9732	0.9763
	B=	1.8377	1.6448	1.4848	1.3507	1.2373	1.1405	1.0571	0.9846	0.9211	0.8651	0.8153
0.80	A=	0.8735	0.9003	0.9200	0.9348	0.9460	0.9547	0.9615	0.9669	0.9713	0.9749	0.9779
	B=	1.7587	1.5709	1.4158	1.2863	1.1772	1.0843	1.0044	0.9350	0.8743	0.8208	0.7733
0.90	A=	0.8802	0.9060	0.9248	0.9388	0.9494	0.9576	0.9640	0.9691	0.9732	0.9766	0.9793
	B=	1.6823	1.4995	1.3492	1.2244	1.1194	1.0302	0.9537	0.8873	0.8294	0.7783	0.7331
1.00	A=	0.8868	0.9115	0.9294	0.9427	0.9527	0.9604	0.9664	0.9712	0.9750	0.9782	0.9808
	B=	1.6085	1.4306	1.2852	1.1647	1.0638	0.9783	0.9050	0.8416	0.7863	0.7376	0.6945
1.10	A=	0.8931	0.9168	0.9338	0.9464	0.9558	0.9630	0.9687	0.9731	0.9767	0.9797	0.9821
	B=	1.5372	1.3642	1.2235	1.1074	1.0104	0.9284	0.8583	0.7977	0.7449	0.6986	0.6575
1.20	A=	0.8992	0.9218	0.9380	0.9499	0.9588	0.9656	0.9708	0.9750	0.9784	0.9811	0.9834
	B=	1.4684	1.3002	1.1641	1.0523	0.9591	0.8806	0.8135	0.7557	0.7054	0.6612	0.6221
1.30	A=	0.9050	0.9266	0.9420	0.9532	0.9616	0.9679	0.9729	0.9768	0.9799	0.9825	0.9846
	B=	1.4019	1.2386	1.1070	0.9993	0.9099	0.8347	0.7706	0.7154	0.6675	0.6254	0.5883
1.40	A=	0.9106	0.9312	0.9458	0.9564	0.9642	0.9702	0.9748	0.9785	0.9814	0.9838	0.9857
	B=	1.3378	1.1792	1.0521	0.9485	0.8627	0.7907	0.7295	0.6769	0.6312	0.5912	0.5559
1.50	A=	0.9159	0.9356	0.9494	0.9594	0.9668	0.9723	0.9767	0.9800	0.9828	0.9850	0.9868
	B=	1.2761	1.1221	0.9994	0.8998	0.8175	0.7487	0.6902	0.6400	0.5966	0.5585	0.5250
1.60	A=	0.9210	0.9398	0.9529	0.9622	0.9691	0.9744	0.9784	0.9815	0.9841	0.9861	0.9878
	B=	1.2165	1.0672	0.9488	0.8530	0.7742	0.7084	0.6526	0.6048	0.5635	0.5273	0.4955
1.70	A=	0.9259	0.9438	0.9561	0.9649	0.9714	0.9763	0.9800	0.9829	0.9853	0.9872	0.9887
	B=	1.1592	1.0145	0.9003	0.8083	0.7328	0.6699	0.6167	0.5712	0.5319	0.4975	0.4673

ϵ		A_1 and B_1 at Holdup Ratio $K/\lambda n$ of										
		0.00	0.05	0.10	0.15	0.20	0.25	0.30	0.35	0.40	0.45	0.50
1.80	A=	0.9305	0.9475	0.9592	0.9675	0.9735	0.9780	0.9815	0.9843	0.9864	0.9882	0.9896
	B=	1.1041	0.9638	0.8537	0.7654	0.6932	0.6331	0.5824	0.5391	0.5017	0.4691	0.4405
1.90	A=	0.9349	0.9511	0.9621	0.9698	0.9755	0.9797	0.9830	0.9855	0.9875	0.9891	0.9905
	B=	1.0510	0.9152	0.8092	0.7244	0.6553	0.5980	0.5497	0.5085	0.4730	0.4421	0.4149
2.00	A=	0.9391	0.9545	0.9648	0.9721	0.9774	0.9813	0.9843	0.9866	0.9885	0.9900	0.9912
	B=	1.0000	0.8686	0.7665	0.6852	0.6192	0.5645	0.5185	0.4794	0.4457	0.4164	0.3906
2.10	A=	0.9431	0.9576	0.9674	0.9742	0.9791	0.9828	0.9856	0.9877	0.9894	0.9908	0.9920
	B=	0.9510	0.8239	0.7257	0.6478	0.5847	0.5325	0.4888	0.4517	0.4197	0.3919	0.3675
2.20	A=	0.9469	0.9606	0.9698	0.9762	0.9807	0.9841	0.9867	0.9887	0.9903	0.9916	0.9926
	B=	0.9039	0.7811	0.6866	0.6120	0.5518	0.5021	0.4605	0.4253	0.3950	0.3686	0.3456
2.30	A=	0.9504	0.9635	0.9721	0.9780	0.9823	0.9854	0.9878	0.9897	0.9911	0.9923	0.9933
	B=	0.8588	0.7401	0.6493	0.5779	0.5204	0.4731	0.4336	0.4002	0.3714	0.3465	0.3247
2.40	A=	0.9538	0.9661	0.9742	0.9797	0.9837	0.9866	0.9888	0.9905	0.9919	0.9930	0.9938
	B=	0.8155	0.7008	0.6137	0.5454	0.4905	0.4456	0.4081	0.3763	0.3491	0.3256	0.3050
2.50	A=	0.9570	0.9686	0.9762	0.9814	0.9850	0.9877	0.9898	0.9913	0.9926	0.9936	0.9944
	B=	0.7739	0.6633	0.5797	0.5144	0.4621	0.4194	0.3838	0.3537	0.3280	0.3057	0.2862
2.60	A=	0.9600	0.9710	0.9780	0.9829	0.9863	0.9888	0.9906	0.9921	0.9932	0.9941	0.9949
	B=	0.7342	0.6275	0.5473	0.4849	0.4351	0.3945	0.3607	0.3322	0.3079	0.2869	0.2685
2.70	A=	0.9628	0.9731	0.9798	0.9843	0.9874	0.9897	0.9914	0.9928	0.9938	0.9946	0.9953
	B=	0.6961	0.5933	0.5164	0.4568	0.4094	0.3708	0.3388	0.3119	0.2889	0.2690	0.2517
2.80	A=	0.9655	0.9752	0.9814	0.9856	0.9885	0.9906	0.9922	0.9934	0.9944	0.9951	0.9957
	B=	0.6596	0.5606	0.4869	0.4301	0.3850	0.3484	0.3181	0.2926	0.2709	0.2522	0.2358
2.90	A=	0.9679	0.9771	0.9829	0.9868	0.9895	0.9914	0.9929	0.9940	0.9949	0.9956	0.9961
	B=	0.6248	0.5295	0.4589	0.4048	0.3619	0.3272	0.2985	0.2744	0.2539	0.2362	0.2208
3.00	A=	0.9703	0.9789	0.9843	0.9879	0.9904	0.9922	0.9935	0.9945	0.9953	0.9960	0.9965
	B=	0.5915	0.4998	0.4323	0.3807	0.3400	0.3070	0.2799	0.2571	0.2378	0.2211	0.2067

Table IV. Functions for the Second Transient Term

ϵn		A_2 and B_2 at Hodlup Ratio $K/\lambda n$ of										
		0.00	0.05	0.10	0.15	0.20	0.25	0.30	0.35	0.40	0.45	0.50
-3.00	A=	0.2013	0.2271	0.2317	0.2198	0.1995	0.1766	0.1544	0.1343	0.1168	0.1018	0.0890
	B=	27.2865	24.9576	22.8689	21.1333	19.7449	18.6479	17.7794	17.0858	16.5252	16.0665	15.6865
-2.90	A=	0.1986	0.2233	0.2271	0.2151	0.1952	0.1729	0.1513	0.1318	0.1147	0.1001	0.0876
	B=	27.0517	24.7335	22.6622	20.9448	19.5719	18.4868	17.6269	16.9395	16.3832	15.9275	15.5495
-2.80	A=	0.1958	0.2193	0.2224	0.2104	0.1908	0.1691	0.1481	0.1291	0.1125	0.0983	0.0862
	B=	26.8214	24.5137	22.4598	20.7603	19.4027	18.3293	17.4781	16.7969	16.2450	15.7924	15.4165
-2.70	A=	0.1930	0.2153	0.2177	0.2056	0.1864	0.1652	0.1447	0.1263	0.1102	0.0964	0.0846
	B=	26.5955	24.2984	22.2616	20.5798	19.2373	18.1756	17.3331	16.6580	16.1106	15.6611	15.2873
-2.60	A=	0.1900	0.2111	0.2129	0.2007	0.1819	0.1612	0.1414	0.1235	0.1079	0.0945	0.0830
	B=	26.3741	24.0874	22.0676	20.4033	19.0757	18.0256	17.1917	16.5229	15.9799	15.5336	15.1621
-2.50	A=	0.1869	0.2069	0.2080	0.1958	0.1773	0.1572	0.1380	0.1206	0.1055	0.0925	0.0813
	B=	26.1571	23.8809	21.8778	20.2309	18.9180	17.8794	17.0540	16.3915	15.8530	15.4099	15.0408
-2.40	A=	0.1837	0.2025	0.2030	0.1909	0.1727	0.1531	0.1345	0.1177	0.1030	0.0904	0.0796
	B=	25.9446	23.6787	21.6923	20.0624	18.7641	17.7369	16.9201	16.2638	15.7299	15.2901	14.9233
-2.30	A=	0.1804	0.1981	0.1981	0.1859	0.1681	0.1490	0.1309	0.1147	0.1005	0.0883	0.0778
	B=	25.7366	23.4810	21.5110	19.8980	18.6141	17.5982	16.7899	16.1399	15.6106	15.1741	14.8098
-2.20	A=	0.1770	0.1936	0.1930	0,1808	0.1634	0.1449	0.1274	0.1116	0.0979	0.0861	0.0759
	B=	25.5330	23.2877	21.3340	19.7377	18.4680	17.4633	16.6634	16.0197	15.4950	15.0620	14.7001
-2.10	A=	0.1735	0.1891	0.1879	0.1758	0.1587	0.1408	0.1238	0.1085	0.0953	0.0838	0.0740
	B=	25.3339	23.0988	21.1612	19.5814	18.3258	17.3322	16.5407	15.9032	15.3832	14.9536	14.5943
-2.00	A=	0.1699	0.1845	0.1828	0.1707	0.1540	0.1366	0.1201	0.1054	0.0926	0.0815	0.0721
	B=	25.1393	22.9143	20.9927	19.4292	18.1875	17.2049	16.4218	15.7906	15.2752	14.8491	14.4924
-1.90	A=	0.1663	0.1798	0.1777	0.1656	0.1493	0.1324	0.1165	0.1023	0.0899	0.0792	0.0701
	B=	24.9492	22.7343	20.8285	19.2810	18.0532	17.0814	16.3066	15.6817	15.1710	14.7484	14.3943

Table IV. (Continued)

		A_2 and B_2 at Holdup Ratio $K/\lambda n$ of										
		0.00	0.05	0.10	0.15	0.20	0.25	0.30	0.35	0.40	0.45	0.50
-1.80	A=	0.1626	0.1751	0.1725	0.1605	0.1446	0.1282	0.1128	0.0991	0.0871	0.0769	0.0680
	B=	24.7637	22.5587	20.6686	19.1370	17.9227	16.9618	16.1952	15.5765	15.0706	14.6515	14.3001
-1.70	A=	0.1588	0.1703	0.1673	0.1554	0.1399	0.1239	0.1091	0.0959	0.0844	0.0745	0.0660
	B=	24.5826	22.3876	20.5129	18.9971	17.7962	16.8460	16.0877	15.4752	14.9740	14.5584	14.2098
-1.60	A=	0.1549	0.1655	0.1621	0.1503	0.1352	0.1197	0.1054	0.0927	0.0816	0.0721	0.0639
	B=	24.4060	22.2210	20.3616	18.8613	17.6737	16.7340	15.9839	15.3776	14.8811	14.4692	14.1233
-1.50	A=	0.1510	0.1607	0.1569	0.1452	0.1305	0.1155	0.1017	0.0895	0.0788	0.0696	0.0618
	B=	24.2340	22.0588	20.2146	18.7296	17.5552	16.6260	15.8840	15.2839	14.7922	14.3839	14.0408
-1.40	A=	0.1470	0.1558	0.1517	0.1401	0.1258	0.1114	0.0980	0.0862	0.0760	0.0672	0.0597
	B=	24.0665	21.9012	20.0720	18.6021	17.4407	16.5219	15.7879	15.1940	14.7070	14.3024	13.9621
-1.30	A=	0.1430	0.1510	0.1465	0.1351	0.1211	0.1072	0.0944	0.0830	0.0732	0.0648	0.0575
	B=	23.9036	21.7480	19.9337	18.4788	17.3302	16.4217	15.6957	15.1080	14.6257	14.2248	13.8873
-1.20	A=	0.1389	0.1461	0.1414	0.1301	0.1165	0.1031	0.0907	0.0799	0.0704	0.0623	0.0554
	B=	23.7453	21.5994	19.7998	18.3597	17.2238	16.3254	15.6073	15.0258	14.5483	14.1510	13.8165
-1.10	A=	0.1348	0.1412	0.1362	0.1251	0.1120	0.0990	0.0871	0.0767	0.0677	0.0599	0.0532
	B=	23.5915	21.4552	19.6703	18.2448	17.1214	16.2331	15.5229	14.9474	14.4747	14.0811	13.7495
-1.00	A=	0.1307	0.1364	0.1312	0.1202	0.1074	0.0949	0.0836	0.0735	0.0649	0.0575	0.0511
	B=	23.4423	21.3157	19.5452	18.1341	17.0231	16.1447	15.4424	14.8730	14.4050	14.0152	13.6865
-0.90	A=	0.1266	0.1315	0.1261	0.1154	0.1030	0.0909	0.0800	0.0704	0.0622	0.0551	0.0490
	B=	23.2978	21.1807	19.4245	18.0277	16.9289	16.0604	15.3658	14.8025	14.3392	13.9531	13.6274
-0.80	A=	0.1225	0.1267	0.1211	0.1106	0.0986	0.0870	0.0765	0.0674	0.0595	0.0527	0.0469
	B=	23.1578	21.0502	19.3082	17.9255	16.8389	15.9801	15.2932	14.7359	14.2774	13.8950	13.5723
-0.70	A=	0.1184	0.1220	0.1162	0.1058	0.0943	0.0831	0.0731	0.0644	0.0568	0.0504	0.0448
	B=	23.0225	20.9244	19.1964	17.8276	16.7529	15.9039	15.2246	14.6733	14.2195	13.8409	13.5211

Table IV. (Continued)

ϵ_n		A_2 and B_2 at Hold up Ratio K/λ_n of										
		0.00	0.05	0.10	0.15	0.20	0.25	0.30	0.35	0.40	0.45	0.50
-0.60	A=	0.1142	0.1172	0.1113	0.1012	0.0900	0.0793	0.0697	0.0614	0.0542	0.0480	0.0428
	B=	22.8919	20.8032	19.0890	17.7340	16.6712	15.8317	15.1600	14.6147	14.1656	13.7907	13.4740
-0.50	A=	0.1101	0.1125	0.1065	0.0966	0.0859	0.0756	0.0664	0.0585	0.0516	0.0458	0.0408
	B=	22.7659	20.6865	18.9862	17.6448	16.5936	15.7636	15.0994	14.5600	14.1156	13.7445	13.4308
-0.40	A=	0.1060	0.1079	0.1018	0.0922	0.0818	0.0720	0.0632	0.0556	0.0491	0.0435	0.0388
	B=	22.6446	20.5746	18.8878	17.5599	16.5203	15.6996	15.0429	14.5094	14.0697	13.7024	13.3917
-0.30	A=	0.1020	0.1033	0.0972	0.0878	0.0778	0.0684	0.0600	0.0528	0.0466	0.0413	0.0368
	B=	22.5280	20.4672	18.7940	17.4794	16.4512	15.6398	14.9904	14.4628	14.0278	13.6642	13.3566
-0.20	A=	0.0980	0.0988	0.0927	0.0835	0.0739	0.0649	0.0570	0.0501	0.0442	0.0392	0.0349
	B=	22.4161	20.3646	18.7047	17.4033	16.3864	15.5842	14.9421	14.4203	13.9900	13.6301	13.3255
-0.10	A=	0.0940	0.0944	0.0882	0.0794	0.0701	0.0615	0.0540	0.0474	0.0419	0.0371	0.0331
	B=	22.3090	20.2666	18.6200	17.3316	16.3259	15.5327	14.8979	14.3820	13.9562	13.6002	13.2986
0.00	A=	---	0.0901	0.0839	0.0753	0.0664	0.0582	0.0510	0.0449	0.0396	0.0351	0.0313
	B=	---	20.1734	18.5399	17.2644	16.2697	15.4855	14.8579	14.3477	13.9266	13.5743	13.2758
0.10	A=	0.0862	0.0859	0.0797	0.0714	0.0628	0.0550	0.0482	0.0424	0.0374	0.0331	0.0295
	B=	22.1090	20.0849	18.4644	17.2016	16.2178	15.4425	14.8221	14.3176	13.9011	13.5525	13.2571
0.20	A=	0.0824	0.0817	0.0756	0.0675	0.0594	0.0520	0.0455	0.0399	0.0352	0.0312	0.0278
	B=	22.0162	20.0011	18.3936	17.1434	16.1703	15.4039	14.7905	14.2917	13.8798	13.5350	13.2426
0.30	A=	0.0787	0.0777	0.0716	0.0638	0.0560	0.0490	0.0428	0.0376	0.0331	0.0294	0.0262
	B=	21.9282	19.9222	18.3274	17.0896	16.1273	15.3695	14.7632	14.2700	13.8627	13.5216	13.2323
0.40	A=	0.0750	0.0737	0.0678	0.0602	0.0528	0.0461	0.0403	0.0353	0.0312	0.0276	0.0246
	B=	21.8450	19.8480	18.2659	17.0405	16.0887	15.3395	14.7401	14.2526	13.8498	13.5124	13.2262
0.50	A=	0.0714	0.0699	0.0640	0.0568	0.0497	0.0433	0.0378	0.0332	0.0292	0.0259	0.0231
	B=	21.7667	19.7787	18.2091	16.9959	16.0545	15.3139	14.7214	14.2394	13.8412	13.5075	13.2243

Table IV. (Continued)

		A_2 and B_2 at Holdup Ratio $K/\lambda n$ of										
		0.00	0.05	0.10	0.15	0.20	0.25	0.30	0.35	0.40	0.45	0.50
0.60	A=	0.0679	0.0662	0.0604	0.0534	0.0467	0.0407	0.0355	0.0311	0.0274	0.0242	0.0216
	B=	21.6933	19.7142	18.1571	16.9559	16.0248	15.2927	14.7070	14.2306	13.8368	13.5068	13.2268
0.70	A=	0.0645	0.0626	0.0569	0.0502	0.0438	0.0381	0.0332	0.0291	0.0256	0.0227	0.0202
	B=	21.6248	19.6545	18.1098	16.9205	15.9997	15.2759	14.6970	14.2261	13.8368	13.5105	13.2335
0.80	A=	0.0612	0.0591	0.0536	0.0472	0.0411	0.0357	0.0311	0.0272	0.0239	0.0212	0.0188
	B=	21.5612	19.5998	18.0674	16.8899	15.9791	15.2636	14.6915	14.2259	13.8411	13.5185	13.2445
0.90	A=	0.0580	0.0557	0.0504	0.0442	0.0384	0.0333	0.0290	0.0254	0.0223	0.0197	0.0176
	B=	21.5025	19.5500	18.0297	16.8639	15.9631	15.2558	14.6903	14.2302	13.8498	13.5309	13.2600
1.00	A=	0.0549	0.0525	0.0473	0.0414	0.0359	0.0311	0.0271	0.0236	0.0208	0.0184	0.0163
	B=	21.4488	19.5051	17.9969	16.8426	15.9517	15.2526	14.6937	14.2389	13.8630	13.5476	13.2798
1.10	A=	0.0519	0.0494	0.0443	0.0387	0.0335	0.0290	0.0252	0.0220	0.0193	0.0171	0.0152
	B=	21.4001	19.4652	17.9689	16.8261	15.9450	15.2539	14.7015	14.2521	13.8805	13.5689	13.3041
1.20	A=	0.0490	0.0464	0.0415	0.0361	0.0312	0.0270	0.0234	0.0204	0.0179	0.0158	0.0141
	B=	21.3564	19.4303	17.9459	16.8144	15.9430	15.2598	14.7140	14.2698	13.9026	13.5945	13.3328
1.30	A=	0.0462	0.0435	0.0388	0.0337	0.0291	0.0251	0.0217	0.0190	0.0166	0.0147	0.0130
	B=	21.3178	19.4004	17.9278	16.8075	15.9457	15.2704	14.7309	14.2921	13.9292	13.6247	13.3660
1.40	A=	0.0435	0.0408	0.0362	0.0314	0.0270	0.0233	0.0202	0.0176	0.0154	0.0136	0.0121
	B=	21.2843	19.3755	17.9146	16.8055	15.9531	15.2857	14.7526	14.3189	13.9603	13.6594	13.4037
1.50	A=	0.0409	0.0382	0.0338	0.0292	0.0251	0.0216	0.0187	0.0162	0.0142	0.0125	0.0111
	B=	21.2558	19.3558	17.9065	16.8083	15.9654	15.3056	14.7788	14.3504	13.9961	13.6987	13.4460
1.60	A=	0.0384	0.0357	0.0314	0.0271	0.0232	0.0200	0.0172	0.0150	0.0131	0.0116	0.0103
	B=	21.2324	19.3411	17.9033	16.8161	15.9824	15.3303	14.8098	14.3865	14.0364	13.7426	13.4929
1.70	A=	0.0360	0.0333	0.0292	0.0251	0.0215	0.0184	0.0159	0.0138	0.0121	0.0107	0.0095
	B=	21.2142	19.3316	17.9052	16.8288	16.0043	15.3598	14.8455	14.4272	14.0814	13.7912	13.5444

Table IV. (Continued)

		A_2 and B_2 at Holdup Ratio $K/\lambda n$ of										
		0.00	0.05	0.10	0.15	0.20	0.25	0.30	0.35	0.40	0.45	0.50
1.80	A=	0.0338	0.0311	0.0271	0.0233	0.0199	0.0170	0.0147	0.0127	0.0111	0.0098	0.0087
	B=	21.2012	19.3272	17.9122	16.8465	16.0311	15.3941	14.8859	14.4727	14.1311	13.8444	13.6006
1.90	A=	0.0316	0.0289	0.0252	0.0215	0.0183	0.0157	0.0135	0.0117	0.0102	0.0090	0.0080
	B=	21.1933	19.3280	17.9242	16.8691	16.0628	15.4332	14.9311	14.5230	14.1855	13.9023	13.6615
2.00	A=	0.0295	0.0269	0.0233	0.0199	0.0169	0.0144	0.0124	0.0108	0.0094	0.0083	0.0073
	B=	21.1907	19.3340	17.9415	16.8969	16.0994	15.4772	14.9812	14.5780	14.2447	13.9649	13.7271
2.10	A=	0.0276	0.0250	0.0216	0.0183	0.0156	0.0133	0.0114	0.0099	0.0086	0.0076	0.0067
	B=	21.1934	19.3452	17.9638	16.9296	16.1410	15.5261	15.0361	14.6378	14.3086	14.0323	13.7974
2.20	A=	0.0257	0.0232	0.0199	0.0169	0.0143	0.0122	0.0104	0.0090	0.0079	0.0069	0.0061
	B=	21.2013	19.3617	17.9914	16.9675	16.1877	15.5800	15.0959	14.7025	14.3774	14.1045	13.8725
2.30	A=	0.0240	0.0215	0.0184	0.0156	0.0131	0.0112	0.0096	0.0083	0.0072	0.0063	0.0056
	B=	21.2145	19.3835	18.0242	17.0105	16.2394	15.6388	15.1606	14.7721	14.4510	14.1815	13.9524
2.40	A=	0.0223	0.0199	0.0170	0.0143	0.0121	0.0102	0.0087	0.0075	0.0066	0.0058	0.0051
	B=	21.2330	19.4106	18.0622	17.0587	16.2961	15.7027	15.2302	14.8466	14.5295	14.2634	14.0372
2.50	A=	0.0207	0.0184	0.0156	0.0131	0.0110	0.0093	0.0080	0.0069	0.0060	0.0052	0.0046
	B=	21.2569	19.4431	18.1055	17.1120	16.3580	15.7715	15.3049	14.9260	14.6129	14.3502	14.1269
2.60	A=	0.0192	0.0170	0.0144	0.0120	0.0101	0.0085	0.0073	0.0063	0.0054	0.0048	0.0042
	B=	21.2861	19.4809	18.1541	17.1706	16.4250	15.8455	15.3846	15.0104	14.7013	14.4419	14.2214
2.70	A=	0.0178	0.0156	0.0132	0.0110	0.0092	0.0078	0.0066	0.0057	0.0050	0.0043	0.0038
	B=	21.3208	19.5241	18.2080	17.2344	16.4971	15.9245	15.4693	15.0998	14.7946	14.5386	14.3209
2.80	A=	0.0165	0.0144	0.0121	0.0101	0.0084	0.0071	0.0060	0.0052	0.0045	0.0039	0.0035
	B=	21.3609	19.5727	18.2673	17.3035	16.5745	16.0087	15.5591	15.1943	14.8930	14.6402	14.4254
2.90	A=	0.0153	0.0133	0.0111	0.0092	0.0077	0.0065	0.0055	0.0047	0.0041	0.0036	0.0031
	B=	21.4064	19.6268	18.3320	17.3779	16.6571	16.0981	15.6540	15.2938	14.9964	14.7469	14.5348
3.00	A=	0.0141	0.0122	0.0101	0.0084	0.0070	0.0059	0.0050	0.0043	0.0037	0.0032	0.0028
	B=	21.4574	19.6864	18.4021	17.4576	16.7449	16.1926	15.7540	15.3984	15.1048	14.8586	14.6493

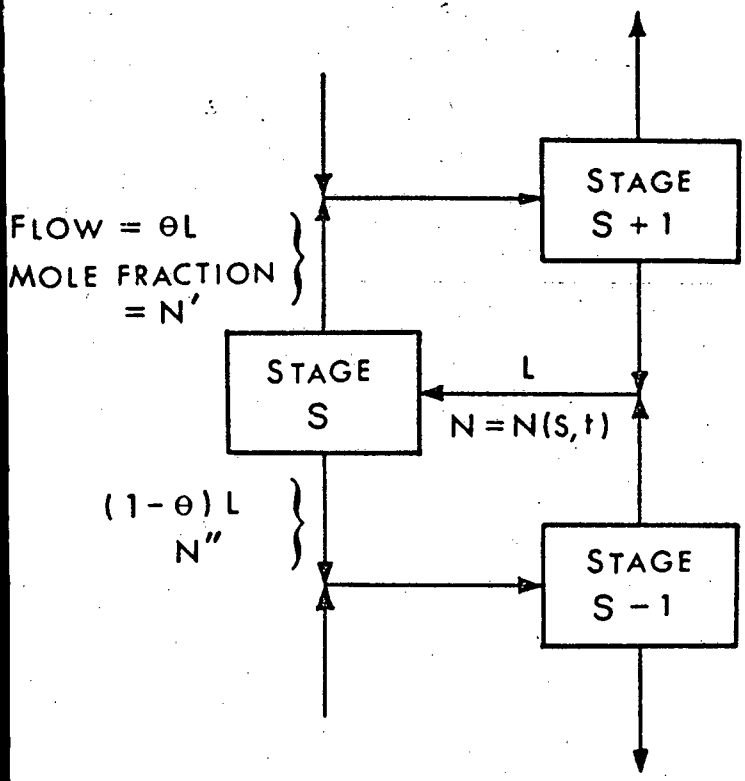

θ = CUT
≃ 1/2 FOR CLOSE SEPARATION
$\left[|\epsilon| = |\alpha - 1| << 1 \right]$

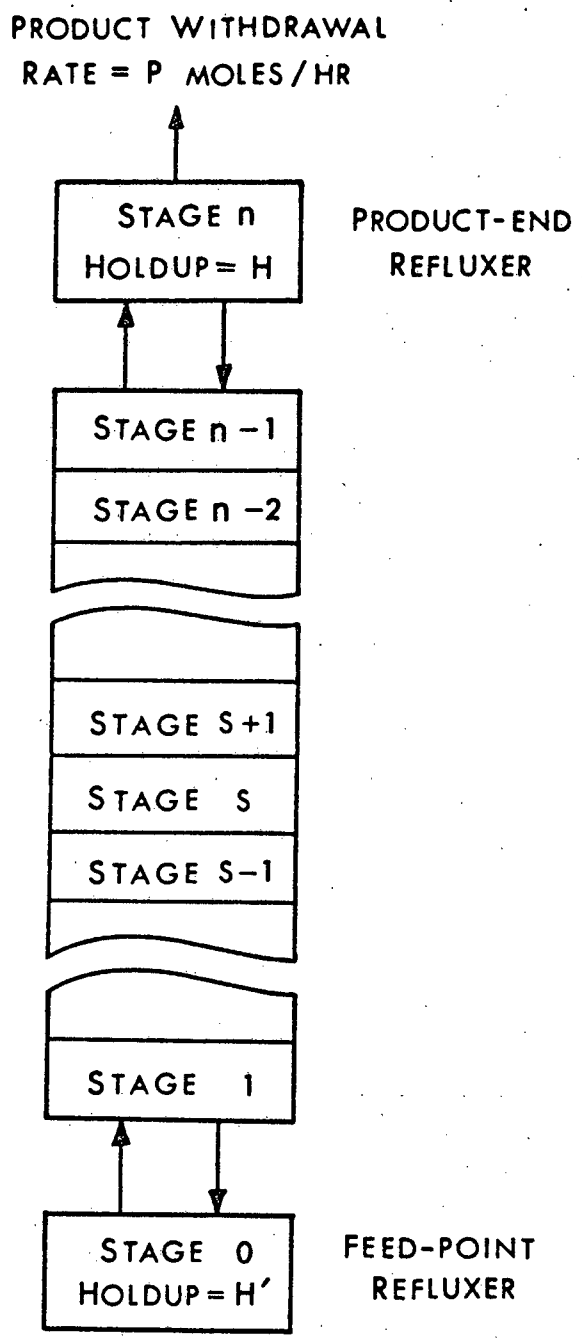

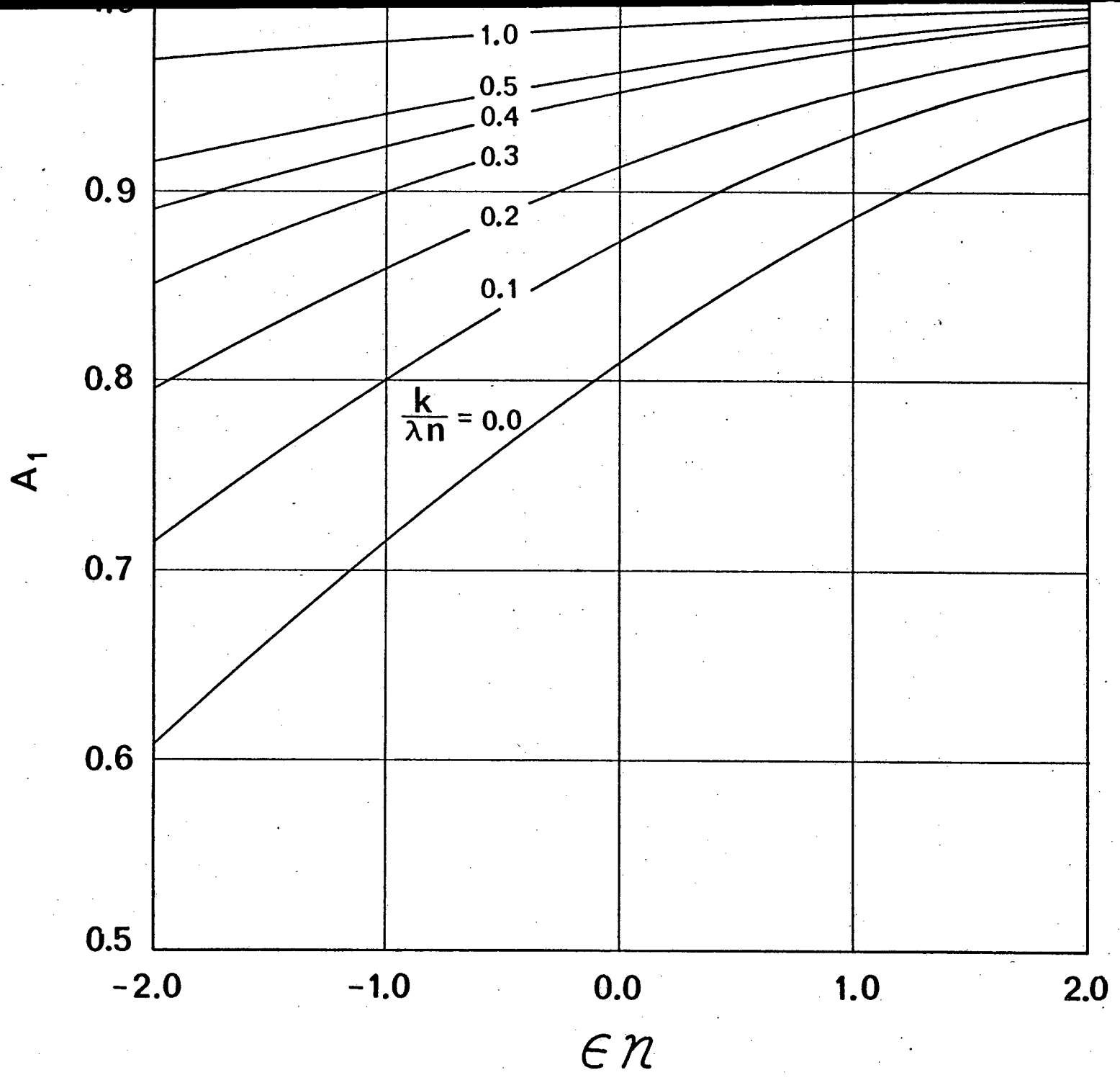
1.0
0.5
0.4
0.3
0.2
0.1
k/λn = 0.0
A1
0.9
0.8
0.7
0.6
0.5
-2.0
-1.0
0.0
1.0
2.0
ϵn

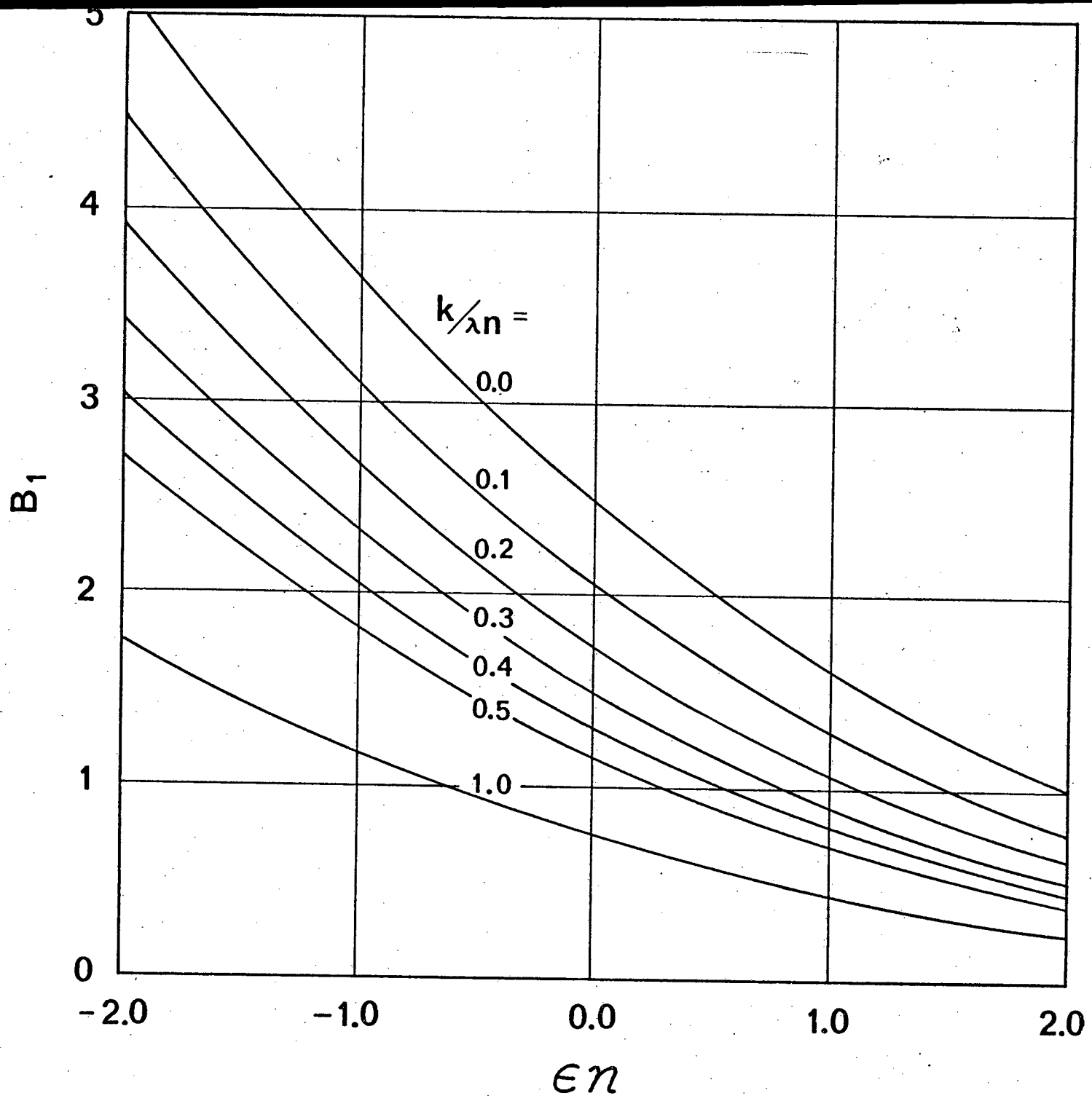
5
4
3
2
1
0
B_1
$k/\lambda n$ =
0.0
0.1
0.2
0.3
0.4
0.5
1.0
-2.0
-1.0
0.0
1.0
2.0
ϵn

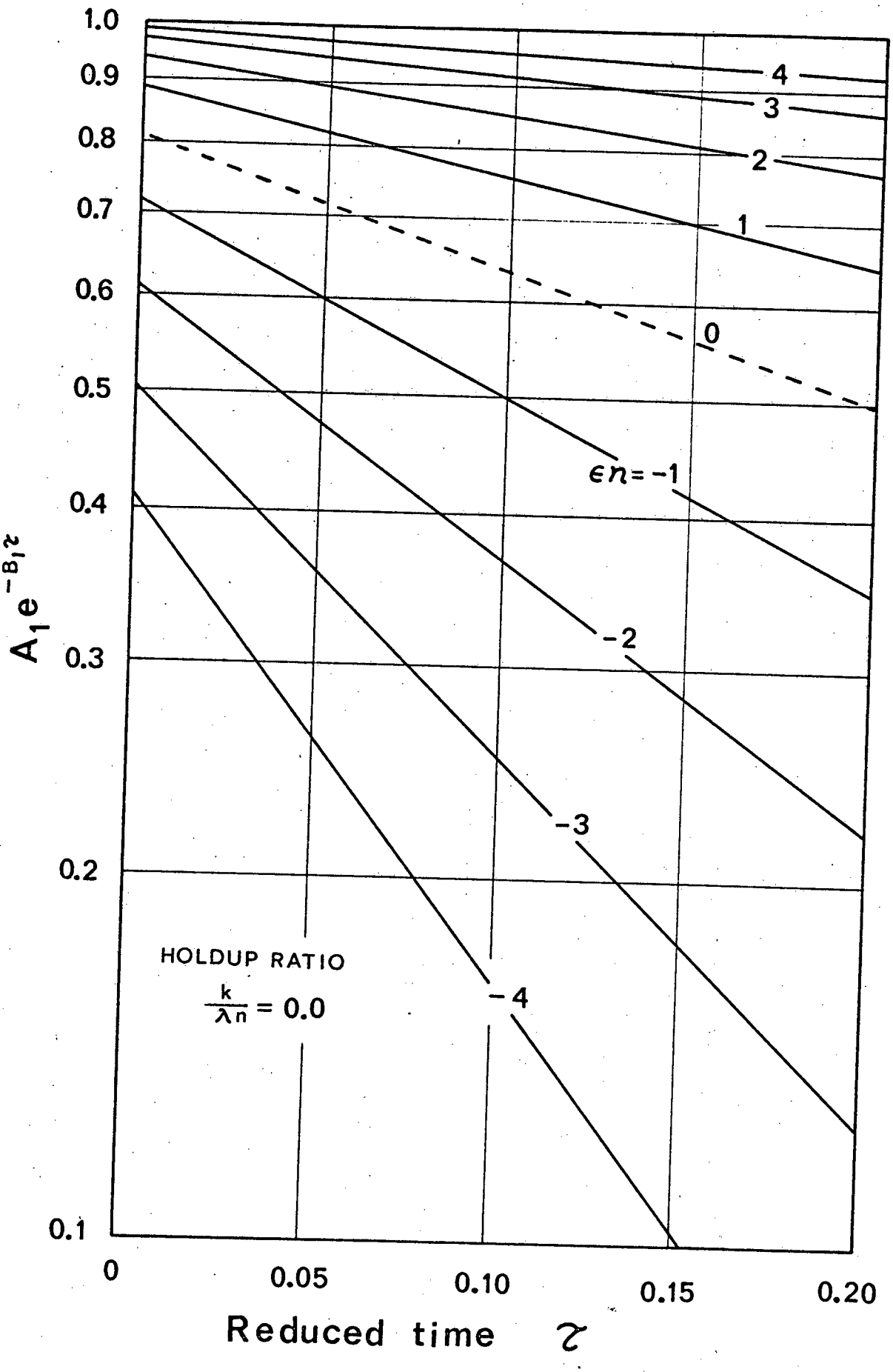
1.0
0.9
0.8
0.7
0.6
0.5
0.4
0.3
0.2
0.1
$A_1 e^{-B_1 \tau}$
4
3
2
1
0
$\epsilon n = -1$
-2
-3
-4
HOLDUP RATIO
$\frac{k}{\lambda n} = 0.0$
0
0.05
0.10
0.15
0.20
Reduced time τ

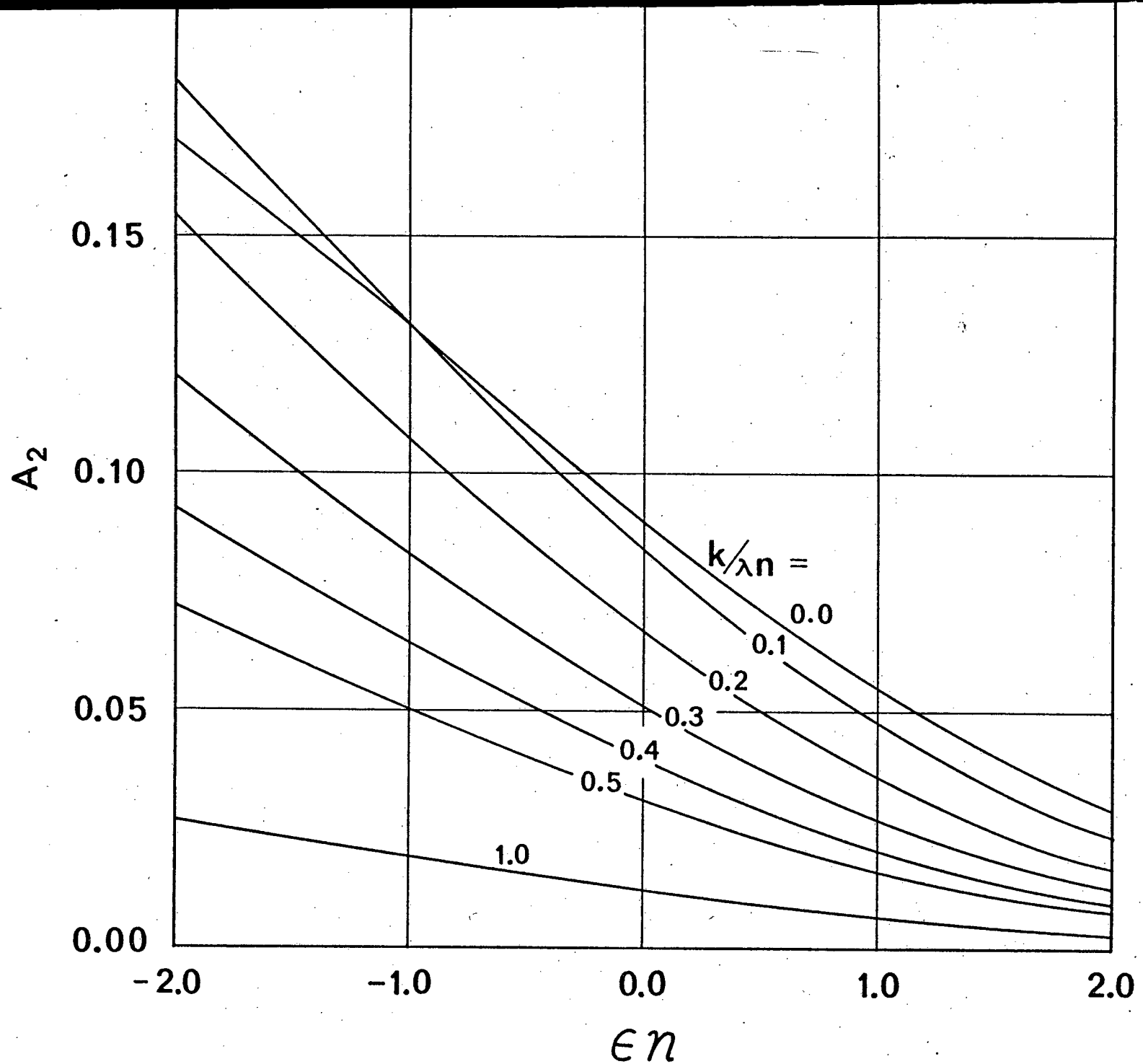
0.15
0.10
0.05
0.00
A_2
$k/\lambda n$ =
0.0
0.1
0.2
0.3
0.4
0.5
1.0
-2.0
-1.0
0.0
1.0
2.0
$\epsilon\eta$

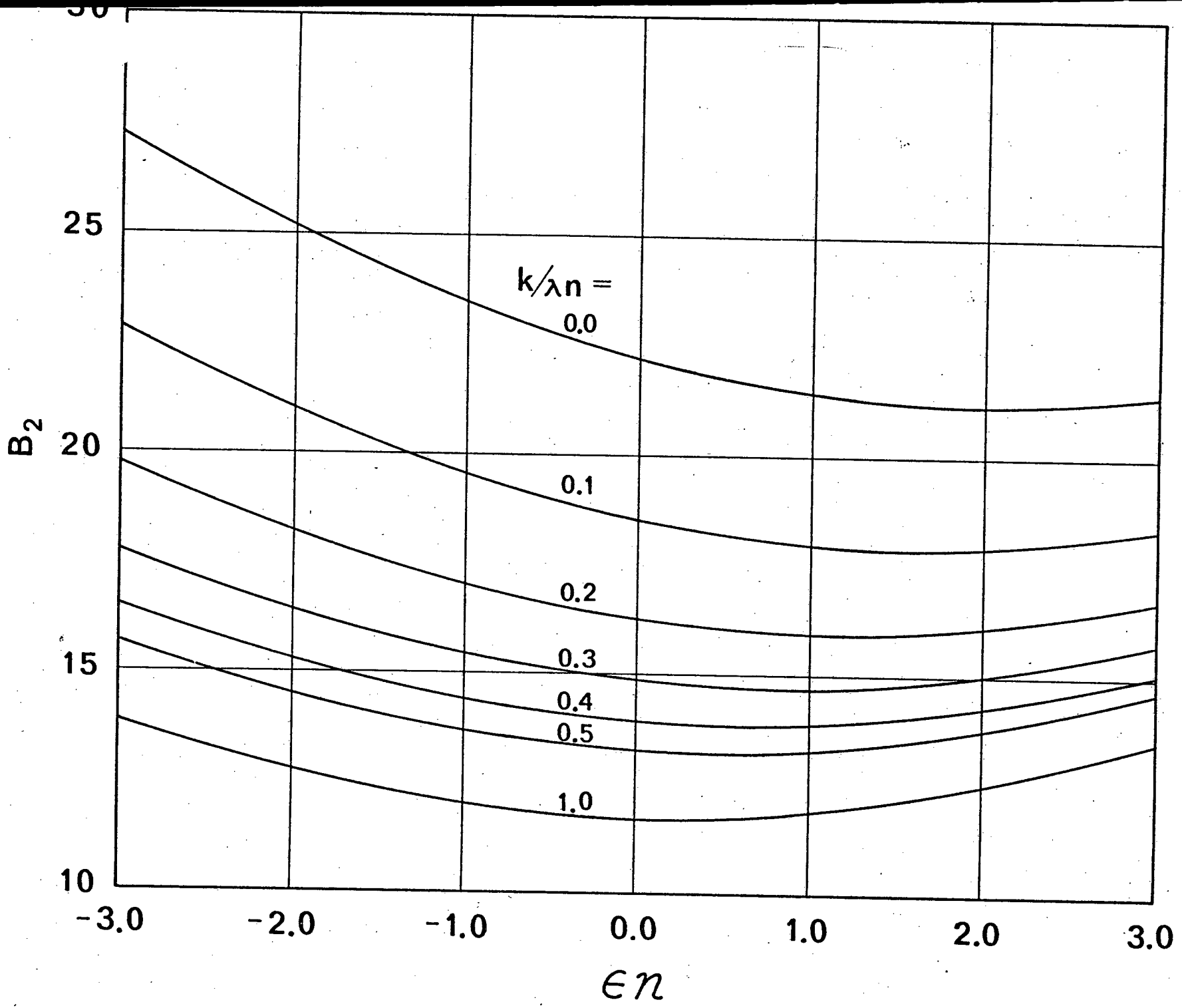
25
20
15
10
B_2
$k/\lambda n =$
0.0
0.1
0.2
0.3
0.4
0.5
1.0
-3.0
-2.0
-1.0
0.0
1.0
2.0
3.0
ϵn

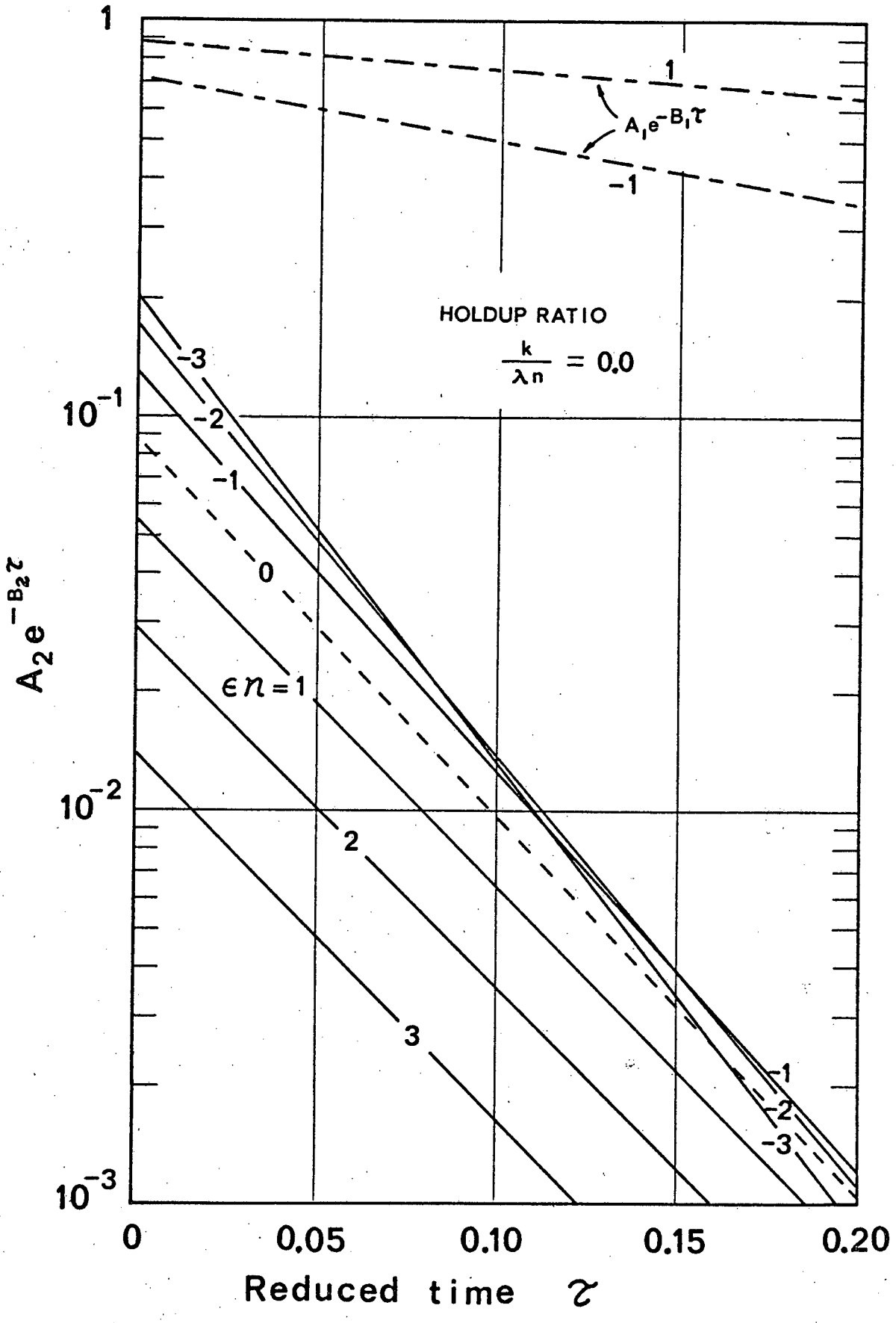
1
10^{-1}
10^{-2}
10^{-3}
$A_2e^{-B_2\tau}$
1
$A_1e^{-B_1\tau}$
-1
HOLDUP RATIO
$\frac{k}{\lambda n} = 0.0$
-3
-2
-1
0
$\epsilon n = 1$
2
3
-1
-2
-3
0
0.05
0.10
0.15
0.20
Reduced time τ

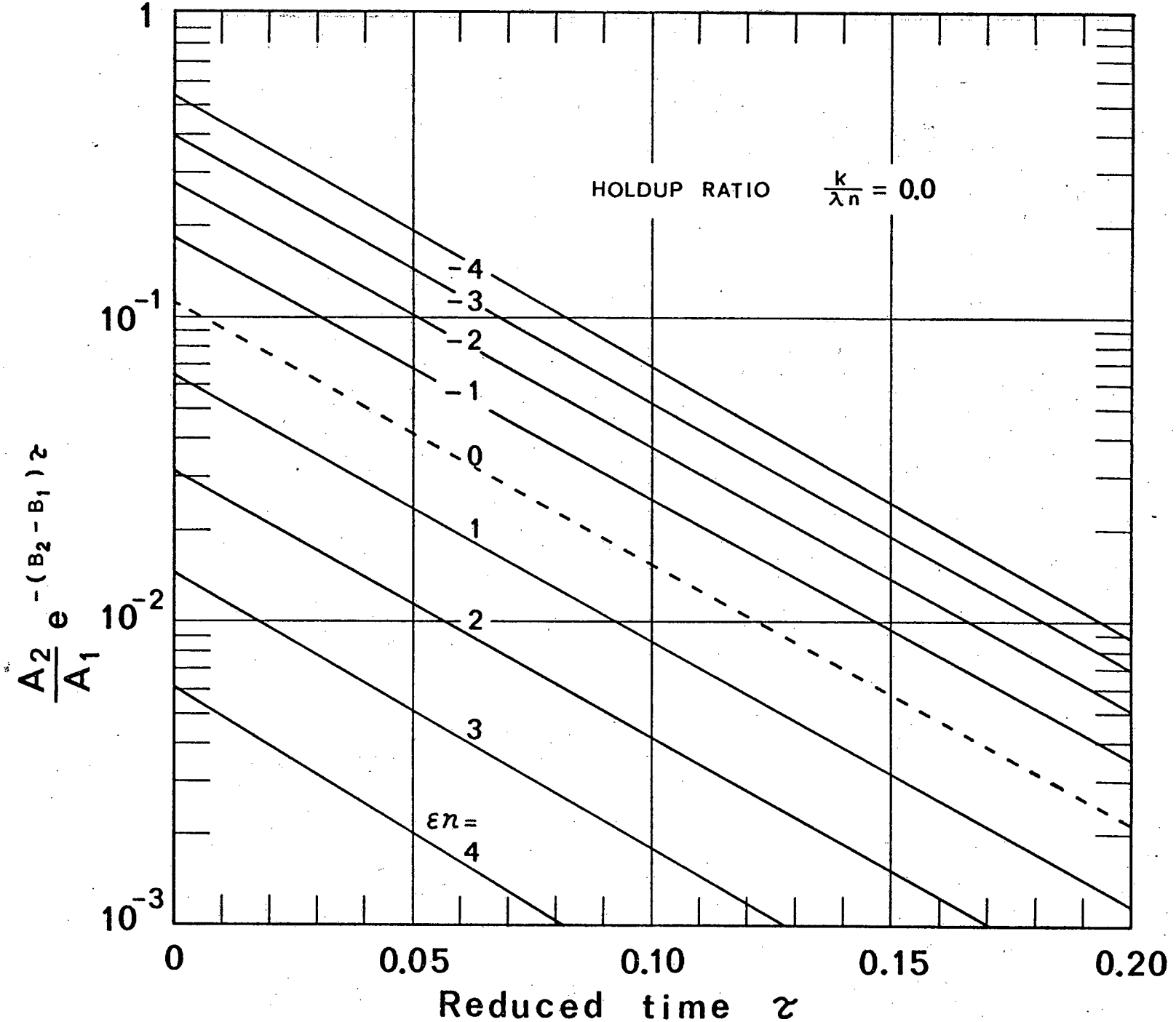
HOLDUP RATIO $\frac{k}{\lambda n} = 0.0$
$\frac{A_2}{A_1} e^{-(B_2 - B_1)\tau}$
1
10^{-1}
10^{-2}
10^{-3}
-4
-3
-2
-1
0
1
2
3
$\varepsilon n =$ 4
0
0.05
0.10
0.15
0.20
Reduced time τ

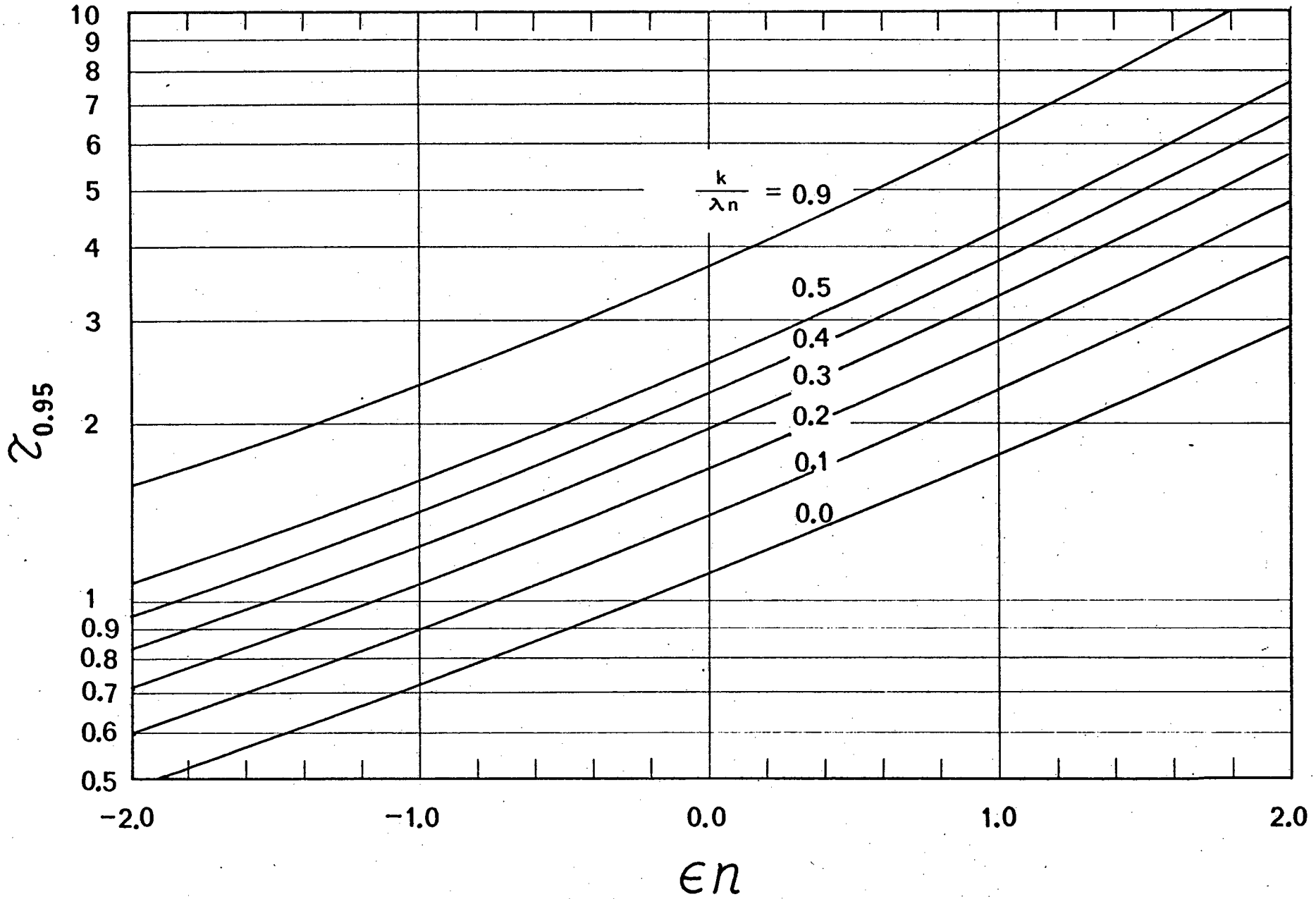
10
9
8
7
6
5
4
3
2
1
0.9
0.8
0.7
0.6
0.5
$z_{0.95}$
$\frac{k}{\lambda n} = 0.9$
0.5
0.4
0.3
0.2
0.1
0.0
−2.0
−1.0
0.0
1.0
2.0
ϵn

FIGURE CAPTIONS

Figure 1 Cascade Notation

Figure 2 Pre-exponential factor A_1 of first transient term

Figure 3 Exponent factor B_1 of first transient term

Figure 4 The first transient term as a function of reduced time τ

Figure 5 Pre-exponential factor A_2 of second transient term

Figure 6 Exponent factor B_2 of second transient term

Figure 7 The second transient term as a function of reduced time τ

Figure 8 Relative importance of the first and second terms

Figure 9 The 95%-equilibrium time